UNIVERSITY OF INSUBRIA

Department of Science and High Technology

Ph.D. Program:

Chemical and Environmental Sciences

-Environmental and Land-

-XXIX Course-

IMPROVING SUSTAINABILITY OF SEDIMENT MANAGEMENT IN ALPINE RESERVOIRS:

Control of sediment flushing operations to mitigate downstream environmental impacts

Dr. Maria Laura Brignoli

Advisor:

Prof. Paolo Espa

Ph.D. Dissertation

October 2016

H.A. Einstein used to tell the story of his father's reaction when he (H.A.) told him that he was going to make the study of sediment transport processes his life's work. His father, the great Albert Einstein, said that he himself had thought the same in his youth, but had decided that the subject was too difficult and that he would stick to nuclear physics.

Abstract

This thesis focuses on the desiltation of Alpine reservoirs in order to sustain their long-term utilization and restore the functioning of the bottom outlets, minimizing at the same time downstream environmental impacts of sediment removal operations. Different case studies of controlled sediment flushing operations (CSFs) are analysed adopting a multidisciplinary approach. In particular, sediment transport and downstream riverbed alteration, ecological impacts on benthic macroinvertebrates and fish, and performance indicators were investigated. These indicators include the cost of the operations (considering both the loss of hydropower and the expenses connected to mechanical excavation) and the flushing efficiency (i.e. the ratio between the volume of evacuated sediment and the corresponding volume of water employed). Moreover, the experimental dataset acquired before, during, and after a sediment removal operation was used to carry out and calibrate a one-dimensional sediment transport model of the monitored event. The CSFs from Cancano and Madesimo reservoirs (Lombardy Region, Italy) and the hydraulic dredging from Ambiesta Reservoir (Friuli-Venezia Giulia Region, Italy) are reported in detail. Furthermore, the main findings from the monitoring campaigns of ten CSFs performed in the Lake Como catchment are discussed. The duration of these operations and the average suspended sediment concentration (SSC) in the outflowing water were constrained, with the specific environmental objective of limiting the downstream fish mortality as predicted by a simple dose/response model. The biomonitoring indicated that this model allowed for a first approximation estimate of the impacts on trout. On the other hand, similar scenarios of sediment removal in terms of duration and average SSC can be identified with analogous predicted impacts on fish but non-negligible differences in flushing efficiency. Therefore, site-specific investigation of environmental impacts may be the key aspect for upgrading the trade-off between economic and environmental needs in planning further operations in the same area. As expected, the monitored riverbed alteration were quantitatively different as a function of the grain size of the flushed sediment. In particular, if the sediment removed was fine (i.e. silt/clay), the observed deposition was limited, and did not represent a permanent alteration of the riverbed substratum. On the contrary, if the sand content in the flushed sediment was relevant, the observed deposition was larger and showed longer persistency. In this case, other management criteria might be developed to take into account not only the effect of the SSC and the duration of the perturbation, but also the riverbed alteration and its dynamics. As ecological impacts, the CSFs had severe effects on both the benthic macroinvertebrates and trout populations. However, the benthic communities were able to recover to the pre-CSF conditions within few months up to one year after the end of the works. A selective pressure on juveniles of the brown trout was detected as well as a

reduction in trout population up to 50%. Regarding the sediment transport modelling, satisfactory agreement was found between the computed pattern of deposits and the observed one along the Liro River after the CSF at Madesimo Reservoir, despite the adopted simplifications. In conclusion, as the control of sediment flushing operations minimizing downstream impacts is only marginally discussed in the scientific literature, the reported experiences can support the planning and the monitoring of more sustainable flushing operations. It is worth noting that the need to upgrade the management of reservoir sediments has increasing global importance, as justified by the aging of existing reservoirs and by the hydropower boom expected within the next two decades in developing countries.

Contents

1 Introduction

1.1 Upgrading in reservoir management: the importance of sediment regime

Water storage in reservoirs is one of the primary elements for coping with the increasing demand of regulated water (White, 2010). Currently, flow regulation through reservoirs increases the naturally available supply for the world irrigation of 40%. Furthermore, ca. 17% of the world electricity is produced by hydropower in 2014. The construction of large dams peaked during 1960s and 1970s (Wisser et al., 2013) and, following a period of relative stagnation during the past 20 years, a boom in hydropower dam construction is expected to increase the global hydropower electricity capacity from 980 GW in 2011 to 1,700 GW within the next 10-20 years (Zarfl et al., 2015). This future development mainly refers to Southeast Asia, South America and Africa where a total of 3,700 dams were planned (83%) or under construction (17%) (Zarfl et al., 2015).

On the other hand, dams disrupt the longitudinal continuity of the river system. They trap all bedload sediment (i.e. the coarser part of the sediment load, that moves in intermittent contact with the bed by rolling, sliding and saltating) and all or part of the suspended load (i.e. finer sediment that is held in the water column by turbulence) depending upon the reservoir capacity in relation to the inflow (Brune, 1953). Downstream of reservoirs, the released water has the energy to move sediment but has little or no sediment load. This clear water is often referred to as *hungry water*, because it may transport sand and gravel downstream without replacement from upstream, resulting in coarsening of the surface layer (i.e. armouring), and thus in incision (Kondolf, 1997). Reservoirs may also decrease the magnitude of floods, which transport the majority of sediment, potentially reducing the effects of *hungry water* (Kondolf, 1997). Sediments accumulating in reservoirs are "resources out of place", because these sediments are needed to maintain the morphology and ecology of the downstream river system, as well to replenish vital land at the coast (Kondolf, 2014a). Moreover, sediment accumulation has relevant negative consequences on the same reservoirs, such as (Palmieri et al., 2003):

- Depletion of storage (reducing flood attenuation capability),
- Abrasion of outlet structures and mechanical equipment,
- Blockage of outlets causing interruption of benefits (e.g. irrigation releases or electricity generation),
- Reducing the ability of the dam to pass floods safely (e.g. by blocking emergency outlet gates),
- Increased loads on the dam.

Nevertheless, reservoirs have traditionally been designed based on the "life of reservoir" concept. Under this paradigm, the designer estimated the rate of sediment inflow and provided storage capacity for 50-100 years of sediment accumulation, thus postponing sedimentation problem and ignoring downstream impacts. Currently, the worldwide annual loss of reservoirs storage through sedimentation is estimated to be around 0.5% (i.e. more than $33{,}000 \times 10^6$ m^3). Even in the Italian Alps, where rates of soil erosion are generally low (e.g. Cerdan et al., 2010), the problem is of growing importance due to the advanced age of many reservoirs and the practical impossibility of building new ones. As it has been pointed out since the nineties (Morris and Fan, 1997), the approach of designing and operating reservoirs must be significantly reviewed accounting for an effective ecosystem management of the downstream rivers that includes not only flow regime but also sediment regime (Wohl et al. 2015). Even if the identification of a suitable sediment management regime must be an important part of designing ecologically sustainable flows downstream of dams and water diversion structures (Wohl et al., 2015; Gabbud and Lane, 2016), up to now, it is not clear what that regime might be (Gabbud and Lane, 2016).

A notable example of recent research efforts in this direction is provided by the Mekong River basin, largely undeveloped prior to 1990, and one of the world most productive and diverse ecosystems. The current impulse to massive hydropower development would lead to a dramatic contraction of the pre-dam sediment load reaching the river delta, unless existing facilities will be modified and new projects are designed and operated to pass sediment downstream (Kondolf et al., 2014b; Wild and Loucks, 2014). In particular, Wild et al. (2015) recently analysed alternative dam siting design and operation to maintain more natural sediment regimes in the Mekong River basin, and identified sediment flushing as a main management strategy. Authors pointed out that devising "environmentally friendly" sediment management techniques, so as not to affect the many ecological features the management efforts attempt to preserve, represents the crucial issue of the upcoming advances. In fact, their modelling results suggested that the main priority to conduct sediment management in the Mekong is maintaining the ecosystem service related to the natural sediment regime rather than preserving storage capacity, at least within a 100 years perspective (see also Kondolf et al., 2014b).

The development of a sound experience in the management of reservoir sediments is even more important if the future climate changes are taken into account. In fact, according to the scenarios produced by different climate models and the current changes in catchments land use and water uses, water resources will become more variable, with more intense floods that may significantly increase sediment yields (Lee and You, 2013; Yasarer and Sturm, 2016).

1.2 Sediment management strategies in reservoirs

A life-cycle management approach would be adopted and the potential for converting the existing dams into sustainable projects would be investigated (Palmieri et al., 2003). Sediment management strategies are not applied in many reservoirs where they could be. Dam operators may be not aware of potential management approaches nor under what conditions different methods are appropriate (Kondolf et al., 2014a). Palmieri et al. (2003) proposed a model to evaluate the technical and economic feasibility of such approaches but the design and implementation as well as the economic analysis are generally rather complex (Coker et al., 2009), justifying the need of a more thorough bibliography on this subject.

Different strategies to counteract the effects of siltation and to extend the useful life of reservoirs are discussed in literature (Kondolf et al., 2014a; Morris and Fan, 1997; Palmieri et al. 2003). Recently, Morris (2015) reported a complete classification of sediment management techniques. Four major types of activities can be undertaken to deal with reservoir sedimentation:

1) Approaches to minimize the amount of sediment arriving to reservoirs from upstream,
2) Methods to route sediment through or around the reservoir to minimize sediment trapping,
3) Methods to remove sediments accumulated in the reservoirs from upstream,
4) Actions to combat sedimentation not involving handling sediment (i.e. “adaptive” strategies).

The first methods address only the reservoir capacity issue but not downstream sediment starvation. The second and third methods maintain reservoir capacity and provide sediment to downstream reaches. The adaptive strategies do not manipulate sediment so they do not deal with the two mentioned problems (i.e. reservoir siltation and downstream sediment starvation). Some case studies related to these four activities are reported by Morris and Fan (1997).

Among sediment management alternatives, sediment flushing has been successfully implemented in many dams globally (Kondolf et al., 2014a). It consists in removing sediment by opening a low-level outlet to produce hydraulic scour. In particular, *free-flow flushing* or *empty flushing* (i.e. employing the complete draw-down of reservoirs) can be an effective way to maintain the storage capacity of small to medium sized reservoir (i.e. with storage capacity less than 10×10^6 m^3- Graf, 2005) silted by fine sediment (Palmieri et al., 2003). Generally, free-flow flushing has been employed at reservoirs having a small hydrologic size (i.e. a capacity to inflow ratio typically below 0.3-0.4), allowing the reservoir to be quickly refilled after flushing (Morris and Fan, 1997), and/or a strongly seasonal flow pattern (White, 2001). Free-flow flushing can be performed during flood season or non-flood season. Although both cases have been successfully employed, flushing during flood season is generally more effective because it provides larger discharges with more erosive capacity (Morris and Fan, 1997). On the other hand, in several cases (i.e. not in the case of recent

structures), the management of reservoir sedimentation through flood season flushing can be prevented by the lack of bottom outlets of a suitable size. Since flushing flows need to pass through the low-level outlet without appreciable backwater, the use of floods exceeding low-level gate capacity may be not feasible (Kondolf et al., 2014a). In these cases, mechanical equipment can be employed to dislodge sediments deposits into the flushing channel, thereby removing sediment faster than it would occur by erosion alone and from an area wider than the flushing channel itself.

Another sediment management technique is represented by dredging consisting in the excavation of material from beneath the water without interfering with normal impounding operation. Dredging is expensive, so it is often used to remove sediment from specific areas near dam intakes (Kondolf et al., 2014a). In hydraulic dredging the sediment is mixed with water and transported from the point of extraction to the point of placement as a sediment-water slurry. Dredged material can be discharged into a containment area or in the river downstream of the dam. Hydraulic dredging can efficiently handle material up to coarse sand (Morris and Fan, 1997).

During sediment flushing, as well as during hydraulic dredging carried out discharging sediment in the downstream river, the high sediment concentration in the sluiced waters could be detrimental for downstream freshwater ecosystems.

1.3 Downstream environmental impacts and sediment transport models

The most striking consequences of sediment flushing may be fish mortality (Baoligao et al. 2016) and severe habitat alterations such as pool-filling (Wohl and Rathburn, 2003). In particular, sediment flushing can deteriorate the quality of downstream water bodies by increasing sediment load and fine sediment deposition in reaches downstream of the dam, contravening national and international standards regarding ecological quality and stream habitats (e.g. Water Framework Directive -WFD- and Habitats Directive in the European Union -EU). Further problems can be connected to the polluting potential of the sediments to be flushed (Frémion et al., 2016; Peter et al., 2014).

In general, despite the antidegradation efforts pursued through water resources acts (e.g. the WFD in EU and the Clean Water Act in the USA), guidelines specifically setting standards for suspended and bedded sediments are still poorly developed (Bryce et al., 2010; Owens et al., 2005). This is the consequence of lacking adequate knowledge about the relationships between sediment pressures and ecological conditions of impacted freshwater ecosystems (Collins et al., 2011). Furthermore, existing thresholds for sediments, both routinely used and being tested, are generally unsuitable for flushing management. Examples such as the Total Maximum Daily Loads (TMDLs), established on a catchment-specific basis in the USA (Mukundan et al., 2012), usually refer to

perturbations due to agricultural practices and urbanization, that last longer and produce lower sediment input than sediment flushing through reservoirs. Similarly, suspended sediment/turbidity standards for coldwater aquatic habitat appear not adequate for managing sediment release from reservoirs (e.g. Crosa et al., 2010; Frémion et al., 2016). Controlling the sediment concentration during flushing operations (i.e. Controlled Sediment Flushing - CSF) may constitute a measure to minimize such adverse ecological effects (e.g. Espa et al., 2015; Peteuil et al., 2013). Quantitative aspects, such as the magnitude, frequency and duration of sediment releases, and the time of the year for the operations would ideally be specified after having assessed the potential environmental impacts, such as the sedimentation affecting fish and benthic macroinvertebrates (e.g. Wohl and Rathburn, 2003; Morris, 2014). Nevertheless, the reliability of sediment flushing is challenged by the uncertainties associated with the modelling of the system during the perturbation (i.e. sediment transport and riverbed scour and fill) as well as in relation to the ecological response (i.e. potential impacts on the biota and its recovery). Analogous perturbations are regularly experienced by river biota during floods where biota is adapted in terms of magnitude and timing; however, the flushing operations may add further and potentially heavier stress to the river environment. The assessment of the flushing impact is especially difficult in mountain streams, where hydraulic conditions and structure of the riverbed vary rapidly over short distances (Rathburn and Wohl, 2001). Furthermore, the control of the sediment load while flushing a reservoir is operationally challenging (e.g. Espa et al. 2015; Peteuil et al. 2013). As highlighted by Rathburn et al. (2013) in the case of a channel sedimentation event, the combination of site-specific field data and the comparison with data collected elsewhere are especially useful to understand whether the recovery potential of the fluvial system is sufficient to adapt to the disturbance. To assess this, sediment transport models play an important role in designing CSF, as they support the prediction of downstream changes.

Sediment transport below reservoirs desilted by flushing has so far received little attention, and only in the last years, research on reservoir desiltation has been focused on the downstream environmental effects of sediment flushing operations (Morris, 2014). Brandt and Swenning (1999) reported a detailed field investigation on the geomorphic effects of a 2-day free-flow flushing operation in the Cachí Reservoir in Costa Rica, where a suspended sediment load of over 850,000 t was measured, with suspended sediment concentration (SSC) peaks of up to 200 g/l. More recently, Liu et al. (2004a, b) reported on two free-flow flushing operations involving two dams in cascade: during the coordinated sediment flushing, very fine sediment (i.e., smaller than 0.02 mm in diameter) constituted the vast majority of the total load, and a SSC peak of 100 g/l was recorded. The authors simulated riverbed dynamics through a one-dimensional (1-D) model, achieving a good agreement between numerical data and field measurements of SSC and erosional/depositional patterns. Wohl

and Cenderelli (2000) presented the geomorphic effects of a reservoir sediment release on the downstream channel, where about 7000 t of silt and sand were deposited mostly in pools. In particular, the downstream displacement of the deposit during the following year was surveyed in the field and numerically investigated by 1-D sediment transport models (Rathburn and Wohl, 2001; 2003): the simulation of the pools' recovery highlighted the need of detailed field observations to support the reliable calibration of the models.

A wider bibliography is available concerning the application of numerical modeling to investigate sediment dynamics inside reservoirs. For instance, 1-D sediment transport models were employed to analyze sedimentation and desilting by flushing (Khosronejad, 2009; Ahn et al., 2013), with the main focus on predicting the efficiency of different operating rules. More refined three-dimensional (3-D) numerical models were also employed with analogous purposes (Gallerano and Cannata, 2011; Haun and Olsen, 2012a). In particular, the spatial distribution of erosional and depositional areas during free-flow flushing operations was investigated by 3-D numerical simulations at both the lab scale (Haun and Olsen, 2012b; Esmaeili et al., 2014) and the full scale (Haun and Olsen, 2012a; Esmaeili et al., 2015). Overall, these studies pointed out that modeling stability and erosion of cohesive sediment banks needs to be advanced to improve the performance of the 3-D models.

2 Objectives and structure of the thesis

The primary objectives of this thesis are the following:

1) To study how sediment release alter or modify sediment transport dynamics in the downstream river causing riverbed alteration,
2) To evaluate the ecological impacts of sediment release on benthic macroinvertebrate and fish,
3) To calibration a one-dimensional (1-D) sediment transport model of a monitored event to evaluate if the model can be used to forecast the sediment transport dynamics of future operations,
4) To discuss the CSFs performed in the last decade at reservoirs located in the Lake Como catchment (Figure 2.2).

The first two objectives are developed in the Chapter 3, 4 and 5, the third in the Chapter 2 and the last one in the Chapter 6 (Figure 2.1).

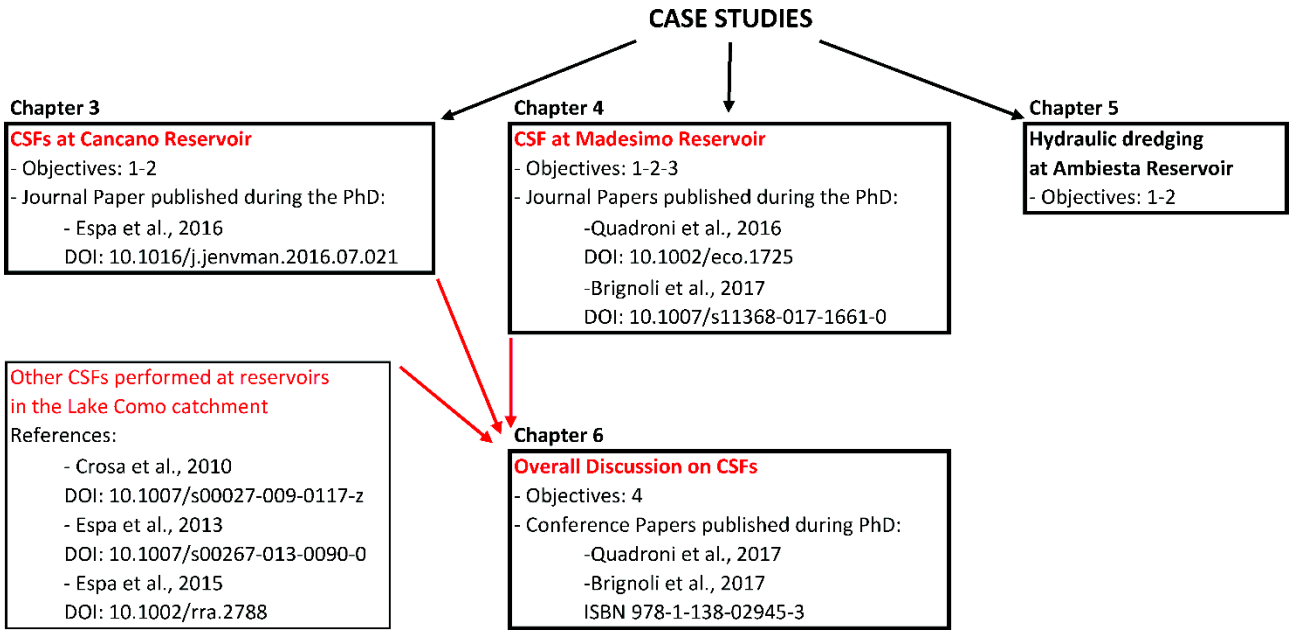

Figure 2.1. Structure of the thesis including main objectives, the papers published during the PhD and the other references used to develop the discussion of Chapter 6.

In the Chapter 3, 4 and 5, the following case studies are reported and discussed individually:

- CSFs at Cancano Reservoir (Valtellina, Lombardia Region, Italy, Figure 2.2),
- CSF at the Madesimo Reservoir (Valchiavenna, Lombardia Region, Italy, Figure 2.2),
- Hydraulic dredging at the Ambiesta Reservoir (Valle di Verzegnis, Friuli-Venezia Giulia Region, Italy, Figure 2.2).

The Chapter 6 provides an overall discussion of the CSFs including:

- The CSFs reported in Chapter 3 and 4,

- The CSFs at Valgrosina and Sernio reservoirs (Figure 2.2). Results related to these operations were previously published in Crosa et al. (2010), Espa et al. (2013;2015) (Figure 2.1)

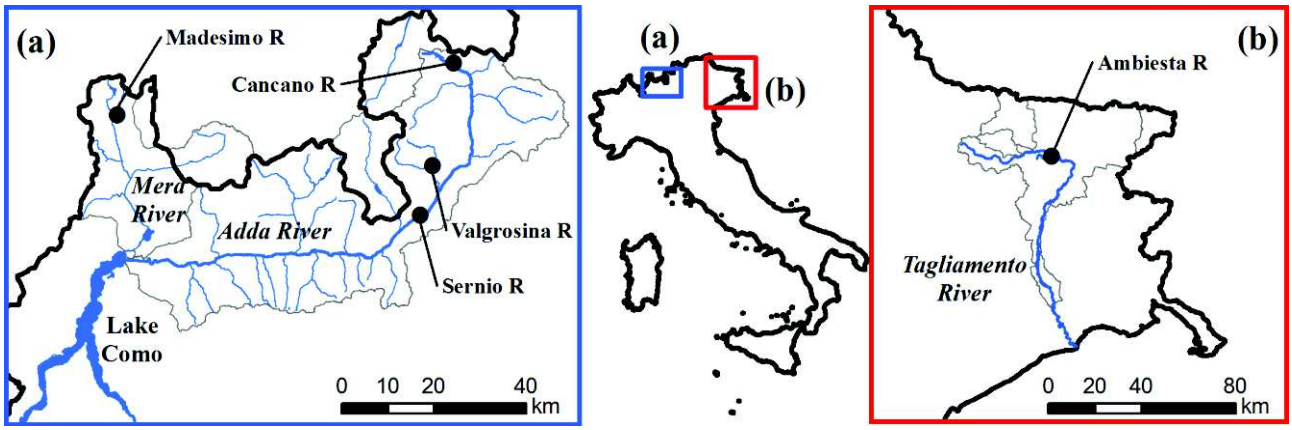

Figure 2.2. Study area. Investigated reservoirs (R) located (a) in the Lake Como catchment and (b) in the Tagliamento River basin.

Each chapter has been structured as a "paper format". For this reason, some repetition in the "Materials and Methods" sections could be observed.

The main points discussed in Chapter 6 are:

- Methods applied to plan and monitor the CSFs,
- Cost and efficiency of the CSFs in comparison with other reported in literature,
- Downstream riverbed alteration as a function of the grain size of the flushed sediment,
- Biological impacts of the CSFs (the short and long-term impacts on benthic macroinvertebrates and fish).

This chapter may provide useful indication for the planning of more eco-sustainable flushing operations developing a sound experience in the management of reservoir sediments. As stated previously, this experience has a key role:

- In preserving the current level of hydropower production ensuring intergenerational equity,
- In maintaining, and possibly upgrading, the ecological quality of downstream freshwater ecosystems,
- In reducing the downstream riverbed starvation,
- In dealing with the expected increase in reservoir sedimentation due to climate changes.

3 Controlled sediment flushing at Cancano Reservoir

This chapter reports on the controlled sediment flushing of the Cancano Reservoir, one of the largest in the Italian Alps. The main aim of the operation was to restore the proper functioning of the bottom outlet, severely buried by a silty deposit of over 15 m of thickness. The CSFs were carried out during low flow season (i.e. between February and April) due to technical constraints; the flushing was spread out over three years and, within each year, over a relatively long period (40-53 days).

3.1 Materials and methods

3.1.1 Study area and monitoring sites

The Cancano Reservoir (123×10^6 m^3) is located in Valtellina (Rhaetian Alps), Northern Italy (Figure 3.1). The Cancano Dam was closed in 1956; main elevation data of the project are as follows:

- - dam crest: 1,902 m above mean sea level (AMSL),
- - power intake: 1,806 m AMSL,
- - bottom outlet, a 1.2 m diameter steel pipe: 1,781 m AMSL.

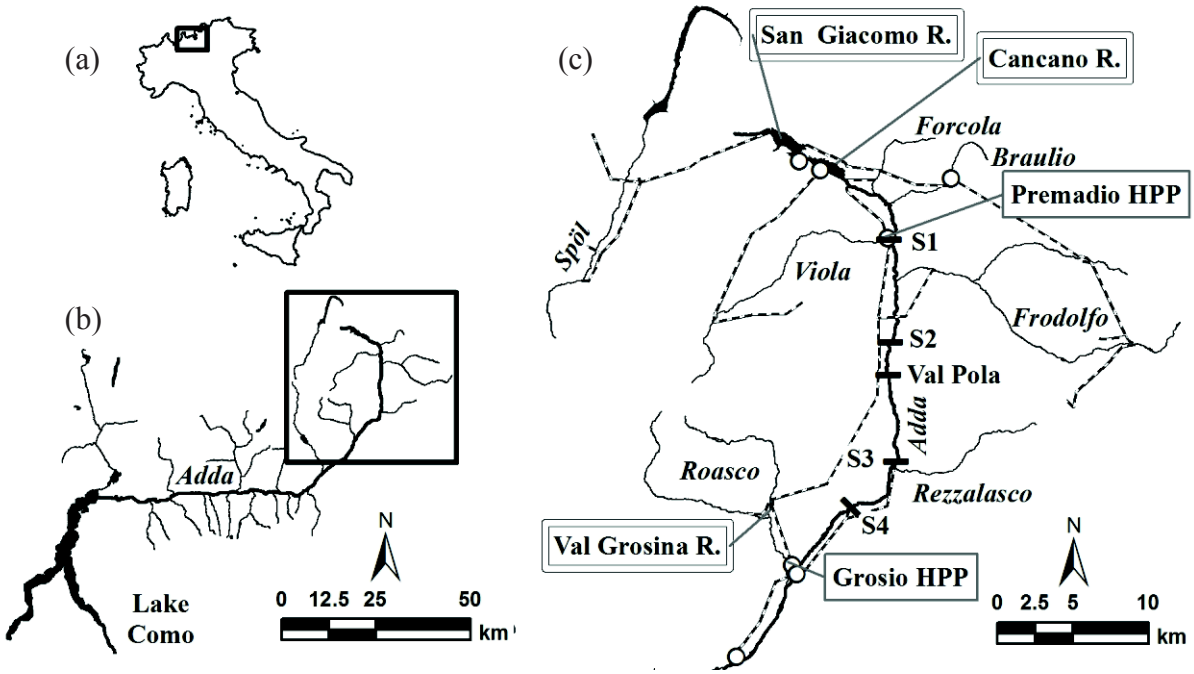

Figure 3.1.Study area. (a) Location in Italy and (b) in the Upper Adda River basin. (c) Main tributaries, water ducts (dashed lines), hydropower plants (HPPs e white circles), reservoirs (R.), and monitoring sites (S1- S4).

The dam impounds the Adda River, the main tributary of Lake Como, 9 km downstream of its springs and immediately downstream from the older San Giacomo Reservoir (64×10^6 m^3 - Figure 3.1). The catchment of the Adda River at Cancano Dam only has 20 km^2 area. Diversion of surrounding streams (Figure 3.1) increases the catchment area up to 370 km^2. More than two thirds

of this area (275 km^2) drain into the San Giacomo Reservoir through the connections to the Spöl, Frodolfo, Braulio, and Forcola streams. The Viola Stream (basin area 75 km^2) is directly channeled to the Cancano Reservoir.

This basin develops in a mountainous area (3769 m AMSL maximum elevation, 33 km^2 glacier covered) with minor anthropogenic activities. Natural runoff is driven by snowmelt, with maximum values in June-July and minimum in January-February.

The two mentioned reservoirs can store approximately 60% of the mean annual runoff of the total catchment area, providing seasonal water storage in the Upper Adda River basin, mainly for peak hydropower. The Cancano Reservoir supplies the Premadio Hydro-Power Plant (HPP) (226 MW installed capacity, 647 m effective head - Figure 3.1). Water discharged by the Premadio HPP is then conveyed to the small Valgrosina Reservoir (1.3×10^6 m^3) to supply the Grosio HPP (430 MW installed capacity, 600 m effective head), the largest in the area (Figure 3.1). From 2007 to 2012 heavy restoration works took place 17 km downstream from the Cancano Dam, in the river area which was affected by a huge rock avalanche mobilizing 34×10^6 m^3 of debris in July 1987. These works included the setting-up of an instream settling basin, hereafter referred to as the Val Pola Pond (Figure 3.2). The settling basin was enlarged during the study period, and its surface area ranged from about 35,000 m^2 in winter 2010 to about 55,000 m^2 in winter 2011 (final configuration).

Figure 3.2. The instream settling basin (the Val Pola Pond) looking upstream before the 2011 flushing event.

The monitored Adda reach develops for approximately 28 km downstream from the Cancano Dam. We displayed four sampling sites (S1, S2, S3, and S4 - Figure 3.1 and Figure 3.3, and Table 3.1) where the following measurements were carried out:

- - S1: Suspended sediment concentration (SSC), water discharge (Q), benthos,
- - S2: Q, benthos, trout,
- - S3: SSC, Q, benthos, trout,
- - S4: benthos.

In order to depict the spatial gradient of the perturbation, the sampling stations were approximately equally spaced, about 7 km; two of them (S1 and S2) were positioned upstream from the Val Pola Pond, and the remaining two (S3 and S4) downstream of the settling basin. Ease of access was also a key determinant in the selection of the sampling sections. Moreover, sites were mainly located close to hydropower intakes (S1, S3 and S4 - see Figure 3.1), where the flow is routinely measured and existing instream structures facilitated the installation and the operation of turbidimeters (S1 and S3).

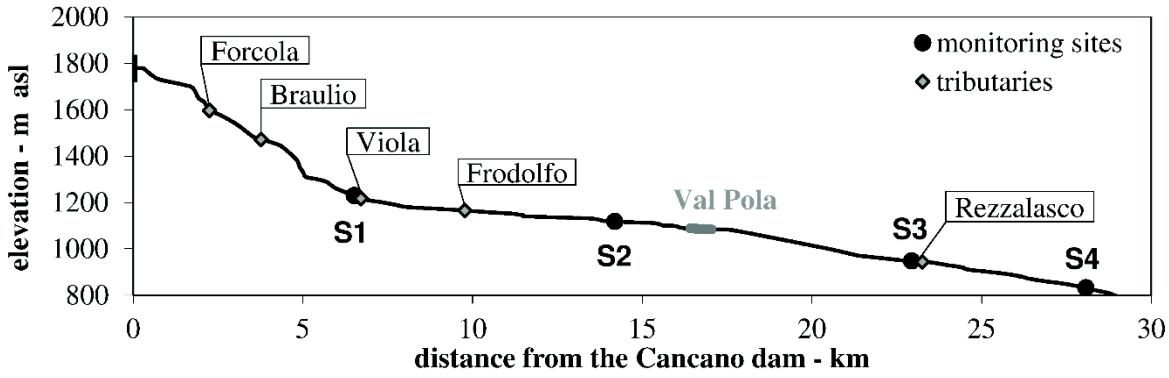

Figure 3.3. Elevation profile of the monitored Adda River stretch. The junctions with the main tributaries, the instream settling basin (the Val Pola Pond), and the monitoring sites (S1-S4) are also shown.

Monitoring sites	S1	S2	S3	S4
distance from dam - km	6.7	14.2	22.9	28.2
elevation - m	1216	1110	940	823
average gradient	0.034	0.011	0.025	0.038
natural basin - km^2	97.5	504.6	598.6	633.5
mean annual natural flow - m^3/s	2.5	12.6	15.0	16.5
minimum flow - m^3/s	0.15-0.25	0.85-1.2	0.90-1.5	0.99-1.6

Table 3.1.Main hydrological characteristics of the four monitoring sites (S1-S4) on the Adda River.

The Adda stretch between the Cancano Dam and S1 is mainly enclosed in a steep canyon with an average gradient of 0.085, which is not safely accessible for monitoring purposes. The river slope is not as extreme below S1, generally ranging between 0.01 and 0.02. The main tributaries, Viola and Frodolfo streams, join to the Adda River between S1 and S2 (Figure 3.1 and Figure 3.3). The monitored river reach displays substantial hydro-morphological alteration. The three mentioned

intakes interrupt its continuity, and the channel is mainly single-thread, incised, and frequently embanked. The mesohabitat is mostly composed of riffles approximately 15 m wide at low flow, with pools in correspondence with the several grade control structures. The bankfull width generally ranges between 20 and 50 m. The substrate is dominated by pebbles ($2 < d < 64$ mm) and cobbles ($64 < d < 256$ mm), with a non-negligible presence of boulders up to 500 mm in diameter.

Water flow is highly regulated as a consequence of massive hydropower development. The environmental flow prescribed by current law is a seasonally modulated Minimum Flow (MF). At least 6% of the natural Mean Annual Flow (MAF) is released downstream of diversions during the low-flow season, i.e. between November and April; during the remaining six months, MF is increased to 10% of the natural MAF (Table 3.1). In general, water discharge remains close to MF during the colder months. On the contrary, from late spring to autumn, because of snowmelt and/or rainfall, the streamflow frequently exceeds the MF in the analysed river reach: Quadroni et al. (2014) measured on average a doubled water discharge compared to MF at S2, S3 and S4.

3.1.2 Sediment flushing operations

The main purpose of the flushing operation was to remove the sediment deposit (approximately 15 m thick) that buried the bottom outlet of the Cancano Dam and begun to threaten the functioning of the power intake. The sediment deposit was fine-grained (about 80% silt and 20% clay), according to the removal of coarser fractions by de-sanding at higher elevation intakes and by settling in the San Giacomo Reservoir.

The flushing operation can be schematically divided into two main stages: in the first one, it was necessary to remove the deposit burying the bottom outlet; in the second one, it was possible to evacuate sediment through the bottom outlet. During the first stage, it was necessary to keep the area dry close to the upstream face of the dam in order to operate earth-moving equipment and mudpumps (Figure 3.4). The removed sediment was therefore moved to the power intake and by-passed downstream from the dam (Figure 3.5). The only possible season to perform such work was between winter and early spring, when seasonal storage is at a minimum and temperature is low enough to prevent abundant snowmelt. During the second stage, when sediment was flushed through the open bottom outlet, it was necessary as well to work in the same low-flow season due to the low capacity of the bottom outlet (Figure 3.5). Due to the limited water availability for transport and appropriate dilution of the evacuated sediment, the operation was spread out over three consecutive years (2010, 2011 and 2012) and, for each year, over a fairly long time period (40-50 days). Moreover, the works were difficult to carry out due to the low temperatures: the daily minimum temperature at the Cancano Dam during the flushing operations was on average -5°C.

Figure 3.4. The Cancano Reservoir during the 2010 flushing event: earth-moving equipment working close to the upstream face of the dam can be seen on the left side of the photograph, the power intake on the right side.

A limit on the SSC (average value per consecutive working period) was fixed using the simple predictive model by Newcombe and Jensen (1996). This model allows to relate the dose, SSC and duration of exposure, to the response, i.e. the effects on fish. These effects are provided through the severity of ill effect - SEV - an index ranging from 0 (no effects) to 14 (100% fish mortality). In particular, we adopted the regression coefficients indicated by Newcombe and Jensen (1996) for juvenile and adult Salmonids and sediment size in the range 0.5-250 mm (Group I). The limit was established downstream of the Val Pola Pond, where the SSC control seemed reasonably reliable. The SSC threshold of 3 g/l was fixed accounting for 40-50 days duration and accepting a SEV of 11, corresponding to a fish mortality of 20-40%. The continuous SSC measurements at S3 were used to verify the maintenance of this threshold. SSC monitoring was continuously carried out also at S1, mainly to control desilting works by mechanical equipment and to regulate upstream water diversion at intakes on tributary streams.

As an extreme measure to avoid intolerable SSC values (approximately above 50 g/l) in the monitored river reach, it was possible to divert the sluiced waters off-stream, conveying them to the Valgrosina Reservoir through the intake slightly downstream of S1. This alternative was particularly suitable to tackle the turning points of the flushing operation when the SSC was out of control; these events are referred to later on as critical phases.

Figure 3.5. (a) The bottom outlet of Cancano Reservoir and (b) the River Adda just downstream of the dam during the 2012 flushing operation.

3.1.3 Sediment monitoring

Optical turbidimeters (Lange Controller SC100®) were installed to continuously gauge SSC at S1 and S3. The SSC measurements were carried out only during the flushing operations. Samples for a posteriori calibration of the raw turbidimeter output were randomly collected during daytime, as close as possible to the probe position, with one liter buckets (n = 294 at S1 and n = 223 at S3). The SSC of these samples was measured in the lab using the Standard Method 2540 D-F (APHA et al., 2005). The raw SSC data (SSC_{TUR}) were correlated to the corresponding lab data (SSC_{LAB}) and linear functions, one per year per station, were obtained through standard least-squares fitting (Figure 3.6). The raw SSC was finally corrected adopting the mentioned linear functions. The agreement between the two measures was generally good and determination coefficients (R^2) ranged between 0.81 and 0.93. The lab-analyzed samples were also used to estimate the time history of SSC in the infrequent occasions when the turbidimeters were out of scale (50 g/l at S1 and 25 g/l at S3).

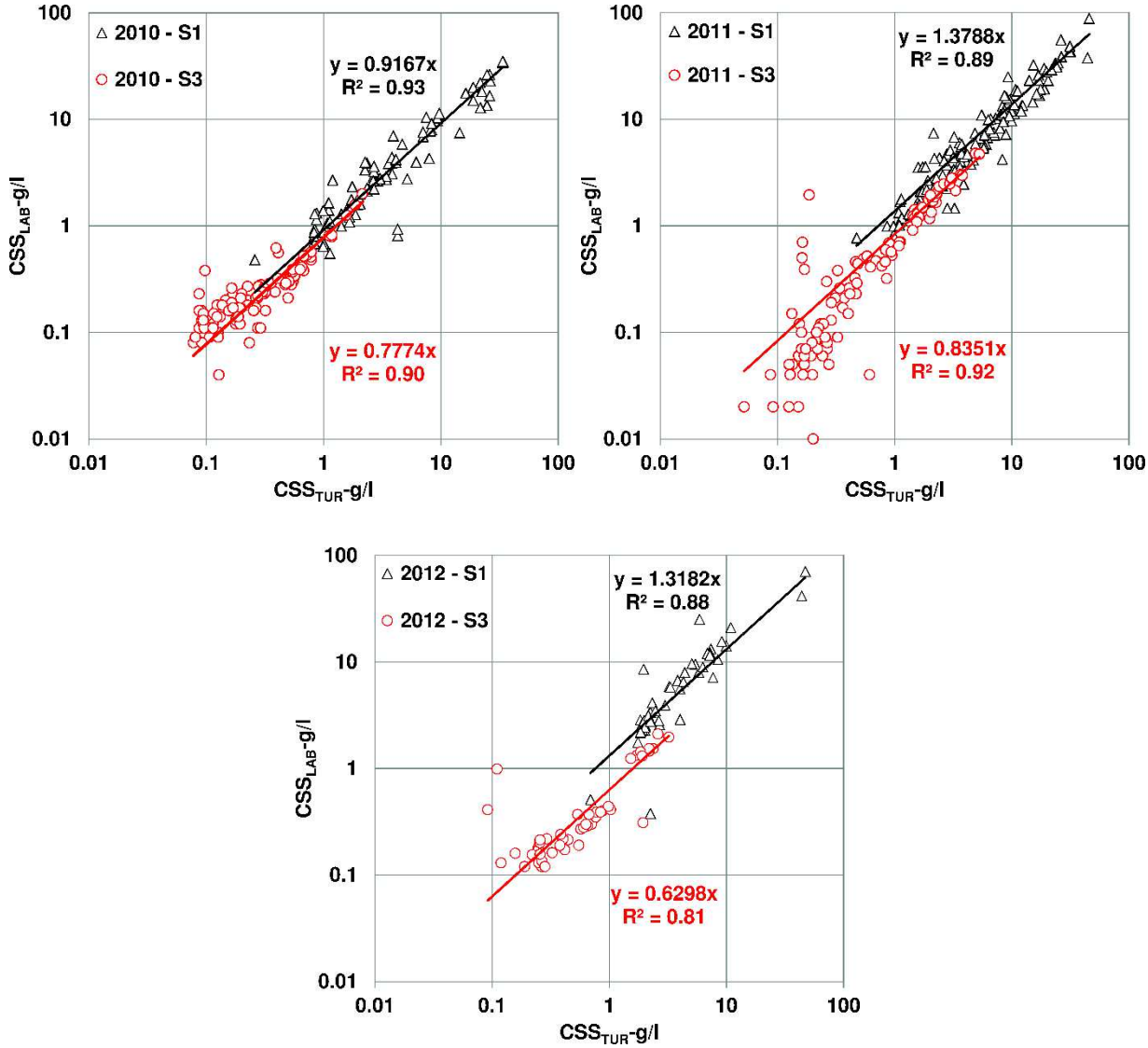

Figure 3.6. Calibration curve for the turbidimeter installed at S1 and S3 using the samples collected during the three sediment flushing operations: raw SSC data acquired in the field (SSC_{TUR}) were correlated to the corresponding laboratory samples (SSC_{LAB}) using linear functions.

Sediment mass flowed through S1 and S3 was computed by time integration of the product between SSC and Q. At S2, where no SSC measurements were carried out, SSC averaged on each flushing event was estimated by mass conservation between S1 and S2, neglecting deposition between the two measurement stations. At S4, SSC was considered equal to S3, accounting for negligible deposition between the two reaches and negligible difference in water discharge (Table 3.1).

The monitored Adda reach was surveyed by visual inspection to roughly check the pattern of sediment deposition after each flushing event; in 2011, the riverbed alteration was also measured in selected transects. Pre-flushing sampling was performed one month before the 2011 operation; post-flushing sampling was carried out at one and nine months after the same event. The whole campaign was performed in low-flow conditions, i.e. with discharge close to MF. The investigation was

conducted between S1 and the Val Pola Pond, i.e. in the river reach where maximum deposition was expected. In particular, the four following transects were monitored:

- - S1A (0.5 km downstream of S1, average slope 0.023, wetted width 14.8 m),
- - S1B (2.5 km downstream of S1, average slope 0.008, wetted width 7.5 m),
- - S2A (close to S2, average slope 0.007, wetted width 12.7 m),
- - S2B (0.6 km downstream of S2, average slope 0.007, wetted width 15.3 m).

Each transect was sampled in three points, two about one meter from the river edge and one in its centre. The content of fine sediment in the uppermost layer of the riverbed was detected through a resuspension technique according to Rex and Carmichael (2002). A McNeil corer with a 135 mm internal diameter tube was used to collect one liter samples of turbid water. All samples were dry-sieved, analysed for the content in silt/clay and then extrapolated to the riverbed after measurement of the water depth, and therefore of the water volume, in the corer tube. An essentially analogous technique was adopted to assess the in-channel fine sediment storage in the Isábena River catchment (NE Iberian Peninsula), which experiences naturally large fine sediment loads as a result of the presence of highly erodible badland formations (Buendia et al., 2013a, 2014).

3.1.4 Benthic macroinvertebrate monitoring

The invertebrate survey was carried out seasonally, from winter 2009 to winter 2013, at the four monitoring sites. The samples were collected with a Surber sampler of 0.1 m^2 area and 500 mm mesh, following the quantitative multi-habitat protocol developed for the computation of the multi-metric index STAR_ICMi. STAR_ICMi is the current Italian normative index, recently developed for WFD inter-calibration purposes. It is ranked into five quality classes (bad, poor, moderate, good, and high), set at 0.24, 0.48, 0.71, and 0.95 respectively (see Espa et al., 2015 for additional detail). According to current Italian law, the quality class assigned to a river reach depends on the annual mean of the STAR_ICMi seasonal values. Total density and two traditional metrics employed to calculate STAR-ICMi (total number of families, and Shannon-Wiener index) were analysed as well.

Temporal and spatial differences in the values of the benthos metrics (i.e. intra-annual differences at each monitoring site and inter-site differences within the same year) were detected through the Kruskal-Wallis test (XLSTAT 2011 software). Invertebrate data collected in 2009, when no flushing works were carried out, were used as reference conditions.

3.1.5 Trout monitoring

Brown trout sampling was carried out in spring and autumn, from 2009 to 2012, at S2 and S3. A removal method with two passes was performed adopting a backpack electrofishing device (ELT60-IIGI 1.3 kW DC, 400/600 V). Trout were counted and measured for total length. Density

was calculated taking into account the sampled area (0.14 ha at S2 and 0.12 ha at S3). As well as for macroinvertebrate, 2009 data were used as reference conditions.

At both monitoring sites, fishing is allowed from March to October with constraints on the minimum size (24 cm at S2 and 30 cm at S3) and maximum number of caught fish (5 per day). Adults are introduced to be fished from March to October; juveniles (Mediterranean stock 50-120 mm) are introduced for stocking, mainly in summer.

3.2 Results

3.2.1 Sediment flushing operations and sediment monitoring

The flushing operations were carried out for 46 days in 2010 (from March 9 to April 24), for 53 days in 2011 (from February 18 to April 11), and for 40 days in 2012 (from February 13 to March 23).

As mentioned in Section 3.1.2, during the first stage of the flushing, the bottom outlet remained closed, since it was obstructed by a thick silt deposit. This stage lasted throughout the first flushing year (2010) and most of the second one (2011). Earth-moving equipment and mud-pumps were employed during daytime to dislodge the silt deposit and to bypass it downstream of the dam. This activity allowed to properly control SSC in the outflow. The SSC pattern detected downstream showed regular daily pulses in response to the dislodging works, while Q varied only slightly. At S1, SSC peaked 10-30 g/l during daytime, dropping to 1-2 g/l during night-time. Q usually ranged from less than 1-2 m^3/s, i.e. 5 to 10 times the MF. At the downstream station S3, Q usually ranged from 3 to 5 m^3/s (about 3-5 times the MF), and SSC was usually over one order of magnitude lower than at S1. An example is provided in Figure 3.7.

46 days after the beginning of the 2011 operation, the silt deposit was cleared sufficiently to allow the opening of the bottom outlet. This gave rise to the second stage of the work, i.e. free-flow sediment flushing through the bottom outlet. After the opening of the bottom outlet, for the entire last week of the 2011 flushing, the SSC control proved to be much more difficult than before. In fact, a noticeable increase in the temperature (daily maximum up to 15°C at the Cancano Dam), determined the significant increase of the runoff in the Cancano Reservoir. Combined to the recently opening of the bottom outlet, this flow increase determined the significant raise of both SSC of the sluiced water and mass of evacuated sediment (Figure 3.7). SSC at S1 averaged 20.1 g/l during the last six days of the 2011 flushing. The same average measured during the previous 46 days was 6.3 g/l. Similarly, almost 65% of the sediment mass flowed through S1 during the 2011 flushing pertains to the last six days, corresponding to an increase of the daily rates from about 550 to 7,600 tons evacuated sediment per day. The SSC at S1 averaged on the whole 2011 working period, approximately 8 g/l, was affected

by this increase, and was the largest if compared to 2010 and 2012 operations (Table 2). During the first day after the opening of the bottom outlet, it was necessary to divert the sluiced waters out of the Adda River. In this occasion, about 5,000-6,000 tons of sediment were conveyed into the Valgrosina Reservoir, thus contributing to a reduction of the SSC peak from approximately 70 g/l at S1 to 6 g/l at S3 (Figure 3.7 and Figure 3.8, Table 3.2).

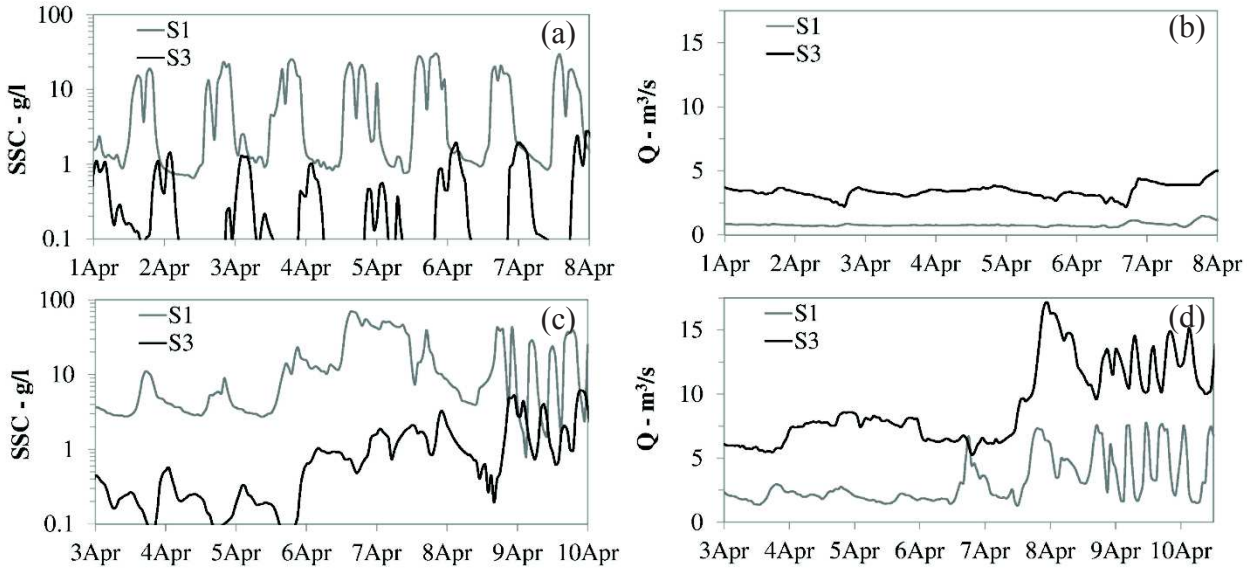

Figure 3.7. Examples of time histories of hourly averaged SSC and streamflow at S1 and S3. (a) (b)During the ordinary flushing control, from April 1 to 7, 2010. (c) (d) During the critical phase following the opening of the bottom outlet and the simultaneous temperature increase in the study area, from April 3 to 9, 2011.

Also at the start of the 2012 flushing it was difficult to control the SSC downstream of the Cancano Dam. In particular, during the final emptying of the reservoir through its bottom outlet, the silt content of the evacuated water was so high that the absolute maximum SSC was measured at both S1 and S3 (Figure 3.8 and Table 3.2). This critical phase had a short duration of less than one day, and off-stream diversion was deemed unnecessary. After that episode, the SSC was satisfactorily controlled for the entire 2012 operation. Both SSC and Q measured at S1 and S3 were comparable to those recorded in 2010 and 2011 before the bottom outlet was opened. Nevertheless, at S3, SSC averaged 0.8 g/l for all of the 2012 flushing, a value almost three times larger than the corresponding ones of 2010 and 2011 (Table 3.2), but still considerably lower than the threshold of 3 g/l fixed before the works.

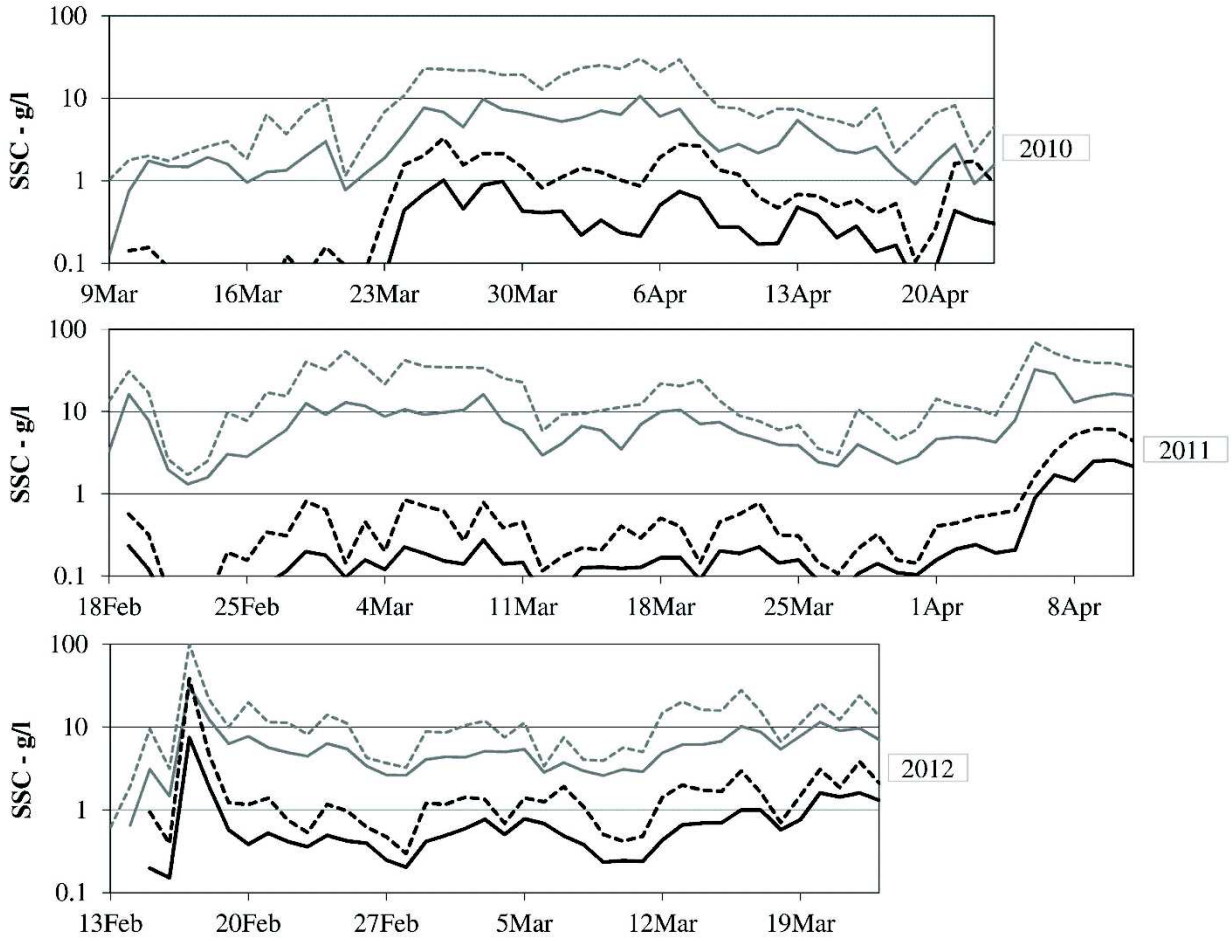

Figure 3.8. Time histories of daily averaged SSC (continuous lines) and maximum hourly SSC (dashed lines) at S1 (gray) and S3 (black) for the three documented flushing events in 2010, 2011 and 2012.

Year	duration day	Sampling site	SSC_{AVE} g/l	SSC_{MAX} g/l	Q_{AVE} m^3/s	M_{AVE} t/day	M_{TOT} t	$M_{SED, S1-S3}$ %
2010	46	S1	3.5	30.2	1.0	320	14620	69
		S2	1.2		2.8			
		S3	0.3	3.3	3.4	100	4,570	
2011	53	S1	7.9	68.9	1.3	1360	70920	79 (*)
		S2	3.1		3.4			
		S3	0.3	6.1	4.8	250	13940	
2012	40	S1	5.9	99.2	0.9	650	26060	54
		S2	2.0		2.8			
		S3	0.8	38.2	3.4	300	12090	

(*) Calculated subtracting the amount of sediment diverted off-stream (ca. 5000-6000 t).

Table 3.2. SSC and streamflow values for the three documented flushing operations. At S1 and S3: average SSC (SSC_{AVE}), maximum SSC (SSC_{MAX}), average Q (Q_{AVE}), average daily flowed mass (M_{AVE}), total flowed mass (M_{TOT}), and percentage of mass deposited in the river reach between S1 and S3 ($M_{SED, S1-S3}$). At S2, where only Q measurement was carried out, SSC_{AVE} was estimated by multiplying SSC_{AVE} at S1 for the ratio between Q_{AVE} at S1 and S2.

3.2.2 Estimates of sediment deposition

A total amount of 110,000 tons of fine-grained sediment flowed through S1 during the flushing of the Cancano Reservoir. About 25% of this sediment mass was detected at S3 in the same period, thus giving average deposition between S1 and S3 of about 75%, at least in the course of the flushing. Comparing the three consecutive years of flushing, a certain variability of the computed percentage deposition can be noticed (Table 3.2).

By far, sediment removal was larger in 2011, when 71,000 tons of sediment flowed through S1 and about 14,000 tons were detected at S3 (Table 3.2). Indeed, riverbed alteration due to flushing was evaluated in this occasion.

Our visual surveys downstream of the Val Pola Pond led us to exclude significant sediment deposition in that river reach. Upstream of the Val Pola Pond, occasional silt deposits of 10-20 cm maximum thickness were found. They were typically located outside of the riverbed wetted by the MF, presumably in areas characterized by slow flow during the flushing. Furthermore, in some low gradient stretches, the riverbed wetted by the MF was covered by a few millimeters thick silt veneer.

Quantitative riverbed sampling in the reach between S1 and the Val Pola Pond (Table 3.3) highlights a moderate increase of the silt/clay fraction, ranging from 0.5 to 1 kg/m^2 as transect average. Nine months after the 2011 flushing, when the second post-event sampling took place, the content of fine-grained sediment was comparable to the pre-flushing one in three of the four investigated transects.

section	silt/clay content - kg/m^2			average difference - kg/m^2	
	Pre	Post1	Post2	Post1-Pre	Post2-Pre
S1A	0.28	2.00	0.05	0.81	-0.44
	1.00	0.95	0.13		
	0.43	1.18	0.20		
S1B	0.19	1.22	0.09	1.08	-0.18
	0.26	1.35	0.04		
	0.24	1.34	0.02		
S2A (*)	-	-	-	0.90	-0.02
	0.60	2.95	0.08		
	0.88	0.32	1.35		
S2B	1.30	1.31	2.63	0.45	0.51
	0.28	0.46	0.88		
	0.82	1.97	0.41		
mean	0.57	1.37	0.54	0.83	-0.03

(*) One of the two points close to the river edge was not sampled due to the high water-level.

Table 3.3. Silt/clay content in the uppermost layer of the riverbed of the four monitored river sections. Pre, Post1 and Post2 indicate the sampling respectively carried out one month before, one month after, and nine months after the 2011 flushing event. For each transect the sampling point located in the centre of the river is reported in the central row.

3.2.3 Benthic macroinvertebrate monitoring

Results of macroinvertebrate survey are provided in Figure 3.9 and Table 3.4.

In 2009, i.e. during the reference year, STAR_ICMi was on average good at all the monitoring sites. Furthermore, a general trend to decrease STAR_ICMi quality as well as density, richness (N families), and diversity (Shannon-Wiener), was noticed in summer/autumn samples if compared to the winter/spring ones. Inter-site differences were not statistically significant for all the considered metrics (Kruskal-Wallis, $p > 0.05$), and the macroinvertebrate communities were mainly composed of the same insect taxa: the Plecoptera Leuctra, the Ephemeroptera Baetis, the Trichoptera Limnephilidae and Rhyacophilidae, and the Diptera Chironomidae, Limoniidae and Simuliidae.

year	season	S1		S2		S3		S4	
		sample	average	sample	average	sample	average	sample	average
2009	winter	-	-	0.86	0.83	1.00	0.85	0.94	0.79
	spring	-		0.92		0.95		0.89	
	summer	-		0.79		0.80		0.62	
	autumn	-		0.75		0.64		0.73	
2010	winter	0.84	0.81	0.79	0.67	0.75	0.74	0.67	0.74
	spring	0.82		0.57		0.92		0.68	
	summer	0.78		0.57		0.72		0.59	
	autumn	-		0.77		0.59		1.02	
2011	winter	0.81	0.66	0.77	0.69	0.88	0.83	0.86	0.81
	spring	0.66		0.60		0.79		0.87	
	summer	0.46		0.75		0.74		0.70	
	autumn	0.70		0.65		0.91		0.84	
2012	winter	0.89	0.74	-	0.74	0.78	0.67	0.89	0.75
	spring	0.77		0.65		0.75		0.77	
	summer	0.63		0.74		0.64		0.68	
	autumn	0.66		0.83		0.52		0.66	
2013	winter	0.95	-	0.73	-	0.70	-	0.61	-

Table 3.4. Seasonal and annual average STAR_ICMi from winter 2009 to winter 2013 at monitoring reaches S1-S4. Quality classes (poor, moderate, good, and high) are bounded at 0.24, 0.48, 0.71, and 0.95, and are respectively evidenced in orange, yellow, green, and blue. Data are not available in 2009 and in autumn 2010 at S1, in winter 2012 at S2. STAR_ICMi annual average is not available in 2009 at S1, and was calculated using only three values in 2010 at S1 and in 2012 at S2.

During the three flushing years, STAR_ICMi quality was generally lower, dropping to averagely moderate at S1 in 2011, at S2 in 2010 and 2011, at S3 in 2012. Comparing the post-flushing sampling (spring) to the corresponding pre-flushing one done in winter, the more noticeable drops in quality were detected at S2 in 2010, at S1 and S2 in 2011. Furthermore, remarkable density decrease, up to 5-10 times, was observed after flushing at all the monitoring sites. Finally, the tendency of STAR_ICMi to decrease during summer/autumn was also ascertained during the flushing years, in a similar way to what was reported in 2009.

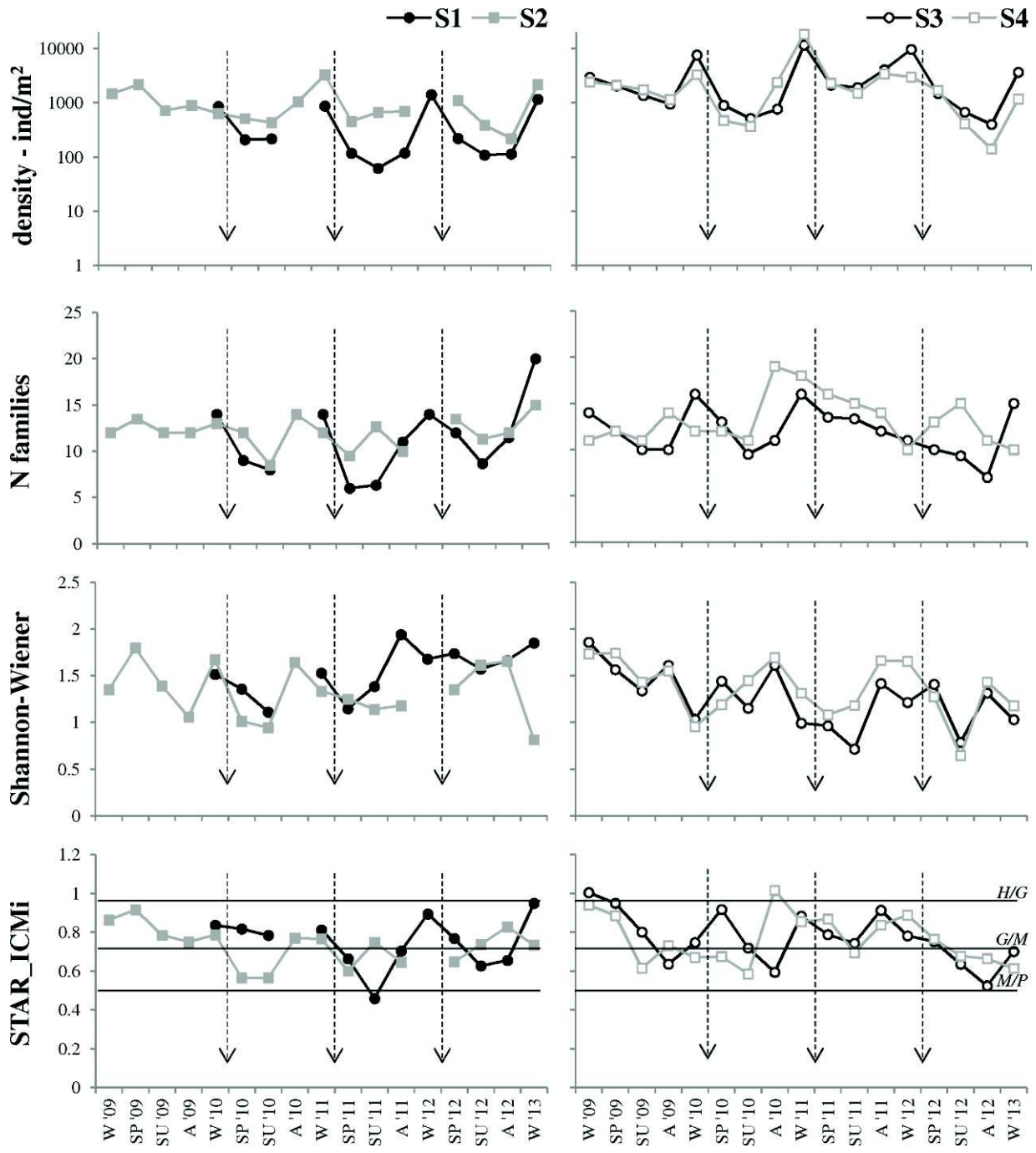

Figure 3.9. Total density, total number of families, Shannon-Wiener and STAR_ICMi index from 2009 (reference year) to winter 2013 at S1-S4. The dashed arrows indicate the flushing events. Data are not available in 2009 and in autumn 2010 at S1, and in winter 2012 at S2.

The lowest STAR_ICMi score (0.46 - poor status), density (62 ind/m^2), and richness (6 families) were recorded at S1 in summer 2011, after the heaviest flushing took place. In the same year, spatial differences in both density and richness were statistically significant (Kruskal-Wallis, $p < 0.05$). Accordingly, the quality at the sites upstream and downstream of the Val Pola Pond was markedly different, being the status of S1 and S2 on average moderate while the one of S3 and S4 good.

Nevertheless, for all the considered metrics and for each monitoring site, inter-annual differences were not significant (Kruskal-Wallis, $p > 0.05$), and no taxa loss or addition was detected at all the sampling sites during the whole study period.

3.2.4 Trout monitoring

Available data concerning trout population are displayed in Figure 3.10 and Table 3.5. Typically, a bimodal distribution of the length structure was detected, allowing differentiating juveniles (0+ and 1+ fish) from adults according to the threshold of about 170 mm.

Overall density was mostly in the range 400-600 ind/ha at both the investigated reaches for the entire study period. In certain samplings, the number of juveniles and their percentage appear low, particularly at S3 in spring 2012 (percentage juveniles below 20%).

In 2010, 2011, and 2012, spring samples can be considered post-flushing samples, as they were collected within two months after the end of the works. At S2, both the overall density (400-500 ind/ha) and the length distribution (60% below 170 mm, 40% above 170 mm) remained approximately constant and comparable to the spring values of the reference year. Similarly, at S3, the total density was approximately stable in spring (around 500 ind/ha with the only exception of 2010 spring), but a significant change of length distribution was observed, with a decrease of juveniles from 75% in 2009 to less than 20% in 2012.

Comparing the post-flushing sample (spring 2010, 2011, 2012) to the previous one (respectively autumn 2009, 2010, 2011), a noticeable decrease of the overall density after each flushing at both monitoring reaches can be ascertained. This density drop range from about 15% at S3 in 2012 to 50% at S2 in 2010. After the 2010 flushing, the density drop estimated as previously mentioned is nearly equal at S2 and S3, both in terms of total density (about 50%) and juveniles density (about 60%). After the 2011 flushing, a total density drop of 35% was measured at S2, but it was due to a noticeable decrease of adults (about 60%), with the juveniles approximately stable. At S3, after the same flushing event, the density drop was even larger (approximately 50%), and also in this case, adult fish (60% decrease) resulted more affected than juvenile group (25% drop). Conversely, at S3 after the 2012 flushing, an overall density drop of about 15% can be evaluated, with juveniles (70% drop) markedly more affected than adults (30% increase).

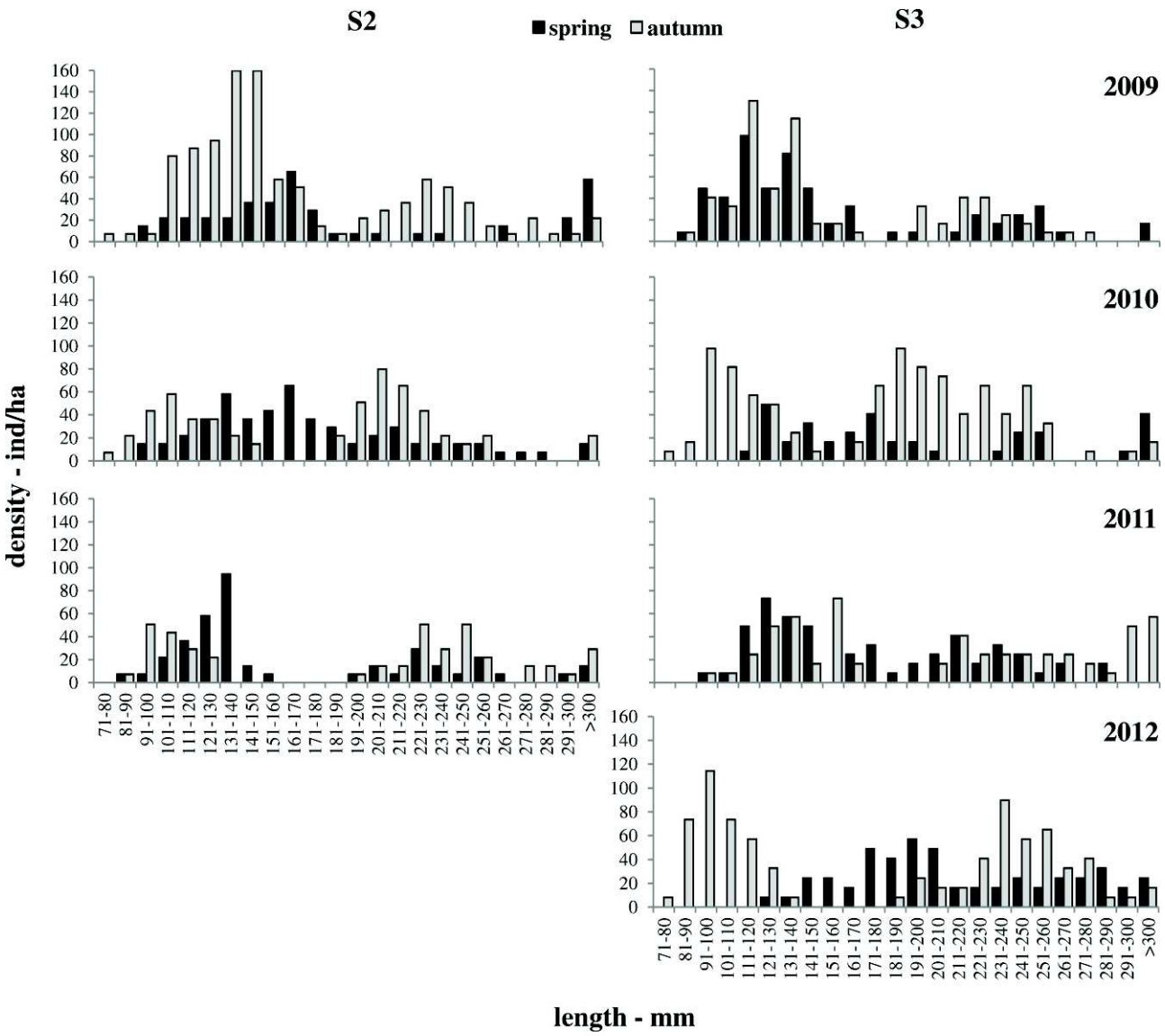

Figure 3.10. Length structure of the brown trout populations at S2 and S3 from spring 2009 to autumn 2012. Data are not available in 2012 at S2.

Year	Season	S2			S3		
		Density	≤170 mm	>170 mm	Density	≤170 mm	>170 mm
2009	Spring	399	60	40	571	74	26
	Autumn	1045	68	32	612	68	32
2010	Spring	515	56	44	335	44	56
	Autumn	581	41	59	955	38	62
2011	Spring	378	65	35	506	53	47
	Autumn	407	38	63	563	45	55
2012	Spring	-	-	-	490	17	83
	Autumn	-	-	-	792	46	54

Table 3.5. Brown trout data at S2 and S3 from 2009 (reference year) to 2012. Percentage of individuals above and below 170 mm in length is provided along with total density. Data are not available in 2012 at S2.

3.3 Discussion

3.3.1 Sediment monitoring and management consideration

This chapter focuses on the sediment flushing works aimed at restoring the functioning of the bottom outlet of the 120 × 10^6 m^3 Cancano Reservoir, one of the largest in the Italian Alps. The flushing operations were carried out in the cold season, but no reasonable alternative seemed possible, due to the peculiarities of the project, particularly the large storage and the small size of the bottom outlet. In several cases, the management of reservoir sedimentation through flushing can be prevented by the lack of bottom outlets of a suitable size. The past engineering practice, in fact, considered the reservoirs as infrastructures with a limited economic life, usually determined by sedimentation, and no sediment management strategies were commonly taken into account. For example, the Sanmenxia Dam on the Yellow River, China, had to be deeply retrofit to improve the sediment-releasing capacity of the bottom outlet structures (Wang et al., 2005).

On the whole, despite the several difficulties met during the desilting works, a satisfactory control of the SSC was achieved: SSC at S3 was maintained significantly below the threshold of 3 g/l, both in terms of average value per flushing event, and, nearly always, in terms of daily average (Figure 3.8).

In particular, SSC control was good for the large majority of the flushing period (approximately 140 days on a total of 150 days). On these days, the typical time pattern of SSC was the periodic alternation between high values due to daytime desilting works and low values due to night-time interruption of the works. Analogous pulses are reported in Espa et al. (2013).

The same degree of SSC control was not possible at the end of the 2011 flushing and at the beginning of the 2012 one. We measured the highest SSCs and the largest mass fluxes through both S1 and S3 during these critical phases. The management, the possible prediction, and the planning of appropriate strategies to deal with such critical phases may represent key aspects of sediment flushing projects, particularly if environmental constrains have to be accounted for. For example, a sharp increase of SSC at the start of free-flow flushing operations, i.e. when bottom outlet structures are opened, can be generally expected (Crosa et al., 2010; Morris and Fan, 1997). Diverting the evacuated water off-stream when SSC cannot be adequately controlled (as it was done in one of the last days of the 2011 flushing) is clearly an extreme action that, if feasible, can be of help, but shifts the problem elsewhere (in the Valgrosina Reservoir in our example).

SSC reduction between S1 and S3 - and consequently the approach of the SSC target at S3 - was achieved by managing both water flow in the regulated tributaries and sediment deposition. In our case study, sediment deposition along the investigated reach would seem marginal. Even if this

result is mostly supported by qualitative evidence (i.e. visual inspection) rather than by detailed riverbed sampling, which was performed only on a few transects, it appears congruent with the small size of the flushed sediment and with the relatively high channel slope. Conversely, the Val Pola Pond played a key role in reducing downstream SSC. The trapping efficiency of the Val Pola Pond can be estimated in 70-80% through the classical USBR formula (Vanoni, 1975) adopting the following input data:

- - 35,000-55,000 m^2 surface area,
- - 3-15 m^3/s inflow and
- - 20% clay (d = 2 μm), 80% silt (d = 31 μm) sediment size distribution.

The sediment mass flowed through S1 and S3 during each investigated flushing allowed to compute deposition ratios ranging from 55 to 80% (Table 3.2), which roughly match the previous trapping efficiencies. The smaller measured deposition ratio concerns the 2012 event, when no off-stream diversion took place at very high SSC and, presumably, the pond was partly filled due to the previous year flushing. Sediment trapped in an instream basin is generally expected to be scoured and transported downstream during subsequent flood events. Alternatively, Morris and Fan (1997) proposed to trap sediment in an off-stream settling basin: in this case, the sediment has to be removed for restoring the basin capacity, thus increasing the cost of the operation.

On average, the cost of the sediment removal at Cancano Reservoir may be estimated in about 45 €/m^3 (50 US$/$m^3$), taking into account both the loss of hydropower at Premadio and Grosio HPPs and the expenses connected to mechanical excavation and maintenance of the working site. The loss of hydropower accounted for about 85% of the sediment removal cost. The cost per unit evacuated volume estimated for the Cancano Reservoir flushing is on top of the range reported for controlled free-flow flushing works in the Adda River basin (5-50 €/m^3, Espa et al., 2013) and it is also comparable to the maximum value (50 US$/$m^3$) for dry excavation by conventional earth-moving equipment in Los Angeles County reported by Morris and Fan (1997). In contrast, sediment flushing is generally considered a rather cheap option for desilting reservoirs (Morris and Fan, 1997). For instance, the unit cost sustained in 2012 for the controlled sediment flushing of the 53 × 10^6 m^3 Genissiat Reservoir (Rhone River, France - Kondolf et al., 2014a; Peteuil et al., 2013) was about 4 € per ton, even though a huge staff was engaged to manage and survey the operation, and only a half of the estimated cost of the operation was due to the hydropower loss. Nevertheless, sediment flushing at Cancano reservoir was expensive and technically difficult. However, it is likely that alternative strategies comprising sediment removal (either by dry excavation or dredging), transport (either by track or piping), and proper disposal would have been far more costly: in fact, great difficulties in transport and in finding suitable disposal sites are typically expected in high-mountain areas. Anyway,

when approaching reservoirs desiltation in a framework of improvement of the overall sustainability, different sediment management alternatives would have to be quantitatively compared: MCDA (Multi-Criteria Decision Analysis) and analogous tools, satisfactorily experimented in the dredging industry (Manap and Voulvoulis, 2014, 2015), could provide the necessary basic framework.

3.3.2 Effects on benthos

Detectable impact (i.e. drift increase) of the sediment load on macroinvertebrate communities may occur at SSC in the order of few hundred mg/l (García Molinos and Donohue, 2011) and sediment deposits of few kg/m^2 (Larsen and Ormerod, 2010; Larsen et al., 2011). Fine sediment infiltration in coarser riverbed substrates revealed key influence on invertebrate also in undisturbed catchments, being assemblages detected in sediment-rich locations relatively poor in density and diversity (Buendia et al., 2013a, 2014).

Impairment of benthos was therefore expected after the flushing operations, especially in the river reach upstream of the instream settling basin. Furthermore, as will be recalled in the following with more detail, noticeable effects of flushing fine sediments were measured on benthic assemblages in the same area (Espa et al., 2013). Like most of the benthic communities found in regulated Alpine watercourses (Espa et al., 2013, 2015; Monaghan et al., 2005; Yoshimura et al., 2006), the particular ones collected in the four monitoring reaches were composed of few resilient taxa, typically subjected to seasonal contraction during the high-flow period.

Sampled data were expected to show:

- - a spatial gradient of the impact, proportionally to SSC that was larger at the upstream reaches,
- - a difference, at least on the short-term impact, between the three operations, since the 2011 CSF was heavier upstream of the Val Pola Pond, and the 2012 flushing was heavier downstream of the Val Pola Pond,
- - a possible cumulative effect, i.e. a progressive decline of the benthic community in the course of the three years of flushing.

These basic hypotheses appear partly confirmed, even if the available data as a whole do not seem consistent with a progressive depletion of the benthic assemblage.

At S1, clear evidence of benthic community impairment due to the flushing operations were recorded. The contraction of the macroinvertebrate community in terms of density, richness and quality was detected after each flushing event. The benthic contraction connected to the seasonal flow increase seems to superimpose on the flushing disturbance: in all the three years of sediment flushing, STAR_ICMi was lower in summer than in spring, i.e. immediately after flushing. Furthermore, as expected, the most severe impact was detected after the 2011 event, characterized by the highest average SSC. Nevertheless, the macroinvertebrate community showed a high resilience and recovered

to the pre-CSF condition within the year, reaching good status in all the winter samples. Comparable density and richness reductions and similar recovery patterns were recorded after four flushing events at the previously mentioned Valgrosina Reservoir (Espa et al., 2013); in that case the duration of each flushing was significantly shorter (two weeks), and the average SSC of ca. 3-5 g/l was smaller if compared to the one at S1. A similar response to a larger dose might suggest an asymptotic behavior, i.e. an analogous response of the benthic assemblage once certain thresholds of SSC and/or duration of the operation are exceeded. The comparable recovery can be justified in both cases by moderate sediment deposition and good water quality. Conversely, a longer recovery time was observed in the Scalcoggia River severely aggraded after a sediment flushing operation, where sand deposition was in the order of hundreds of kg/m^2 (see Section 4.3.1.4).

In the downstream monitoring reaches, after each flushing event, a non-taxon-specific and relatively short-term density reduction occurred as well, but the response of the macroinvertebrates to the flushing disturbance is not as clear as at S1, and the superposition of further pressures cannot be ruled out. For example, at S2 a quality drop of one class was measured after all the three flushing, but no evident difference between 2010 and 2011 was noticed.

Downstream of the Val Pola Pond, at sampling reaches S3 and S4, the macroinvertebrate data are quite similar, according to nearly equal SSC perturbation. The status of the benthic community maintained averagely good after the 2010 and the 2011 flushing events, characterized by the same averaged SSC. A more pronounced sensitivity of the benthic assemblage to the flushing perturbation was noticed after the 2012 event, when average SSC measured at S3 was approximately triple than in the previous years, even if smaller in comparison to S1 and S2. On the other hand, starting from summer 2012, STAR_ICMi dropped to moderate at both S3 and S4, up to winter 2013. A possible explanation could be found in the release of sediment stored in the Val Pola Pond after flow increase. However, our SSC measurements, concerning only the periods when flushing was carried out, prevent from supporting such a hypothesis.

3.3.3 Effects on trout

A recent meta-analysis on the effects of sediments on a variety of biological endpoints for lotic fish (Chapman et al., 2014) supports the general consensus that sediments in both suspended and deposited forms have negative consequences on fish feeding behaviour and embryo development and survival; whereas, fish abundance was not found to be significantly associated with sedimentation. Michel et al. (2013) suggest to consider possible adaptive responses of the Salmonid fish to fine sediment pulses (maximum SSC tested of 5 g/l and maximum exposure of 24 days).

The trout response to the flushing disturbance could be analysed under the same hypotheses formulated for the benthos: variability of the impact according to the spatial gradient and the

magnitude of the flushing disturbance, possible cumulative effects. A heavier impact on juveniles could also be expected, along with an impairment of natural reproduction since in the present case study the flushing season overlaps with the period of more marked sensitivity of trout to enhanced fine sediment loads (Kemp et al., 2011), i.e. the incubation stage (over winter in the study area).

In particular, according to the Newcombe and Jensen (1996) (N&J) model, SEVs of about 11 and 10 can be calculated for each flushing at S2 and S3, thus giving trout mortality in the ranges 20-40% and 0-20% respectively. Substantial agreement with the N&J model was found in a reach unaltered by stocking/fishing by Espa et al. (2013): the authors measured trout density reduction of 2-52% after flushing events with 10-11 SEV, recording heavier impact on juveniles.

On one hand, fish data would seem to support a relatively moderate impact of the flushing on the trout population. For example, trout populations sampled at S2 and S3 did not change significantly in overall density for the whole study period. The measured values, mostly in the range 400-600 ind/ha, are considered poor/moderate for Alpine watercourses below 1500 m elevation (OFEFP, 2004), and are comparable to those detected in other regulated Alpine rivers (Ortlepp and Mürle, 2003; Unfer et al., 2011).

Moreover, at both sampling reaches, overall density measured in spring remained approximately constant and similar to the reference year value. It is worth noting that the spring sample is reasonably less influenced by summer stocking than the autumn one and that, in the three years when flushing was carried out, the spring sampling may be considered as a post-event one.

On the other hand, a noticeable decrease of the overall density after each flushing at both monitoring sites can be deduced after comparison of the pre-CSF sample (autumn 2009, 2010, 2011) to the post-CSF one (spring 2010, 2011, 2012). Interestingly, the total density decreases evaluated as mentioned range from about 15% at S3 in 2012 to 50% at S2 in 2010, showing good agreement with trout mortality estimated through the N&J model. Nevertheless, the previous hypotheses concerning a spatial gradient of the impact, its proportionality to the flushing magnitude, and a more severe impairment of juveniles are not fully confirmed. For example, after the 2010 flushing, a nearly equal density drop was noticed at S2 and S3. After the 2011 flushing, the total density drop was larger at S3 than at S2, and, at both stations, it followed the significant decrease of the adults number while the juveniles resulted only slightly perturbed, particularly at S2.

The forcing of stocking and fishing seems therefore to hide the effect of the flushing on the trout population, thus preventing detailed quantitative analysis. It could be concluded that the whole fish dataset seems inconsistent with a remarkable alteration of the trout population, at least within the limits where the usual practices of stocking and game fishing were carried on during the study period.

4 Controlled sediment flushing at Madesimo Reservoir

This chapter reports on the sediment transport and the in-channel sedimentation after a CSF performed from a small hydropower reservoir in the central Italian Alps. This operation was performed during three days in the mean flow season. After a short description on the main characteristics of this particular CSF, the main findings related to sediment transport and riverbed sedimentation (obtained in a 3.6 km reach below the dam before, during, and after the desilting operation) were reported. A 1-D sediment transport model was implemented for the investigated CSF event. Moreover, the results of the biomonitoring on macroinvertebrates and fish were discussed.

4.1 Materials and methods

4.1.1 Study area and monitoring sites

The Madesimo Dam regulates the Scalcoggia River. The dam is located 6.4 km downstream from the river's main spring and 1.6 km upstream from the confluence with the Liro River (Figure 4.1). Approximately 14 km downstream from this confluence, the Liro joints the Mera River, in turn the second largest tributary of Lago di Como. The Madesimo is a concrete gravity dam and it was closed in 1964. The dam crest is at 1,526 m AMSL. The bottom outlet is equipped with a square vertical-lift gate that has a side length of 2.6 m and a sill at 1,509 m AMSL. The original gross and effective storage capacity of the reservoir were 0.161×10^6 m^3 and 0.126×10^6 m^3, respectively. At the catchment scale, it can be considered a relatively small reservoir: for comparison, the Spluga and Isolato reservoirs, which are also shown in Figure 4.1, store 33 and 1.8×10^6 m^3, respectively. The pre-flushing reservoir bathymetry, carried out in July 2010, indicated a historic loss of storage capacity of about 46,000 m^3. According to the estimates provided by the company managing hydropower in the area, the average annual rate of storage loss at Madesimo reservoir is about 1.6%, a high value if compared to surrounding reservoirs (i.e. 0.17% and 0.30% for Spluga and Isolato). Sediment trapped in the Madesimo Reservoir is mostly silt and sand, as it will be later described. Water resources in the area are massively exploited for hydropower generation. The Madesimo Reservoir supplies water to the Isolato-Madesimo hydropower plant (17 MW installed capacity, 8 m^3/s rated discharge - hereafter Q). This plant and the Isolato- Spluga hydropower plant (43 MW installed capacity, 7 m^3/s rated Q) drains into the Isolato Reservoir. In turn, the Isolato Reservoir supplies water to the Prestone hydropower plant (25 MW installed capacity, 18 m^3/s rated Q) that releases water into the Prestone Reservoir (0.06×10^6 m^3) (Figure 4.1).

The basin of the Scalcoggia River at the Madesimo Reservoir has an area of 25.2 km^2 with an altitude ranging from 1,500 to 3,200 m AMSL. The land is mostly covered by forest and scarcely

vegetated rocks, with 2% of urbanized area. The basin runoff is essentially snowmelt driven, with the maximum Q normally observed between late spring and early summer. Mean annual Q at the Madesimo Dam is 1.3 m^3/s. The basin area of the Liro River at the Isolato Dam is 55.3 km^2, with a mean annual Q of 3 m^3/s. Further downstream, at the Prestone Dam, the catchment area and the mean annual Q of the Liro River are 126.5 km^2 and 6.4 m^3/s, respectively. A minimum flow that equates 7.6 and 12.9% of the mean annual Q is currently set downstream of the Madesimo and the Isolato dams.

The Scalcoggia River downstream of the Madesimo dam can be divided in three parts: the upper one is 1.1 km long, followed by a 180 m drop and a final stretch of about 350 m (Figure 4.2). The channel is very steep with 2-5 m bankfull width; it has bedrock morphology and step-pool mesohabitat. According to field observations and following the Udden-Wentworth scale, the substrate is dominated by cobbles (64< d<256 mm), with a non negligible presence of boulders up to 1,000 mm in diameter.

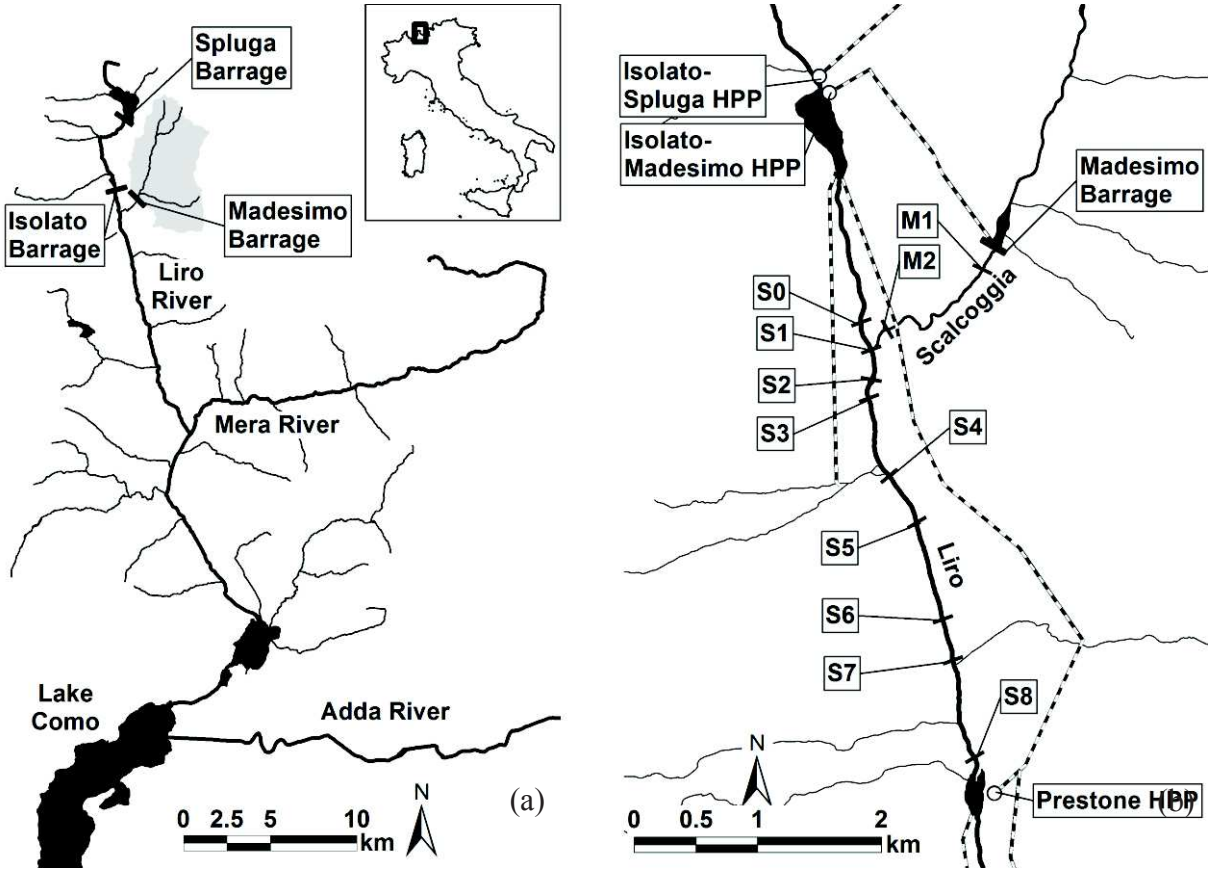

Figure 4.1. Location map. (a) Position in the Northern Italy and catchment area of the Scalcoggia River at the Madesimo Dam. (b) Monitoring sites and hydropower system with main channelling (white and black lines) and hydropower plants (HPPs, white circles).

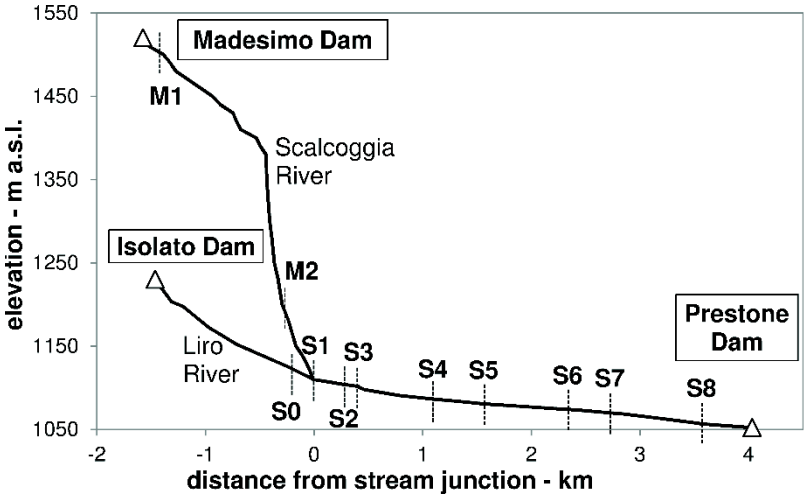

station id.	sampling
M1	GR, benthos
M2	GR
S0	benthos, fish
S1	GR
S2	GR, McNeil
S3	GR
S4	GR
S5-up	GR
S5-down	GR, SSC, grain size of suspended sediment
S6	GR, McNeil
S7	GR
S8	GR, McNeil, SSC, grain size of suspended sediment, benthos, fish

Figure 4.2. Longitudinal elevation profile of Liro and Scalcoggia rivers showing the measurement sites (M1, M2 and from S0 to S8) and dams. Field surveys performed at each site are specified to the right (i.e. deposit thickness measurements with graduated rod -GR, McNeil samples, SSC measurements, collection of suspended sediment to characterize the grain-size, benthic and fish sampling)

The Liro River between the Isolato dam and the Prestone Reservoir is 5.6 km long (Figure 4.2) with an average bankfull width of 10-20 m. The substrate is dominated by cobbles (64<d<256 mm) with sporadic areas where pebbles (2<d<64 mm) are predominant; boulders up to 500 mm in diameter are also present. The Liro River between Isolato dam and the Scalcoggia confluence has a step-pool morphology; from the stream junction to the Prestone Reservoir, the channel is 3.6 km long (see Section 4.1.3) and develops a plane-bed morphology (as per Montgomery and Buffington, 1997).

4.1.2 The 2010 Controlled Sediment Flushing - CSF

Planning and execution of the 2010 CSF were strongly conditioned by the limits imposed by the local Authorities to mitigate the downstream environmental impacts. These limits concerned the duration of the operation (i.e. max. 3 days) and the maximum SSC acceptable in the Liro River downstream from the Scalcoggia confluence. The maximum SSC was set at 10 g/l as the average value permitted during the whole operation. This value was based on an estimation of the likely CSF effects on the trout community in this stream. This estimate was derived from the N&J model, as reported and discussed by Espa et al. (2013) and in the Section 3.1.2 for other CSF in the same area. The target evacuation volume of sediment (ca. 15,000 m^3) and the freshwater volume (2-2.5 × 10^6 m^3) allocated in the upstream reservoirs (e.g. Spluga and Isolato, see Figure 4.1) were the variables used to keep the SSC within the limits (i.e. to transport and dilute the sediment load in the Liro River).

The second half of October was selected as the most adequate period to balance technical and environmental requirements and to keep the system under control i.e. accounting for water availability in the upstream reservoirs and preserving the safety use of earth moving equipment within the reservoir. The CSF was carried out after the full drawdown of the reservoir. Mechanical equipment

was employed to dislodge the sediments and discharge them into the flushing channel. Excavation was performed only during daytime, while during the night water entering the reservoir was left free to flow into the flushing channel and released downstream without mechanically incrementing the sediment load. Clear water released from the Isolato Reservoir was maximum during the daytime (i.e. up to ca. 10 times higher than Q flushed from Madesimo Reservoir), and it was reduced during the night (i.e. ca. 3 times higher).

4.1.3 Sediment monitoring

Eight and two monitoring sites (Figure 4.1 and Figure 4.2) were surveyed along the Liro and Scalcoggia River, respectively; the measurements carried out in each site are indicated in Figure 4.2. Sites were selected accounting mainly for variation in channel slope and ease of access.

Monitoring sections	Distance (km)	Slopes (m/m)	Thickness (mean, m)	Thickness (SD, m)
M1	-1.5	0.123	0.240	0.103
M2	-0.24	0.340	0.149	0.064
S1	0	0.021	0.008	0.008
S2	0.28	0.021	0.009	0.007
S3	0.41	0.017	0.043	0.013
S4	1.1	0.013	0.056	0.017
S5 up	1.55	0.010	0.203	0.066
S5 down	1.57	0.009	0.040	0.018
S6	2.34	0.008	0.053	0.025
S7	2.73	0.012	0.019	0.007
S8	3.56	0.017	0.010	0.007

Table 4.1. Distance, mean channel slope and thickness of sediment deposits after the CSF at each monitoring sections. The distances of the monitored sections are given from the stream junction of the rivers Liro and Scalcoggia; the mean channel slope of the monitored reaches is computed by the thalweg elevations of the two surrounding topographic sections; mean and standard deviation (SD) of the sediment thickness are computed from 10 graduated rod measurements.

The topographic survey between S1 and S8 comprises sixteen cross sections, approximately 250 m spaced; the exact distances and the mean slopes are reported in Table 4.1. Downstream from S3 the channel displays substantial morphologic alteration due to alignments and embankments. At S5 there is a bridge with an approximately horizontal sill that created a backwater effect during the CSF.

Data collected during the CSF included measurements of Q, SSC and dissolved oxygen (DO). Q downstream of the Isolato Reservoir was recorded every 5 minutes, and the same was done for the inflow into the Madesimo Reservoir. Downstream, at S5, SSC and DO was continuously recorded, by means of an optical turbidimeter (Lange Controller SC100®) installed in one of the pillars of the bridge (see Figure 4.1 for location details). The turbidimeter was set to record 5-min average samples with 3 Hz sampling frequency. Further downstream, turbidity measurements were conducted at S8

by means of a portable turbidimeter (Partech 740®), only during daytime. The aim of this was to verify the likely downstream reduction of SSC due to in-channel deposition; there, SSC records were also taken at 5-min interval. Water and sediment samples for a posteriori calibration of the turbidimeters were collected as close as possible to the probes by means of 1-liter handheld buckets. Samples were randomly taken during daytime. Overall, 35 samples were collected in S5 and 37 in S8. The sediment concentration of these samples was determined in the laboratory following the Standard Method 2540 D-F (APHA et al., 2005). The raw turbidimeter data (SSC_{TUR}) were correlated with the corresponding values obtained in the laboratory (SSC_{LAB}), and at-a-site specific calibration power functions ($SSC_{LAB} = a \times SSC_{TUR}^{b}$) were obtained through standard least-squares fitting. The raw SSCs values detected in the field were then corrected using these statistical functions. Once the full SSC records were compiled, the suspended sediment load was computed by time integration of SSC measured at S5 times the flow rate calculated as a sum of Q from the Madesimo and the Isolato reservoirs. In particular, the water flow gauged at the Isolato Reservoir was routed to S5 by simply adding a constant time shift (30 minutes, based on the average flow velocity until the confluence). The flow released from the Madesimo Reservoir did not change significantly in the course of the CSF, thus, a constant value of $Q = 1.4$ m^3/s was used.

Additional samples were collected in S5 and S8 to determine the grain-size of the suspended load (i.e. in this work we express this as a daily average). The same procedure described in Espa et al. (2013) was adopted. One litre samples were collected during daytime at a rate of 6 per hour. The turbid water was poured into an Imhoff cone and allowed to settle for one hour. The clear supernatant was then discarded while the remaining sediment and water were stored in a bucket. These samples were analysed in the laboratory by dry sieving and gravitational settling.

Data from turbidimeters is considered representative of the total sediment concentration for the silt/clay fraction, whose presence in the riverbed deposits was negligible (see Section 4.2.1.2). Therefore, SSC measurements and suspended sediment sampling were basically employed for the quantification of the silt/clay fraction of the sediment transported during the CSF.

The total amount of flushed sediment was assessed through ADCP bathymetric surveys in the reservoir carried out before (July 2010) and after (November 2010) the CSF. In order to quantify the volume of sediment deposited along the study reach and its spatial variability, we visually inspected the sites and performed volumetric riverbed sampling three weeks before (on September 29th, 2010) and three weeks after (November 12th) the CSF. The volumetric riverbed sampling was performed in S2, S6 and S8 (Figure 4.2) to examine the alteration of the substrate (i.e. fine sediment infilling) after the CSF. In order to normalize the measurements between sections only the riverbed wetted by the minimum flow (i.e. $Q = 0.4$ m^3/s) was investigated. Each transect was sampled at three points,

two of them one meter from the channel edges and one in the centre. In the post-CSF survey, care was taken to sample the riverbed in the same points as we did in the pre-CSF campaign; this was achieved using a known distance from previously marked points. Sampling was carried out by means of a McNeil corer (McNeil and Ahnell, 1964; Lambert and Walling, 1988) with a 135 mm internal diameter tube. Water depth at the sampling points ranged from 0.1 to 0.3 m. Particles larger than 32 mm (i.e. very coarse gravel and even larger) were taken out before sampling the fines in order to limit bias caused by large clasts (as per Evans and Wilcox, 2014). The collected samples were dried and sieved in the laboratory. Each sample weighed ca. 1.5 kg. As indicated by Rex and Carmichael (2002), to take the finer materials into account, one litre of turbid water was also collected after the removal of core samples, keeping the corer firmly placed on the streambed and stirring up suspendable sediment within the tube, trying to keep the same level of agitation in all the samples. Samples were also dried and sieved in the laboratory, analysed for SSC and grain-size, and then extrapolated to the corresponding water volume measured in the tube. For each grain-size class, the computed sediment mass was added to the corresponding core sample in order to obtain the complete grain-size distribution.

The thickness of fine sediment freshly deposited on top of the coarse surface layer after the CSF was determined using a graduated iron rod. At each transect (Figure 4.2), the height of the sediment was measured at 10 randomly selected points. At S5, these measurements were performed upstream and downstream from the bridge (S5-up and S5-down, respectively). The average deposit thickness and the standard deviation (SD) of the 10 measurements were computed for each site. The observation error was estimated at ± 1 cm. The volume of deposited sediment related on each stretch (i.e. identified by two succeeding transects), was estimated assuming that the deposition changed linearly and adopting the average wetted widths. For the Liro River, these channel widths, ranging from 13 to 29 m, were derived from a steady state flow simulation adopting the mean Q observed during the CSF (i.e. 11 m^3/s - modelling details are reported in the Section 4.1.5). The total sedimentation volume was then obtained by adding the volumes estimated in each reach. On the other hand, the estimation of the volume of sediment deposited along the Scalcoggia River was performed with a simpler procedure adopting the average value of channel widths (i.e. 3 m); altogether, allowing to construct the budget between the released and the deposited sediments.

4.1.4 Biomonitoring

The biological survey was carried out at three biomonitoring sites (BSs): M1 on the Scalcoggia River, and S0 and S8 on the Liro River (Figure 4.1). These BSs were selected to assess the effects of the maximum (M1) and reduced (S8) sediment disturbance, and those of the diluting flows (S0). The site S0 is upstream the Scalcoggia confluence; it is characterized by an average slope of 0.055.

Routine water quality analyses performed by the local environmental protection agency ruled out any significant organic pollution at BSs. These analyses were carried out monthly, from 2009 to 2011, and did not include the flushing period. According to these analyses, SSC was usually less than 10 mg/l and DO ranged between 8 and 13 mg/l.

4.1.4.1 Benthic macroinvertebrate monitoring

The benthic macroinvertebrate survey was carried out seasonally (i.e. on February, May, September and November) at S0 and S8, from 2009 to 2011 (overall 12 samples per site), to characterize the assemblages before the CSF and to assess the recolonization patterns. A different schedule was adopted at M1, where one pre-CSF (one month before the event) and five post-CSF (respectively 1, 4, 5, 8 and 11months after the event) sampling campaigns were conducted. Samples were collected with a Surber sampler of 0.1 m^2 area and 500 μm mesh following the quantitative multi-habitat protocol developed for the computation of the multi-metric STAR_ICMi (see Section 3.1.4). The total density and three traditional metrics employed to calculate the STAR_ICMi [total number of families, number of Ephemeroptera, Plecoptera and Trichoptera families (EPT) and Shannon–Wiener index] were analysed as well. Temporal and spatial differences in the values of the benthos metrics (i.e. pre-CSF/post-CSF differences at each BS and between BSs, inter-annual differences at each BS and inter-site differences within the same monitored year) were investigated using the Kruskal–Wallis test. The Bray–Curtis index (BCi) was used to quantify the compositional dissimilarity between samples. It ranges from 0 to 1, with 0 being complete similarity and 1 being complete dissimilarity. To track the flushing response, the BC distances were represented in a two-dimensional ordination space using a non-metric multidimensional scaling (NMDS). M1 assemblages were not included in the NMDS, as they were too dissimilar from those collected at S0 and S8. Finally, the analyses of similarities (ANOSIM) was used to test the macroinvertebrate assemblages for significant differences between pre-CSF and post-CSF samples within the same BS and between BSs, between different years at each BS and between BSs within the same monitored year. The Kruskal–Wallis test, BCi computation and NMDS were performed by XLSTAT 2011 software, and the ANOSIM was carried out with PAST 3.09 software.

4.1.4.2 Fish monitoring

Fish sampling was performed annually (in autumn) at S0 and S8, from 2009 to 2011, using a backpack electrofishing device (ELT60-IIGI 1.3kW DC, 400/600 V, removal method with two passes). Fish were identified to species level, counted and measured for total length. Population densities were calculated taking into account the sampled area (641 and 1,333 m^2 at S0 and S8, respectively). The length structures of the most abundant populations were depicted. There are different rules for recreational fishing in the investigated sites of the Liro River. In particular, at S0

fishing is allowed from March to October, with constraints on the size (for brown trout – Salmo trutta trutta – 240 mm) and number of individuals that can be fished (max. five specimens per day). Fishing is forbidden at S8. Brown trout juveniles (Mediterranean stock 50–120 mm) are restocked every summer in the investigated Liro River.

4.1.5 Numerical simulation

4.1.5.1 The model

The 1-D model applied to simulate sediment transport and deposition during the CSF was the SRH-1D v.3.0 (Sedimentation and River Hydraulics - One Dimensional; Huang and Greimann, 2012). This model is habitually used by the US Bureau of Reclamation to simulate flows and sediment transport in river networks (e.g. Huang and Greimann, 2012; Ruark et al., 2011). The model can also be applied to examine sedimentation in reservoirs, thus providing alternative sediment management options. For instance, Morris (2014) reported the application of SRH-1D for predicting the pattern of sediment deposition inside the Peligre Reservoir (Haiti) under different operating rules. SRH-1D can simulate, within the limits of the 1-D approximation, sediment transport in natural rivers similar to those which occurred during the studied CSF (i.e. unsteady sediment transport, unsteady flow with possible transition between sub and super-critical flow).

The model uses a single depth-averaged advection-diffusion equation to simulate transport of total load of multiple size fractions. The sediment transport mode (suspended or bed load) is determined as a function of the Rouse coefficient Z (Greimann et al., 2008):

$$Z = \frac{w_f}{k\, u^*}$$

where w_f = particle fall velocity, k = von Kármán constant and u* = shear stress.

Particles smaller than 62.5 μm in diameter (i.e. silt and clay) are defined as cohesive sediment and they are handled differently from larger ones (i.e. non-cohesive sediments). For non-cohesive sediments, the appropriate formula to calculate the sediment transport capacity has to be selected by the user (as indicated by Huang and Greimann, 2012). The model takes into account the non-equilibrium transport by incorporating an "adaptation length" (L_{tot}) that quantifies the travel distance required for a packet of sediment for reaching a new equilibrium concentration, when it moves from one reach to another characterized by different shear stress. The adaptation length is computed according to Greimann et al. (2008). Three user-defined parameters control L_{tot} i.e. the suspended sediment recovery factor for deposition and for scour (α_d and α_e, respectively) (Han and He, 1990; Ahn and Yang, 2015), and the bedload adaptation length coefficient (b_L) (Huang and Greimann 2012) (Table 4.2). L_{tot} is computed as:

$$L_{tot} = (1 - f)\,(b_L\,h)\; + f\left(\frac{Q}{\alpha\,W\,w_f}\right)$$

where f = fraction of the suspended load related to the total load, h = average depth at the cross section, Q = flow rate and W = width of the cross section. In particular, SRH-1D assumes that the suspended sediment recovery factor is constant, but different values are used for α_d and α_e, and the program automatically selects the correct one (Huang and Greimann, 2012). For cohesive sediments, two kinds of erosion (i.e. surface and mass erosion) and deposition (i.e. full and partial deposition) are simulated. The bottom shear stress is compared to critical values in order to select which of them may occur. The equations used in model deposition are the Krone's (1962) full deposition formula and the van Rijn (1993) partial deposition formula. The model applies a modified version of the formula reported by Partheniades (1965) for surface erosion; the mass erosion equation is similar to that used for surface erosion (Huang and Greimann, 2012).

Name	Symbol	Default	Benchmark	Range	Ref.	Process/Quality
Suspended sediment recovery factor for deposition	α_d	0.25	0.25	0.05-1	b, f	Total adaptation length (L_{tot})
Suspended sediment recovery factor for scour	α_e	1	1	0.05-1	b, f	
Bedload adaptation lenght coefficient	b_L	0	0	0-10	c	
Active layer thickness multiplier	nalt	2	0.55	0.5-2	e	Bed material mixing
Weight of bedload fractions	χ	-	0	0-1	c, d	
Manning's parameter (s $m^{-1/3}$)	n	-	0.04	0.03-	4	Riverbed

Table 4.2. Parameters examined in the sensitivity analysis. Starting left, columns respectively report the name of the parameter, the adopted symbol, the default value, the value in the benchmark simulation, the investigated range, the main references, and the process/quantity controlled. In the references column, a = Arcement and Schneider 1989; b = Han and He 1990; c = Lai and Greimann 2011; d = Ruark et al. 2011; e = Huang and Greimann 2012; f = Ahn and Yang 2015

Bed material mixing is modelled by dividing the bed into an active layer and a series of underlying inactive layers; erosion and deposition of sediment can occur only from the active layer (Figure 4.3). The active layer thickness is determined as the product of a length scale related to the riverbed sediment size (i.e. the geometric mean of the minimum and maximum sizes of the coarsest size class), and a user-defined dimensionless parameter (i.e. the active layer thickness multiplier, hereafter referred to as *nalt*, Table 4.2). As part of the bed material mixing module, the user must also specify the weight of bedload fractions (χ, Table 4.2), which is a parameter that controls the weighing

of the bedload grain-size distribution during the transfer of materials between the active layer and the underlying layer. If $\chi = 0$, the grain-size distribution of the sediment that is transferred to the sub-layer is equal to the active layer grain-size distribution. If $\chi = 1$, the grain-size distribution of the sediment that is transferred to the sub-layer is equal to the bedload grain-size distribution (Ruark et al., 2011).

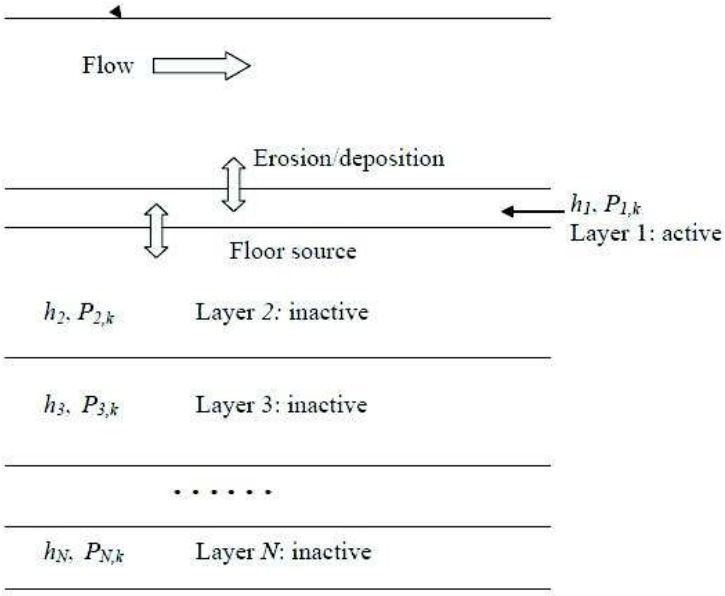

Figure 4.3. Conceptual model of bed mixing (Huang and Greimann, 2012)

4.1.5.2 Boundary conditions and bed material properties

The Liro River between the Scalcoggia confluence and the Prestone Reservoir (from S1 to S8) was modelled using the available topography (see Section 4.1.3) and adding further cross sections generated by linear interpolation at a maximum distance of 10 m. The duration of the simulation was set in relation to the duration of the CSF operation (i.e. 66 hours), with 1-min time step. Q at S1 (i.e. upstream flow boundary condition) was calculated similarly to Q at S5 (see Section 4.1.3) applying a constant time shift of 15 minutes for the Q gauged at the Isolato Reservoir. Normal depth (i.e. uniform flow depth) was selected as the downstream boundary condition at the end of the modelled reach (S8). In fact, the water level at the downstream Prestone Reservoir was low enough to not affect flow conditions in S8 during the CSF. For the upstream sediment boundary condition, a temporal series of sediment load at S1 was deduced from available measurements as reported later in the paper (see Section 4.2.3.1). A constant value of Manning's roughness coefficient (n = 0.04 s/m$^{1/3}$) was assigned to the whole study reach. The time span between SSC peaks detected between sections S5 and S8 during the CSF (approximately 15 minutes when Q was maximum) allowed for the estimation of the average velocity corresponding to a known Q. Then, in order to calibrate this parameter, the model was run under steady flow conditions (for more details see Section 4.1.5.3) matching the computed average velocity with the estimated one. The obtained value also agrees with those reported

for straight and stable channels with pebble substrate in classic literature (n = 0.03-0.05, Arcement and Schneider, 1989).

Only two layers (i.e. active and inactive) were used to model the riverbed, and just a single size class (i.e. pebble 64<d<128 mm) was adopted. This size is approximately the coarsest one observed on the riverbed surface along the study reach. Even though this schematization is fairly rough, it prevented the simulated riverbed to contribute to sediment transport and deposition. In fact, the scouring of riverbed material was not observed after the CSF and the contribution of riverbed material to the sediment transport is considered negligible compared to the sediment flushed from the reservoir. Therefore, the case study can be considered essentially a depositional case.

4.1.5.3 Sediment transport parameters and sensitivity tests

Preliminary steady flow simulations were performed to evaluate the range of Froude number and bed shear stress, adopting the riverbed schematization previously described, and with no sediment input as the upstream boundary condition. Minimum and maximum Q observed during the CSF (i.e. Q_{min} = 5 m^3/s, Q_{max} = 15.4 m^3/s, see Section 4.2.1) were selected for this purpose. For Q = Q_{min}, the calculated Froude number ranged from 0.2 to 1; while for Q = Q_{max}, the Froude number ranged from 0.6 to 1.5, with supercritical flow occurring in three reaches, covering about 10% of the channel length. In the two simulations, the shear stresses ranged from 5 to 75 N/m^2 and from 35 to 140 N/m^2, respectively. The minimum shear stress was always obtained in S5-up. The deposition of cohesive sediment can occur only if the shear stress is lower than the critical shear stress for surface erosion that is generally below 1-3 N/m^2 (van Rijn, 1993; Yang, 2006). Therefore, there was no need to perform a calibration of these parameters since negligible deposition of cohesive sediment was expected under the analysed conditions (default values were used).

Non-cohesive sediment transport was computed by means of Yang's unit stream power formula for sand (1979) and for gravel (1984) which are appropriate owing to the size of the flushed sediment and suitable for both subcritical and supercritical flow (Yang, 2006). The Yang's Sand (1979) transport formula is the following:

$$\log C_t = 5.165 - 0.153 \log\left(\frac{w_f\, d}{\nu}\right) - 0.297\left(\frac{u*}{w_f}\right) + \left(1.78 - 0.36\, log\left(\frac{w_f\, d}{\nu}\right) - 0.48\, log\left(\frac{u*}{w_f}\right)\right)\log\left(\frac{V\, S}{w_f}\right)$$

where C_t = total concentration in parts per million by weight, w_f = particle fall velocity, d = sediment particle diameter, ν = kinematic viscosity of water, u* = shear stress, V = average flow velocity and S = energy slope. The Yang's Gravel (1984) transport formula is:

$$\log C_t = 6.681 - 0.633 \log\left(\frac{w_f\, d}{\nu}\right) - 4.816\left(\frac{u*}{w_f}\right) + \left(2.784 - 0.305\, log\left(\frac{w_f\, d}{\nu}\right) - 0.282\, log\left(\frac{u*}{w_f}\right)\right)\log\left(\frac{V\, S}{w_f} - \frac{V_{cr}\, S}{w_f}\right)$$

where V_{cr} = critical average flow velocity at incipient motion.

Dry specific weight was set to 1.85 ton/m^3 for small cobbles, 1.49 ton/m^3 for sand and 1.10 ton/m^3 for silt/clay. Non-cohesive particle fall velocity was calculated using classical values recommended by the Interagency Committee (1957), assuming a shape factor of 0.7 and water temperature of 10°C (i.e. values observed during CSF samplings).

The sensitivity analysis concerned two sets of parameters (Table 4.2): i) parameters related to the bed material mixing (χ and *nalt*); and ii) parameters controlling the total adaptation length (α_d, α_e and b_L). Default values of the parameters are the following: $\alpha_d = 0.25$, $\alpha_e = 1$, $b_L = 0$, *nalt* = 2. There was not a default value for χ although Lai and Greimann (2011) reported that most sediment transport models assume χ equal to 0. Our analysis was performed adopting the same range of the parameters used by Ruark et al. (2011). These authors developed a method for assessing the influence of parameter uncertainty in sediment transport modelling and applied this method to the SRH-1D model in two distinct flume experimental cases (one erosional and one depositional). Finally, and although in the present study *n* was evaluated through velocity estimates, its influence on the numerical output was also tested, assuming the previously reported standard range for straight and stable channels with cobble substrate. The influence of the parameters on the numerical solution was assessed by comparing several simulations to a specific one that will be referred to as benchmark simulation (Table 4.2).

4.2 Results

4.2.1 The sediment flushing operation

The CSF was performed between the 19th and the 21st of October 2010 for a total of 66 hours (Figure 4.4), a relatively short duration if compared with analogous operations performed in the same region (Espa et al. 2013, 2015). During the first day, from 6:00 to 8:00 am, the Madesimo Reservoir was emptied and, short after, the mechanical removal of bottom sediments started. Earth-moving equipment worked from 8:00 am until 6:00 pm, except for the third day (when the work was completed at 3:00 pm).

Figure 4.4. Madesimo Reservoir. Photos taken the 19th October (a) in the morning and (b) in the evening, (c) the 20th October in the morning and (d) 21st October in the morning.

4.2.1.1 Flow and sediment transport

Q released from the Isolato Dam (Figure 4.5) ranged approximately from 10 to 14 m^3/s during daytime and decreased to 4 m^3/s during the night. In the last CSF day, after the end of the excavation works, Q was maintained at 10 m^3/s until 11pm. The water entering the Madesimo Reservoir was about 1.4 m^3/s during the whole operation. Time series of SSC at S5 and S8 are provided in Figure 4.6; the transformation of the raw SSC data was carried out by means of the calibration curves reported in Figure 4.7. The flow hydrograph at S1 is also reported in Figure 4.6.

A regular daily pulse (analogous to those described in Espa et al. 2013) is noticeable in the observed SSC at S5, with daily peaks between 10 and 15 g/l and nocturnal values below 1 g/l. The average SSC for the whole sediment flushing period was 2.9 g/l. The temporal pattern of SSC observed in the lowermost downstream section (S8) is analogous to that recorded in S5, except for the mentioned time shift (see Section 4.1.5.2). The total suspended sediment load at S5 was 7,800 tons. The suspended loads for the first, second and third days were 3,700, 2,400, and 1,700 tons, respectively.

Figure 4.5. Liro - Scalcoggia River confluence during the CSF

The grain-size distribution of the suspended load at S5 and S8 (calculated as the average of the three daily distributions weighed according to the respective daily flowed masses) is shown in Figure 4.7. The suspended sediment collected in the two sites was very similar in grain-size: 21% was very fine sand (62.5 μm<d< 125 μm), 64% silt (4 μm <d<62.5μm) and 7% clay (d<4 μm). Taking into account the silt/clay fraction found in suspension, the total silt/clay load is quantified at 5500 tons.

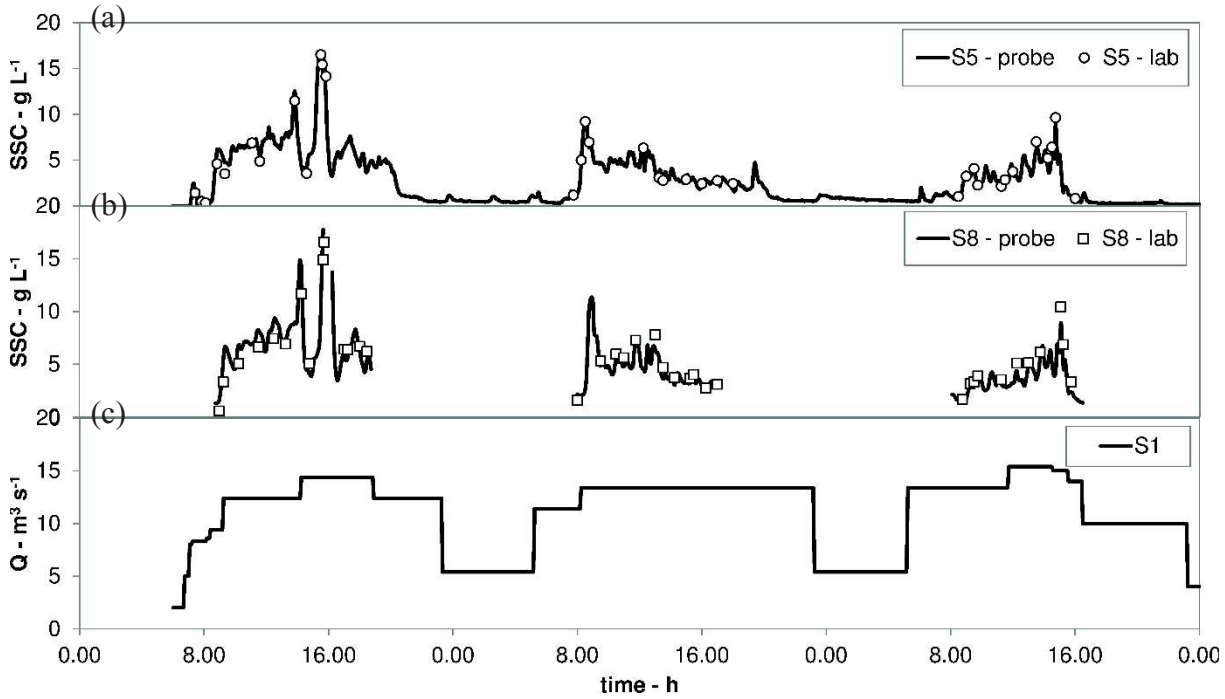

Figure 4.6. Time series of SSC and Q from 19th to 21st October, 2010. (a) SSC by calibrated turbidimeter (black line) and lab samples (white circles) at S5. (b) SSC by calibrated turbidimeter (black lines) and lab samples (white squares) at S8. (c) Streamflow at S1 (black line).

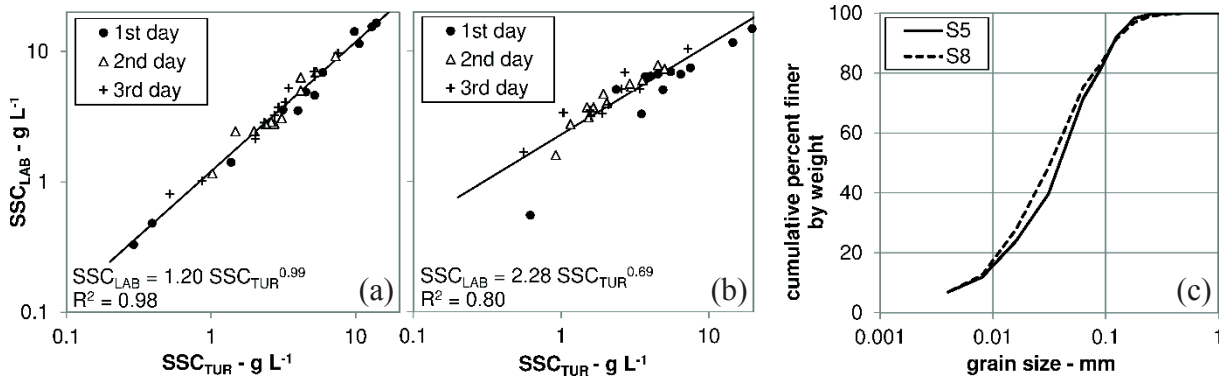

Figure 4.7. Calibration curve for the turbidimeter (a) installed at S5 and (b) operated at S8 using the samples collected during the CSF. Raw SSC data acquired in the field (SSC_{TUR}) were correlated to the corresponding laboratory samples (SSC_{LAB}) using a power function. (c) Grain-size distribution of suspended sediment collected at S5 and S8.

4.2.1.2 Riverbed deposits

Photographs of some monitoring sites before and after the CSF are provided in Figure 4.8. In general, deposited sediments were rather uniformly distributed throughout the cross sections between S1 and S8. Lateral-accretion deposits thicker than the channel deposits were observed only occasionally. The mean thickness of the deposits and their standard deviation, recorded during the post-CSF field survey along the Liro River, are given in Table 4.1. Mean values from 0 to 20 cm were found. The maximum sedimentation occurred at S5-up (Figure 4.8c); whereas the minimum was recorded in reaches where the slope exceeded 0.015 (S1, S2, S7 and S8; Table 4.1). The total volume of deposited sediments is estimated at ca. 3,000 m^3, corresponding to a mean value of 0.84 m^3/m (i.e. deposition per unit channel length) and 0.05 m (thickness of the deposit). A similar field evaluation, although less detailed, allowed estimating ca. 1,000 m^3 of sediment deposited along the Scalcoggia River after the flushing operation, with the thickness of its deposits in pools up to 0.3 m. In particular, the mean deposit thickness measured at M1 was 0.24 m (SD = 0.103 m, where SD is standard deviation). Grain-size distributions of McNeil samples at S2, S6 and S8 are provided in Figure 4.9. Collected samples were analysed individually but only two curves per site (before and after CSF) are presented in the figure and in Table 4.3 and Table 4.4. They were obtained by summing the weights of each sediment size class according to the sampled volume.

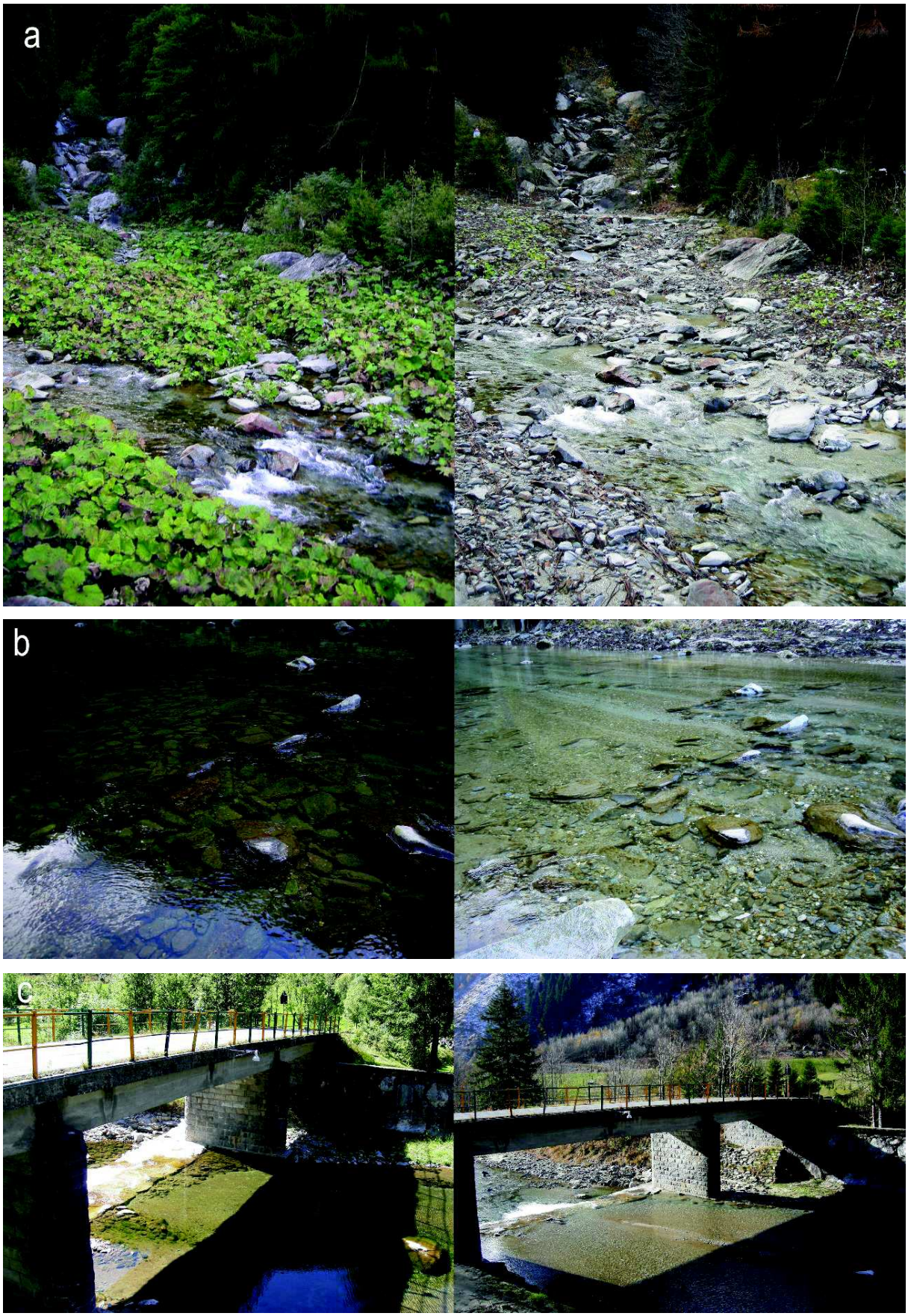
a
b
c

Figure 4.8. Photos taken three weeks before and three weeks after the sediment flushing: 8a) S1;8 b) S3; 8c) S5- up (upstream of the bridge); (d) S5-down (downstream of the bridge)

Riverbed samples highlight the increase of sand after the CSF and, consequently, the relative decrease of gravels. The characteristic diameter (d_{50}) of the pre-CSF samples was 6-7 mm, while after the CSF it decreased to 2 mm in the two downstream sites (S6 and S8). The reduction is less marked in S2 (field observations support this low deposition at S2, see Table 4.1). The content of particles smaller than 125 μm did not change significantly; deposition of this fraction is very low in the entire study reach (Table 4.3). The average proportion of particle size smaller than 2 mm (i.e. sand and silt/clay particles) per unit area obtained after the McNeil coring are reported in Table 4.4. This proportion varied between 8 and 27 kg/m^2 and from 21 to 40 kg/m^2 in the pre and post-CSF situations, respectively, increasing from 1 kg/m^2 at S2 to 30 kg/m^2 at S8. Most of the deposited sediment was sand, whereas the deposition of silt/clay was low (i.e. from 0.9 to 2 kg/m^2 and from 0.5 to 1.2 kg/m^2 in the pre and post-CSF samples, respectively). The average grain-size of the sand deposits was estimated summing the weights of each size class for all the pre and post-CSF samples and calculating the difference. The proportion of sands in the deposits was the following: 38% very coarse, 34% coarse, 22% medium and 6% fine (the proportion of very fine sand was also negligible).

Monitoring	clay/silt (%)	sand (%)	gravel (%)	<125 μm (%)
S2				
Before flushing	1.4	21.2	77.5	2.1
After flushing	1.0	28.0	71.0	1.8
Difference	-0.4	6.9	-6.4	-0.3
S6				
Before flushing	2.3	21.2	69.0	4.3
After flushing	1.5	28.0	47.9	2.6
Difference	-0.4	6.9	-21.0	-1.7
S8				
Before flushing	0.3	12.3	87.4	0.5
After flushing	0.6	48.1	51.2	2.1
Difference	0.4	35.8	-36.2	1.6

Table 4.3. Major grain-size and content of sediment smaller than 125 μm into the McNeil samples at S2, S6 and S8.

Monitoring	Before flushing		After flushing		Difference	
sections	mean	SD	mean	SD	mean	SD
S2	20.4	9.0	21.6	7.2	1.2	15.6
S6	27.0	16.9	40.0	13.4	13.0	30.0
S8	8.0	2.1	38.3	10.2	30.3	8.2

Table 4.4. Mass per unit area (average and standard deviation - SD) of sediment smaller than 2 mm. Analyzed samples were obtained through McNeil corer at three points in sections S2, S6 and S8, before and after the CSF.

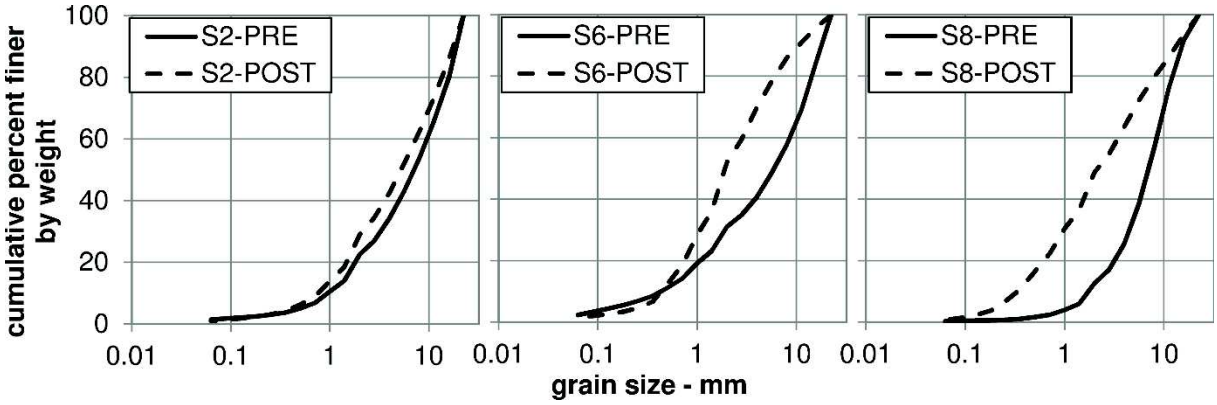

Figure 4.9. Grain-size distribution of McNeil samples at S2, S6 and S8. Each curve was obtained summing three samples, two collected 1 m from river edges and one in the centre of the stream. Particles larger than 32 mm were excluded.

4.2.1.3 Sediment budget and cost of the operation

The sediment balance, subdivided between cohesive and non-cohesive sediment, si summarized in Table 4.5 The volume of sediment released from the Madesimo Reservoir and estimated through bathymetric survey was 16,000 m^3. The sediment export downstream from S8 was 12,000 m^3, according to the estimates of sand deposits in the study reaches (i.e. 1,000 m^3 along the Scalcoggia River and 3,000 m^3 between S1 and S8 in the Liro River). The mass of sediment that flowed through S1 was 20,400 tons (i.e. 5,500 tons of silt/clay and 14900 tons of sand) of which 15,900 tons of sediment were transported through S8 in the course of the CSF (calculated from the adopted specific dry sediment weights).

Cross-section	Mass flown			Reach	Deposition
	Non-cohesive (tons)	Cohesive (tons)	Water (tons)		Non-cohesive (tons)
MD	16,400	5,500	278,000		
				MD-S1	1,490
S1	14,900	5,500	2,646,000		
				S1-S5	2,920
S5	11,980	5,500	2,646,000		
				S5-S8	1,550
S8	10,430	5,500	2,646,000		

Table 4.5. Mass balance of the sediment evacuated in the CSF of the Madesimo Reservoir. MD in the cross-sections column indicates Madesimo Dam. The mass flown through the reported cross-sections is provided in terms of both cohesive (silt/clay) and non-cohesive (sand) sediment. As observed in the field, deposition only concerned non-cohesive sediment.

The cost of releasing a unit volume of sediment was about 6.5 €/ m^3, an estimate that takes into account the loss of hydropower production at Prestone and Isolato-Madesimo hydropower plants and the expenses related to the earth-moving equipment. This unit price sits in the low range of values reported by Espa et al. (2013) for controlled free-flow flushing operations in the neighbouring Adda River (5-50 €/m^3). Sediment flushing efficiency, calculated as the ratio between the volume of evacuated sediment and the volume of water used throughout the operation (i.e. including water for dilution purposes) was 0.006.

4.2.2 Ecological impacts

4.2.2.1 Effects on benthic macroinvertebrate

The main results of the macroinvertebrate monitoring are reported in Table 4.6 for M1 and in Figure 4.10 and Figure 4.11 for S0 and S8. Figure 4.12 shows the relative abundance of the main families in all of the collected samples.

		Month(s) before/after the flushing event					
		-1	1	4	5	8	11
Density (ind.m^{-2})	Plecoptera	319	3	28	45	132	70
	Ephemeroptera	144	0	1	6	4	122
	Trichoptera	85	4	17	3	5	55
	Diptera	1918	2	1771	686	1309	544
	Other taxa	13	0	9	148	137	115
	Total	2479	9	1826	888	1587	906
Metric	N families	20	6	15	16	17	17
	EPT	9	4	6	8	6	7
	Shannon-Wiener	1.23	1.68	0.25	0.80	1.13	1.99
	STAR_ICMi*	0.92 (G)	0.62 (M)	0.61 (M)	0.63 (M)	0.69 (M)	0.76 (G)

*Quality classes are reported within brackets: G=good and M=moderate

Table 4.6. Time evolution (from one month before to eleven months after the flushing event) of the composition of the macroinvertebrate community (single taxon and total densities) and of four community structure metrics at M1.

At the three BSs, the density and number of families of the pre-CSF benthic communities were similar. Moreover, the same families were mainly detected: the Plecoptera Leuctridae and Nemouridae, the Ephemeroptera Baetidae and Heptageniidae, the Trichoptera Limnephilidae and Rhyacophilidae, and the Diptera Chironomidae and Simuliidae. However, the community collected at M1 in summer 2010 (i.e. the only available pre-CSF sample) was dissimilar from the corresponding S0 and S8 ones ($BCi_{M1–S0}$ = 0.68; $BCi_{M1–S8}$ = 0.79), which were comparable with each other (BCi_{S0-S8} = 0.20). In fact, the community at M1 was dominated by Chironomidae, while the other two were mainly composed of Baetidae and Simuliidae. After the CSF (i.e. in autumn 2010), the dissimilarity between the three BS communities increased ($BCi_{M1–S0}$=0.99, $BCi_{M1–S8}$=0.95, $BCi_{S0–S8}$ = 0.62) and returned to nearly pre-CSF values about 9 months later (i.e. in summer 2011).

In general, no significant differences in both benthos metrics (Kruskal–Wallis, $p>0.01$) and community composition (ANOSIM, $p>0.01$) were found before and after the CSF at S0 and S8, nor cross-comparing the two BSs. Moreover, for the two Liro sites, neither inter-annual differences nor inter-site differences within the same monitored year were statistically significant (Kruskal–Wallis and ANOSIM, $p>0.01$). The post-CSF assemblages collected at M1 were significantly different from those of S0 and S8 (ANOSIM, $p<0.01$). A more detailed description of the time evolution of the

benthic communities, with a focus on the comparison between pre-CSF/post-CSF samples, is reported in the succeeding text for each BS.

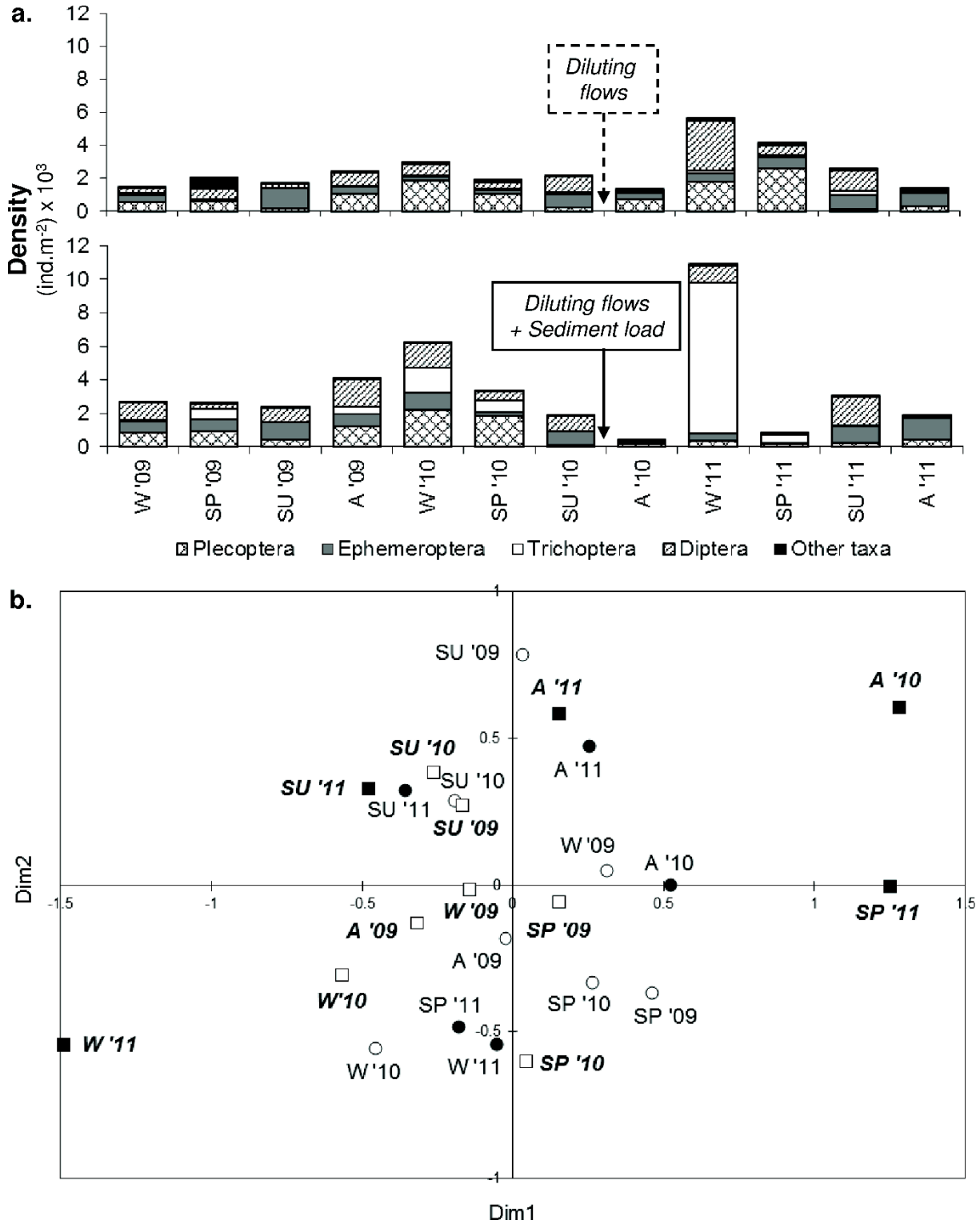

Figure 4.10. (a) Temporal trend (all seasons from 2009 to 2011) of the composition of the macroinvertebrate communities (single taxon and total densities) at S0 and S8. Arrows indicate disturbances due to the flushing event. (b) NMDS between these communities using the BC distances (circle = S0 sample and square = S8 sample, white = pre-CSF sample and black = post-CSF sample).

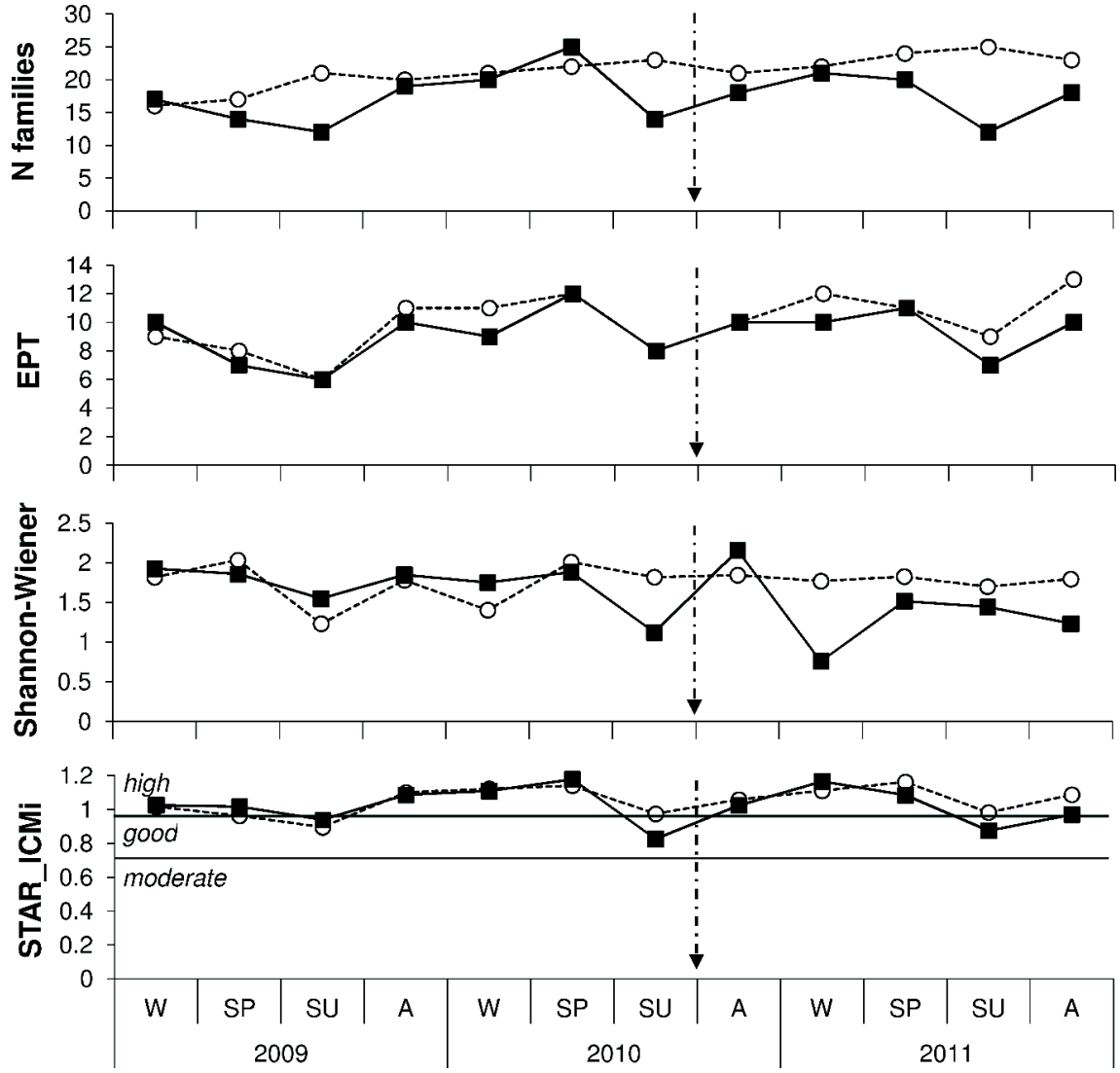

Figure 4.11. Temporal trend (all seasons from 2009 to 2011) of four metrics on the structure of the macroinvertebrate communities at S0 (circle) and S8 (square). Arrows indicate the flushing event.

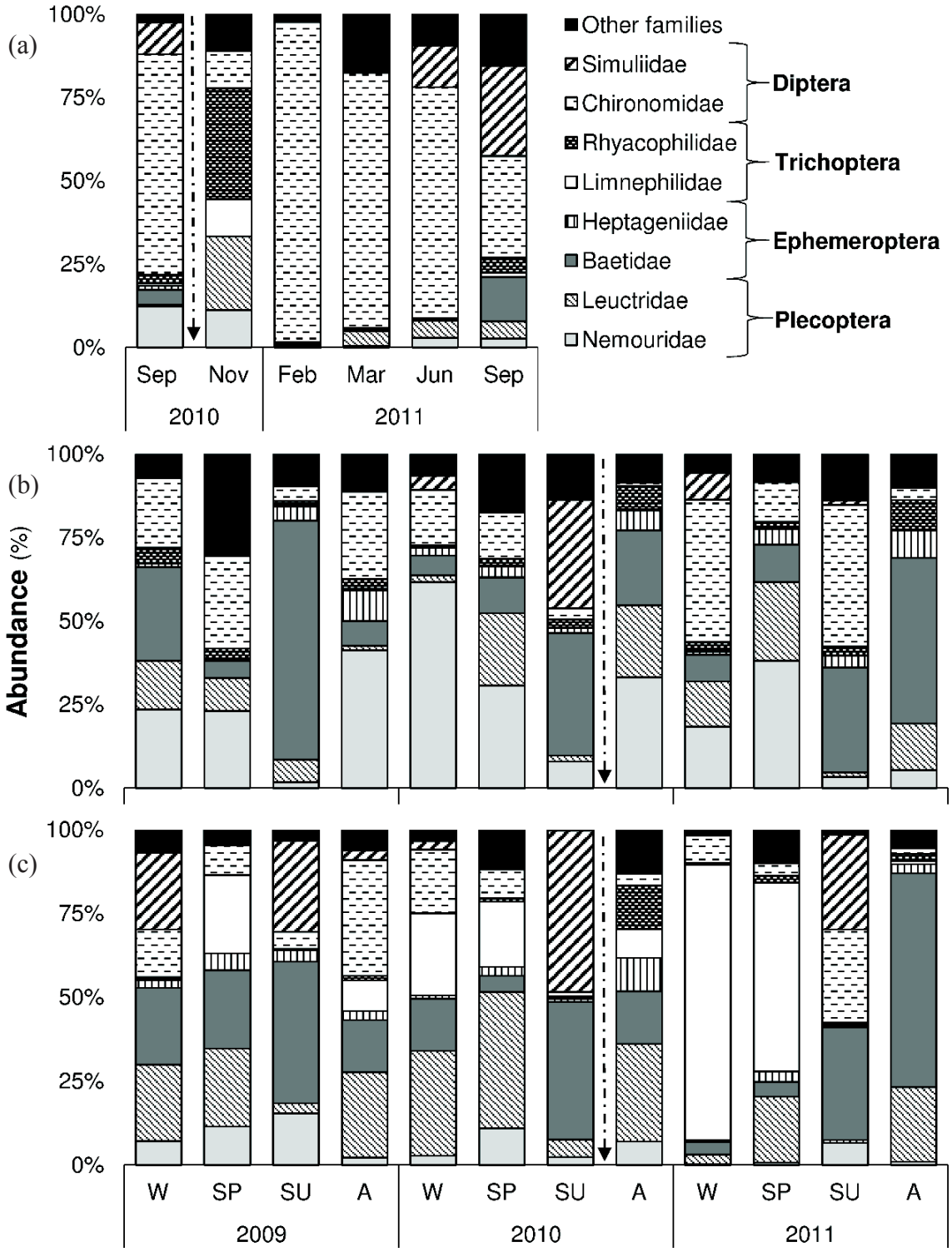

Figure 4.12. Relative abundance of the main families of the benthic macroinvertebrates collected (a) at M1, (b) at S0 and (c) at S8.

At M1, a total density decrease of 99.6% was recorded 1 month after the CSF. The number of families and EPT also decreased by 70.0% and 55.6%, respectively, and the STAR_ICMi quality class dropped from good to moderate. The minimum value of Shannon–Wiener was detected 4 months after the CSF, when the community was dominated by Chironomidae. Except for Chironomidae and Leuctridae, the other families recovered slowly in density, and the community did

not return to the pre-CSF condition after 1 year from the CSF. Nemouridae and Heptageniidae did not reach the pre-CSF density, and no aquatic beetles were found. The density of Naididae increased, and freshwater worms belonging to the families Enchytraeidae, Lumbricidae and Lumbriculidae, which were not sampled before flushing, were collected. Similarly, the total density, number of families and STAR_ICMi values never reached the pre-CSF ones during the monitored period.

At S0, a total density reduction of 39.1% was recorded 1 month after the diluting flows released during the CSF. However, comparable reductions were also observed in other occasions, and the same low densities of the first post-CSF sample (i.e. autumn 2010) were also recorded in autumn 2011. The NMDS in Figure 4.10b (stress value = 0.116) shows that the community composition was similar in all S0 samples, with small differences linked to seasonality. During the 3 years of monitoring, the lower EPT and STAR_ICMi values were recorded in summer.

At S8, a total density reduction of 79.7% and the minimum density were recorded 1 month after the sediment flushing (i.e. in autumn 2010). The NMDS in Figure 4.10b emphasizes a considerable difference of the post-CSF community composition up to summer 2011. The boom of Limnephilidae observed 4 months after the flushing event (i.e. in winter 2011) was also detected by the Shannon–Wiener index. In the third post-CSF sample (i.e. in spring 2011), Limnephilidae constituted more than 50% of the community. In summer 2011, the community approximately recovered to the pre-CSF conditions. Only Nemouridae and Heptageniidae had lower densities than before the CSF. However, the metrics plotted in Figure 4.11 did not detect the effects of the flushing activities. On the contrary, they show a rather regular seasonal trend, with a summer decrease of the number of families, EPT and STAR_ICMi, with the last always lowering from high to good.

4.2.2.2 Effects on fish

At both S0 and S8, only brown trout and bullhead (Cottus gobio) were sampled in the three monitoring campaigns. The results of the fish survey are reported in Table 4.7 and Figure 4.13.

The trout density was lower at S8 (2,140 ind/ha on average) than at S0 (3,172 ind/ha on average), where no specimens longer than 270 mm were caught. At both BSs, the trout length structure usually had a bimodal distribution, and a density reduction was observed in the post-CSF sample. At S0, the density decrease approximately amounted to 36%, mainly affecting 0^+ individuals (i.e. mostly the stocked ones). However, a comparable contraction could be noticed when comparing the first and the second pre-CSF samples. At S8, the density decrease was larger (i.e. 55%), and mainly concentrated on 1+ individuals.

The bullhead population at S8 was more well-structured, in terms of length classes, and had a higher density (547 ind/ha on average) than that at S0 (183 ind/ha on average). The densities recorded at both BSs after the CSF were slightly lower than those of the 2010 pre-CSF samples, but higher

than the 2009 ones. No 0^{+}-1^{+} individuals were detected in all of the S0 samples and in the S8 post-CSF sample. However, at S8, the juvenile density decreased by approximately 70% between 2009 and 2010 (i.e. before the CSF took place).

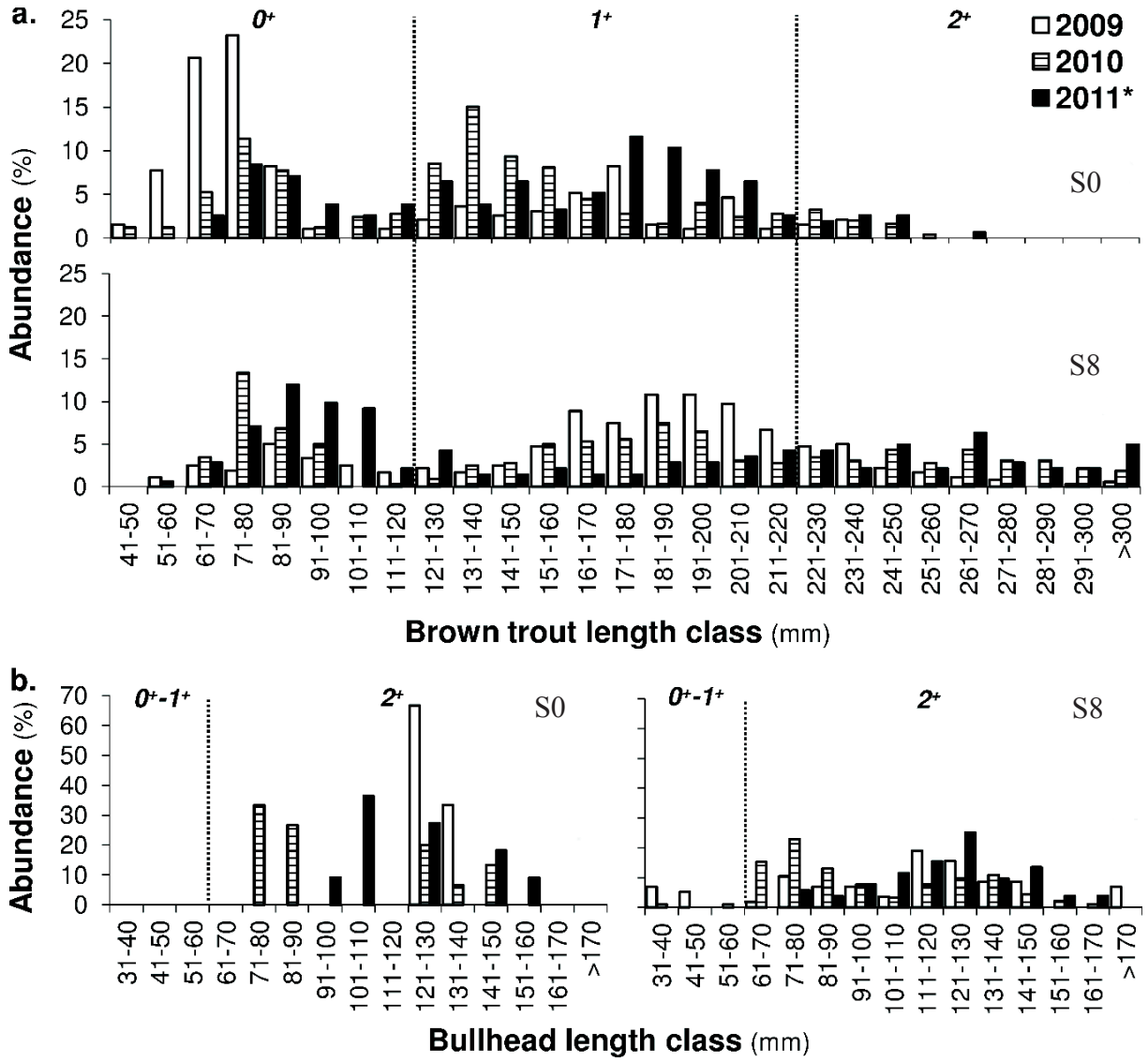

Figure 4.13. Length structure of brown trout (a) and bullhead (b) populations sampled in autumn 2009 and 2010 (pre-CSF samples), and in autumn 2011 (post-CSF sample indicated by an asterisk) at S0 and S8. Age classes were identified according to Unfer et al. (2011) for brown trout and Tomlinson and Perrow (2003) for bullhead.

				Density (ind.ha^{-1})		
		LC	AC	2009	2010	2011*
Brown trout	S0	≤120	0^+	2,018	1,291	699
		≤220	1^+	1,050	2,298	1,572
		>220	2^+	115	283	191
		Total		3,182	3,872	2,461
	S8	≤120	0^+	529	715	462
		≤220	1^+	1,919	1,016	273
		>220	2^+	480	685	341
		Total		2,927	2,416	1,076
Bullhead	S0	≤60	0^+-1^+	0	0	0
		>60	2^+	94	235	219
		Total		94	235	219
	S8	≤60	0^+-1^+	56	15	0
		>60	2^+	410	677	482
		Total		467	692	482

*Post-CSF sample

Table 4.7. Density of brown trout and bulhead at S0 and S8 in the three monitoring campaigns (2009-2011). Age classes (AC) were determined through length classes (LC), according to Unfer et al. (2011) for brown trout and Tomlinson and Perrow (2003) for bullhead.

4.2.3 Numerical modelling

4.2.3.1 Model outcomes

The simplified sedigraph at S1 adopted as the upstream sediment boundary condition is shown in Figure 4.14. It was derived from the available experimental dataset. The starting point was a simplified time series for silt/clay concentration at S1 (Figure 4.14), deduced from SSC measured at S5. The schematization showed variations between night-time and daytime, when excavation in the reservoir took place. The concentration of silt/clay during night-time was assumed constant at 0.36 g/l. Then, three daytime concentrations were computed (one per day) based on the observed silt/clay load (2,650, 1,700 and 1,150 tons, respectively; see Section 4.2.1.1). The time series of total sediment load was then derived from the previous measurement, assuming a constant percentage of sand. In this way, the total mass of sediment that flowed through S1 (20,400 tons; see Section 4.2.1.3) during the CSF fulfilled both the total balance and the grain-size distribution of the inflowing sediment (i.e. 27% silt/clay fraction and 73% sand; see Section 4.2.1.3). Sand was divided uniformly into the standard five grain-size classes. According to the observational evidence (see Section 4.2.1.2) the fraction of inflowing sediment coarser than sand was set to zero. Sediment load at S1 during daytime, was thus set to 20, 12 and 12 g/l respectively for the first, second and third day of the CSF. The estimated sediment concentration at M1, S1 and S8 averaged 66.0 g/l, 6.8 g/l and 5.8 g/l over the entire operation period.

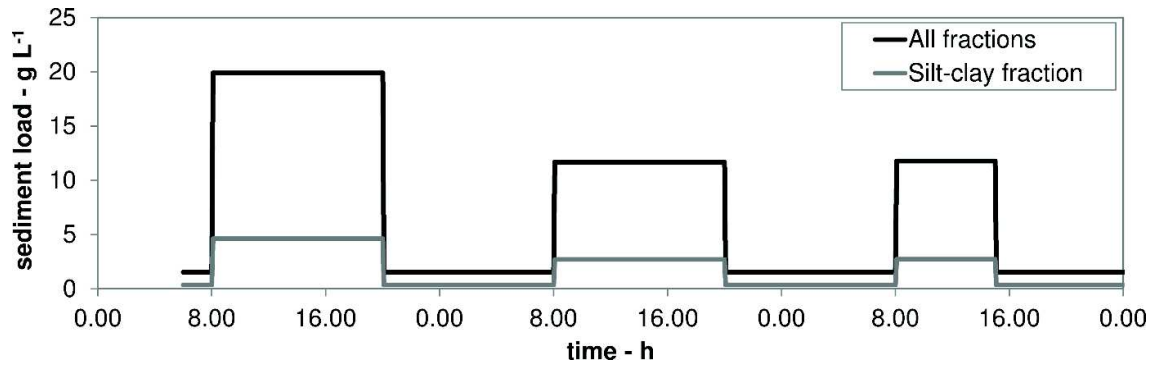

Figure 4.14. Schematic time series of sediment load adopted as the upstream sediment boundary condition for the modelling.

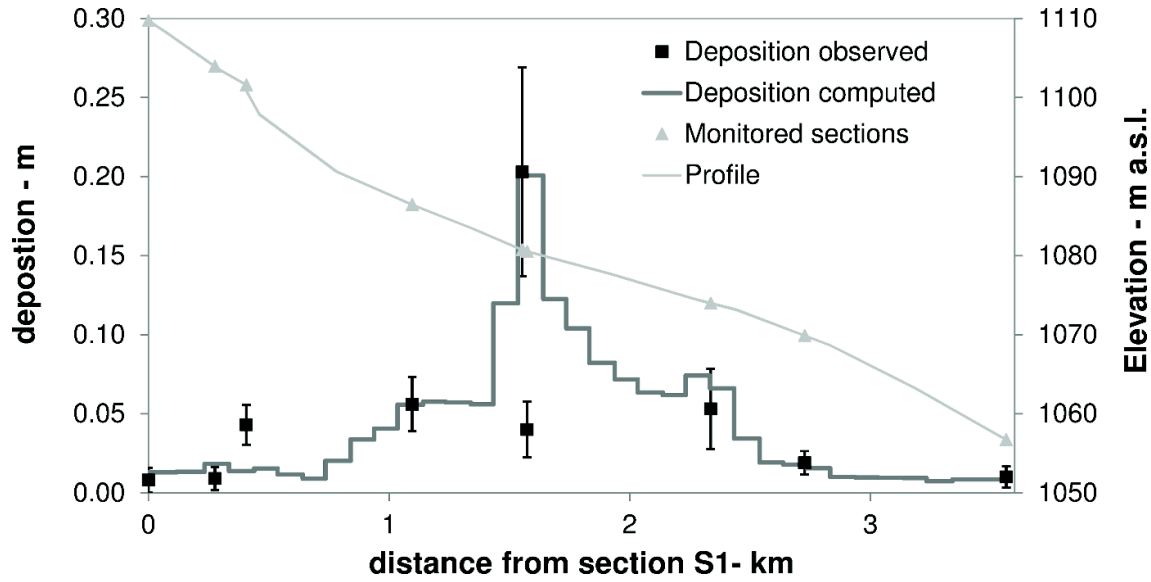

Figure 4.15. Comparison of the measured sediment deposit thickness (mean±SD) and the computed pattern, as averaged over 100 m long reaches, between S1 and S8.

A satisfactory agreement between the computed and the observed depositional pattern (Figure 4.15) was obtained by adopting the default values for the total adaptation length parameters (see Section 4.1.5.3) and setting $\chi = 0$ and *nalt* = 0.55 (corresponding to an active layer thickness of 0.05 m). We therefore adopted this as the benchmark simulation for further comparisons. In particular, the simulated sediment mass deposited after the CSF (hereafter $M_{dep,tot}$) was nearly equal to the estimated value (i.e. 4,470 tons; see Section 4.2.1.3). The largest deposition was obtained in the middle part of the study reach, where the elevation profile is characterized by a lower slope (0.008). The average grain size of the computed sediment deposits was 35% very coarse sand, 33% coarse sand, 20% medium sand, 9% fine sand, and 3% very fine sand; and, as expected, 0% of silt/clay. The coarsest deposits were found at S1 (i.e. 49% very coarse sand); whereas the finest were located in S5-up (i.e. 22% very coarse sand). Such proportions are in the same order of those obtained from the McNeil samples (see Section 4.2.1.2). Moreover, the negligible deposition of sediment below fine sand agrees with results of riverbed substrate sampling (Table 4.3).

4.2.3.2 Sensitivity tests

The model sensitivity to bed material mixing parameters was assessed through nine simulations carried out with *nalt* = 0.5-1-2 and χ = 0-0.5-1. The parameters controlling the total adaptation length were set to default. $M_{dep,tot}$ increased almost linearly with increasing *nalt;* conversely, $M_{dep,tot}$ decreased linearly with the increase of χ (Figure 4.16). $M_{dep,tot}$ ranged from 2,000 to 8,000 tons in the mentioned intervals of the parameters. Several simulations carried out with different *nalt*-χ pairs were therefore capable of reproducing $M_{dep,tot}$ similar to that estimated from field measurements. For example, the benchmark simulation (*nalt* = 0.55, χ = 0) and the simulation with *nalt* = 1.60, χ = 1 gave the same $M_{dep,tot}$. However, the spatial distribution of the deposits showed some differences (Figure 4.16), with the benchmark pattern more similar to the observed pattern upstream from S5 and in the final studied km. The maximum deposit thickness was 0.2 m for the benchmark simulation and 0.12 m for the other one (i.e. *nalt* = 1.60, χ = 1). The composition of the deposited sediments was affected by the variation of χ but not by *nalt*, i.e. with χ = 1 the grain-size was coarser than with χ = 0 (very coarse sand formed 50% of the total deposited sediment, against 35% obtained in the benchmark simulation). Anyway, in both cases the deposition of particles smaller than fine sand was negligible.

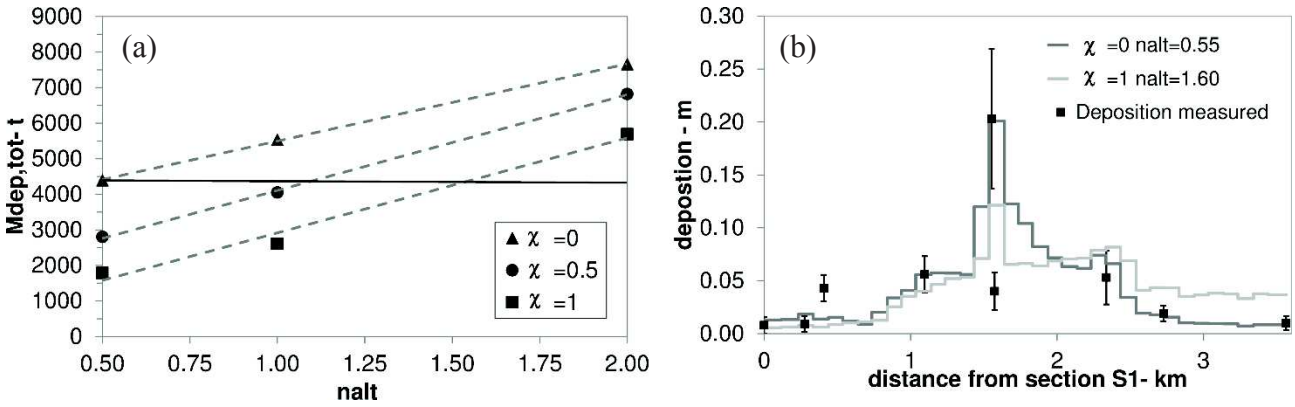

Figure 4.16. (a) Computed amount of sediment deposition ($M_{dep,tot}$) as a function of the parameters nalt and χ. The horizontal line represents the field estimated value of $M_{dep,tot}$. (b) Computed depositional patterns varying the values of χ and nalt. Note that χ was set to 1 (upper limit) and 0 (lower limit) and the associated nalt (respectively 0.55 and 1.60) was calibrated to achieve the observed $M_{dep,tot}$.

The model sensitivity to the variation of the next parameters was generally lower; for instance, the default value of the recovery factor for deposition α_d was 0.25; if α_d is reduced to 0.05 keeping the other parameters as in the benchmark simulation, $M_{dep,tot}$ decreases of about 10% from about 4,500 to 4,000 tons. Conversely, if α_d is set to 1, both $M_{dep,tot}$ and the spatial depositional pattern are equal to those obtained from the benchmark simulation. Varying in the same way both the recovery factor parameter for scour α_e (from 0.05 to 1 - default value), and the bedload adaptation length coefficient b_L (from 0 - default value - to 10), did not significantly influence the numerical solution in comparison to the benchmark. Finally, the decrease of Manning's coefficient *n* resulted, as expected, in a

reduction of the computed $M_{dep,tot}$. In particular, the decrease of *n* from 0.05 to 0.04 caused a reduction in $M_{dep,tot}$ of about 10%, and the further decrease from 0.04 to 0.03 led to another comparable reduction. Worth to notice that the grain-size of the deposited sediment was not affected by the *n* value; in the three tested cases, deposits consisted of about 70% of very coarse and coarse sand. All the numerical simulations discussed in this subsection are summarized in Table 4.8, where the adopted parameters and the main output $M_{dep,tot}$ are reported.

Id	Parameters						Output	
	nalt (-)	χ (-)	n ($s\ m^{-1/3}$)	α_d (-)	α_e (-)	b_L (-)	$M_{dep\ tot}$ tons	Difference %
Benchmark	0.55	0	0.04	0.25	1	0	4,490	
1	0.5	0	0.04	0.25	1	0	4,390	-2%
2	1	0	0.04	0.25	1	0	5,530	23%
3	2	0	0.04	0.25	1	0	7,660	71%
4	0.5	0.5	0.04	0.25	1	0	2,800	-38%
5	1	0.5	0.04	0.25	1	0	4,050	-10%
6	2	0.5	0.04	0.25	1	0	6,820	52%
7	0.5	1	0.04	0.25	1	0	1,780	-60%
8	1	1	0.04	0.25	1	0	2,600	-42%
9	2	1	0.04	0.25	1	0	5,690	27%
10	1.16	1	0.04	0.25	1	0	4,490	0%
11	0.55	0	0.05	0.25	1	0	5,070	13%
12	0.55	0	0.03	0.25	1	0	3,890	-13%
13	0.55	0	0.04	0.05	1	0	4,070	-9%
14	0.55	0	0.04	1	1	0	4,410	-2%
15	0.55	0	0.04	0.25	0.05	0	4,410	-2%
16	0.55	0	0.04	0.25	1	10	4,460	-1%

Table 4.8. Comparison between the benchmark simulation and the further sensitivity analysis simulations. The parameters varied compared to the benchmark simulation are in red. The reported output is the sediment mass deposited in the simulated reach at the end of the simulation ($M_{dep,tot}$). Percentage differences are computed relatively to the benchmark. Simulations 1-10 concern model sensitivity to the parameters controlling bed material mixing. Simulations 11-12 concern model sensitivity to the Manning's parameter. Simulations 13-16 concern model sensitivity to the parameters controlling the total adaptation length.

4.3 Discussion

4.3.1 Ecological impacts

4.3.1.1 Characterization of the benthic and fish communities at BSs

The macroinvertebrate assemblages at the BSs were congruent with those usually detected in regulated Alpine watercourses (Robinson et al., 2004; Monaghan et al., 2005; Espa et al., 2013). Most of the sampled families have adaptations enabling them to live in a disturbed environment (Matthaei et al., 1996). The S0 and S8 assemblages both varied seasonally, showing a summer contraction probably associated to insect life cycles and streamflow increase due to snowmelt. This contraction

was more prominent at S8, where streamflow during the snowmelt period was higher because of the larger residual basin (Quadroni et al., 2014). A similar contraction was recorded in the Alpine Roseg River in Switzerland when ice melting was at its maximum (Burgherr and Ward, 2001).

Brown trout was the dominant fish species at the BSs, displaying densities considered good for Alpine water courses below 1500 m elevation (OFEFP, 2004), and larger than those reported for the Alpine rivers Spöl (Ortlepp and Mürle, 2003) and Ybbs (Unfer et al., 2011), in Switzerland and Austria, respectively. In spite of the fishing ban, the trout density was lower at S8 than at S0, probably because of differences in stream morphology (e.g. absence of refugia, such as boulders and pools at S8) and trout migration from S8 to the close Prestone Reservoir. The trout length structure was congruent with stocking and fishing activities; nevertheless, a bimodal distribution was usually recorded in the Ybbs River, where only low-scale catch and release fishery occurred (Unfer et al., 2011). Beyond trout, bullhead were also caught at both BSs. Bullhead is a bottom-dwelling species listed in Annex II of the EU Habitats Directive (92/43/EEC) and is quite rare at the European level (Legalle et al., 2005). The larger bullhead density recorded at S8 than at S0 may again be explained by the differences in stream morphology (i.e. bullhead prefer riffles than step-pools, Vezza et al., 2014). Moreover, the differences in stream morphology could have determined the differences in sampling efficiency. Comparable bullhead densities were found in the Alpine rivers Adda (Espa et al., 2015) and Reppisch (Utzinger et al., 1998), located in Italy and Switzerland, respectively.

4.3.1.2 Ecological effects of the flushing operations

Remarkable changes in streamflow and related hydrodynamic forces, sediment transport and riverbed morphology occurred at the BSs during and after the CSF from the Madesimo Reservoir. All of these physical factors were suggested to significantly influence both macroinvertebrate (e.g. Kennen et al., 2010; Jones et al., 2012; McMullen and Lytle, 2012; Buendia et al., 2014; Booker et al., 2015) and fish (e.g. Poff and Allan, 1995; Kondolf, 2000; Bilotta and Brazier, 2008; Chapman et al., 2014) communities.

As expected, the impacts on the benthic communities measured at the three BSs were quantitatively different, as a response to quantitatively different degrees of stress. A short-term density reduction of 40% was observed at S0, which was only subjected to the diluting discharges. These effects seemed comparable with those commonly recorded during the seasonal streamflow increase due to snowmelt. A higher impairment (i.e. a density decrease of 80% and a change in community composition that recovered in about 9 months) was detected at S8, where the disturbance due to sediments, both transported and deposited, superimposed that of the diluting flows. However, the most severe impairment occurred at the site closer to the flushed reservoir, where almost all of the computed metrics dropped after the CSF, and the recovery was slower and still incomplete 1 year

after the operations. Although the fish results were more difficult to interpret because of trout fishing and stocking and difficulty in bullhead capture, they would seem to indicate the impairment of trout juveniles at the BS affected by the sediment increase.

The flow and sediment effects will be discussed separately in the two following sections.

4.3.1.3 Flow effects

The significant reduction of the macroinvertebrate density and the change in the community structure after experimental peak flows were documented both in the laboratory channel (Mochizuki et al., 2008) and in the field (Robinson et al., 2004). McMullen and Lytle (2012) quantified that macroinvertebrate abundance was approximately halved within 10 days from flood events, with no substantial difference between natural and managed ones. Buendia et al. (2014) reported that the benthic community recovered within a few days after a 1-year flood that mobilized the riverbed of the Isabena River in the southern Pyrenees (Spain). Habitat complexity and the availability of low velocity microhabitats are key factors that enable both macroinvertebrates and fish to withstand floods. According to Wilcox et al. (2008), benthic organisms can better resist high flows in streams organized into alternating sequences of steps and pools. Thompson et al. (2011) only detected a slight brown trout displacement, mainly of 0^+ individuals, after a pulse flow from 0.5 to 18.5 m^3/s in a bedrock reach of the Silver Creek in California (United States), characterized by a large number of flow refugia. All of these findings may explain both the moderate density reduction of benthos and the absence of relevant effects on fish at S0, where the diluting flows released during the CSF were approximately 25 times larger than MF. For the same reasons, the higher effects of the streamflow increase alone can be hypothesized at S8, where the stream morphology was poorer. There, the estimated average bed shear stress increased from 12 Pa at MF to 80 Pa during the CSF (estimated using the open-channel uniform-flow basic formulae for wide rectangular cross sections with a Manning's coefficient of 0.04 $m^{1/3}$ s as suggested by Arcement and Schneider (1989) for straight and stable channels with cobble substrate). An increase in bed shear stress from 0.1–7 to 40 Pa (i.e. over the sediment entrainment threshold) was associated with an average increase in the mayflies drift rate (by a factor of 35) on patches of sandy bed material in an upland gravel-bed stream (Ribera Salada) in the Catalan Pre-Pyrenees (Spain) (Gibbins et al., 2010).

4.3.1.4 Sediment effects

The sediment effects due to the CSF on the benthic community can be schematically divided into short term and long-term ones. The former are associated with the significant increase in sediment load that can trigger several responses (Jones et al., 2012). The most immediate response is an increase in macroinvertebrate drift and a subsequent depletion of the benthos assemblage. The long-term effects are associated with the sediment deposition after the CSF, which can determine a

reduction in the periphyton food supply (Luce et al., 2013) and persisting habitat alteration (Jones et al., 2012), thus tangling the recolonization of the benthic taxa. In our case study, both effects were strictly associated to the streamflow increase during the CSF. In fact, as mentioned earlier, the streamflow increase could have determined the increase of the benthic drift during the CSF. However, the diluting flows reduced both the sediment load and the sediment deposition, and, therefore, their negative effects on the benthic assemblage. The detectable impacts of the sediment load on macroinvertebrate communities may occur at SCs and deposition considerably lower than those reported in this study. García Molinos and Donohue (2011) found that a 3-h pulse of approximately 0.20 g/l SSC, repeated for 5 consecutive days, determined significant macroinvertebrate drift in a headwater stream (River Liffey) in County Wicklow (Ireland). A similar result was obtained by Larsen and Ormerod (2010) after the addition of approximately 4–5 kg/m^2 of fine sand in two headwater tributaries of the Usk River in Wales. In addition, Larsen et al. (2011) found a taxon-specific response to the addition of 0.6–18 kg/m^2 of inert sand to the riverbed. Filter feeders, swimmers and k-selected taxa with gill respiration and requiring attachment to the substrate (e.g. Baetidae and Heptageniidae) were affected, while fine detritus feeders, burrowers and taxa with tegumental respirations and shorter life cycles (e.g. Chironomidae and Oligochaeta) were favoured. Accordingly, at M1, after the CSF, some Oligochaeta families appeared or increased in abundance. Moreover, at S8, the increase in the sand content in the riverbed substrate probably supplied Limnephilidae with the suitable materials for the construction of their cases (Statzner, 2011). Commonly drifting taxa (i.e. Chironomidae and Leuctridae) rapidly recovered at both the sediment-impacted sites, possibly recolonizing via incoming drift. Although at S8 the community recovery was faster than at M1, because of the lower disturbance, at both BSs, Nemouridae and Heptageniidae did not regain their pre-CSF densities after 1 year from the operations. Espa et al. (2013) found the same result for Heptageniidae (Ecdyonurus and Rhithrogena), while the opposite situation was detected in the case of Nemouridae (Protonemura). This discrepancy could be ascribed to the higher taxonomic resolution adopted by Espa et al. (2013) and highlights the importance of the macroinvertebrate identification to species level, as suggested by Monk et al. (2012).

Fish showed more resistance than benthos to transported and deposited sediments. Chapman et al. (2014), in their recent meta-analysis, did not find a significant association between fish abundance and sedimentation. Adaptive responses to sediment pulses may prevent fish from dying (Michel et al., 2013). However, SC values recorded at S8 could have caused the density reduction of trout juveniles. This result agrees with the findings of Espa et al. (2013), which reported the contraction of trout juveniles after 2 weeks of 3-4 g/l average SSC in the Alpine Roasco Stream in Italy. Moreover, the documented increase of the sand content in the S8 substrate could have interfered with trout

spawning. In fact, the proportion of sand in the substrate that is critical for salmonid embryos and eggs was estimated at approximately 10–15% (Lapointe et al., 2004; Louhi et al., 2008).

4.3.1.5 Management consideration

The EU policy on energy and environment is currently focused on the increase in the use of renewable energy sources and on the sustainable management of natural resources. All EU member states have to contribute to the increase in the use of renewable energy sources, up to 20% of the overall community energy consumption, by 2020 (Directive 2009/28/EC). Additionally, all European watercourses must achieve good ecological status or potential (i.e. a slight deviation from a type-specific reference condition) by 2027 (WFD).

Sustained long-term preservation of reservoir storage is crucial to maintain the current hydropower production in the Alps, where many reservoirs are more than 50 years old. Therefore, the current challenge is to tackle reservoir siltation while respecting WFD constraints on the ecological quality of the downstream freshwater ecosystems.

In this case study, clear water releases from the Isolato Reservoir considerably reduced the ecological impacts of the CSF from the Madesimo Reservoir on the downstream Liro River. The STAR_ICMi stream quality detected at S8 remained high after the CSF. On the contrary, at M1, where the sediment stress was markedly higher, a quality decrease from good to moderate was measured.

However, care should be taken when evaluating the ecological stream quality through the STAR_ICMi. In fact, as previously observed by Espa et al. (2015), this multi-metric index would seem to overestimate the status of the benthic community in certain circumstances. Indeed, it assigns a relevant weight to metrics associated with organic pollution, which was not of concern in the investigated area. Moreover, it only takes into account the relative abundance of the sampled families; for example, the STAR_ICMi quality of the M1 post-CSF sample was moderate, although the total density was only 9 ind/m^2. A more adequate index should be developed to specifically evaluate the sediment pressure in the Alpine context, following the example of Extence et al. (2013).

4.3.2 Numerical modelling for sediment flushing

4.3.2.1 Use of numerical modelling

Sediment dynamics inside reservoirs have been frequently analysed by 1-D sediment transport models, including sedimentation and desilting by flushing, with the main focus on predicting the efficiency of different operating rules. For instance, pressure flushing operations were simulated in the Sefid-Roud Reservoir in Iran (Khosronejad, 2009) and in the Lewis and Clark Lake in the US (Ahn et al., 2013). Similarly, Valette and Jodeau (2012) simulated various drawdown scenarios of the Tolla Reservoir (France) to predict the resulting sediment loads.

More refined three dimensional (3-D) numerical models were also employed with analogous purposes (Haun et al., 2012a). The spatial distribution of erosional and depositional areas during free -flow flushing operations was investigated by mixing lab-scale experiments and 3-D modelling in the Kali Gandaki Reservoir in Nepal (Haun et al., 2012b) and in the Dashidaira Reservoir in Japan (Esmaeili et al., 2014). Additionally, full scale 3-D simulations of free-flow flushing operations performed in the Angostura (Costa Rica) and in the Dashidaira reservoirs were respectively carried out by Haun et al. (2012a) and Esmaeili et al. (2015). The comparison with bathymetrical data acquired during the operations highlighted the need for further improvement in the modelling of bank stability and erosion of cohesive sediment to increase the accuracy of the results.

Only recently, research on reservoir desiltation has been directed at understanding the downstream environmental effects of sediment flushing operations (Morris, 2014). An interesting attempt to numerically assess the compatibility of sediment flushing was performed by Gallerano and Cannata (2011). As a first step, they calculated a target sediment load of 25 g/l by modelling the sediment transport in the catchment of the Pieve di Cadore Reservoir in Italy during a 10-year flood. Then, they applied a 3-D model to simulate pressure flushing operations in the reservoir, thus determining the appropriate discharge to outflow the target sediment load. Authors reported that downstream fish population could withstand this sediment load without significant losses according to the N&J dose/response model. However, the downstream geomorphic effects of the investigated sediment flushing were not explored.

Only some papers deal with sediment transport downstream of reservoirs desilted by sediment flushing, using both numerical and experimental approaches. Brandt and Swenning (1999) reported a detailed field investigation on the geomorphic effects of a 2-day free-flow flushing operation in the Cachí Reservoir in Costa Rica, where a suspended sediment load of over 850,000 tons was measured, with SSC peaks of up to 200 g/l. More recently, Liu et al. (2004a, b) reported on two free-flow flushing operations involving two dams in cascade: Dashidaira and Unazuki (Japan). Riverbed dynamics were modelled with a 1-D model, and a good agreement was generally found between numerical data and field measurements of SSC and erosional/depositional patterns. The study focused basically on particles smaller than 0.02 mm in diameter, which accounted for the vast majority of the total load, and a SSC peak of 100 g/l was measured downstream of the Dashidaira Dam (i.e. the most upstream one) during coordinated sediment flushing. Overall, compared to our study case, the flushing operations reported by Brandt and Swenning (1999) and Liu et al. (2004a, b) displayed significantly larger Q (100-500 m^3/s), and SSC peaks were at least an order of magnitude higher than those estimated for the Madesimo CSF. Furthermore, the implementation of mitigation measures and the related ecological effects of the flushing operations were not reported. In contrast, for the CSF at

the Madesimo Reservoir, the SSC of the sluiced water was controlled, and ecological surveys were carried out to assess the impact on downstream biota. Analogous investigations of the downstream environmental effects of CSFs from reservoirs located in Lake Como catchment are provided by Espa et al. (2013, 2015). In these cases, the efficiency of sediment removal was constrained by the environmental measures enforced by regional Authorities, such as the SSC limit, implemented to minimize downstream effects (see Section 6.3). Average allowable SSC from 1.5 to 4 g/l were basically derived using the N&J model (see Section 6.1), as in case of the Madesimo study. Similar limits on SSC were also set to manage the *environmentally friendly flushing* from the Genissiat Dam (France) described by Peteuil et al. (2013) (see Section 6.2). It is worth noting that in our case, SSC thresholds did not fully meet the standards for riverine ecosystem protection mainly because of the sand (which was detected through turbidity measurements only marginally) that was sluiced from the dam.

In addition to the downstream geomorphic effects occurring shortly afterwards the sediment flushing, the time required to recover the pre-release conditions in the perturbed channels was also examined. For instance, Wohl and Cenderelli (2000) presented the geomorphic effects of a sediment release from the Halligan Reservoir in the US on the downstream pool and riffle channel. About 7,000 tonnes of silt and sand were deposited mostly in pools and whole runoff of the year after was needed to remove them. Moreover, two reaches were surveyed in detail and numerically investigated using 1-D sediment transport models (Rathburn and Wohl, 2001; 2003); the simulation of the recovery of the pools highlighted the need of detailed field observations to perform reliable model calibration.

4.3.2.2 Modelling of the Madesimo dam flushing event

Overall the 1-D approximation can be considered adequate to replicate the depositional pattern observed after the investigated CSF. In fact, the deposited sediment resulted rather uniformly distributed throughout the cross sections. This pattern can be explained by the simple shape of the cross sections, approximately rectangular, and by the channel morphology, mostly straight.

The river's transport capacity of non-cohesive sediments was computed by Yang's unit stream power formulas for sand (1979) and for gravel (1984). Yang's unit stream power formulae were used by Rathburn and Wohl (2001) to simulate pool scouring (see Section 4.3.2.1), giving satisfactory results. More recently, Ahn et al. (2013) used Yang's sand equation and extended the equation to cohesive sediment to numerically model sediment flushing (see Section 4.3.2.1). Yang (2006) found that the accuracy of Yang's unit stream power formulas was less sensitive to the variation of some parameters, such as the relative depth, the Froude number and the sediment load, in comparison to the other tested formulas. Moreover, they are appropriate for supercritical flows. López et al. (2014) tested the predictive power of ten bed load formulas against bed load rates observed in a large

regulated river (Ebro River, Spain), where they found that the Yang (1984) formula gave one of the best performances and that it was not as sensitive as other formulae to grain-size.

In the case of the Madesimo study, only a first-approximation scheme was adopted to model some elements, particularly the riverbed grain-size distribution. As it is well known (e.g. Bunte and Abt, 2001), quantitatively describing river-bed material in gravel- and cobble-bed streams is a rather complicated task, and the user is frequently required to make a number of informed decisions that depend on the objectives of the study and the conditions of the stream. Indeed, our case study was characterized by coarse river bed substrate and sediment transport composed mainly by materials finer than gravel, with no observed scouring; the choice was thus to adopt a basic representation of the river bed (see Section 4.1.5.2).

After the calibration of the parameters, we detected significant agreement between the observed and the calculated depositional patterns. It is worthy to remark that the volume of sediment deposited downstream of the reservoir was estimated through measurements of deposit thickness with a graduated rod. Even though this technique has been commonly used to measure the fraction of pool volume filled with fine sediments (e.g. Hilton and Lisle, 1993), it only provides basic estimates of the actual deposition, thus potentially affecting model calibration. In the case of the Liro River we believe, however, that the major source of uncertainty is most likely related to the limited number of monitoring sites. Nonetheless in some sites the thickness was only few centimetres and, therefore, the uncertainly of the estimates is of the same order of the magnitude of the measurement error.

Overall, our investigation indicates that the SRH-1D model can effectively support the further planning of analogous CSF, provided that a careful calibration of the parameters is performed using site-specific data. In particular, the sensitivity analysis highlighted the predominant effect of the bed material mixing parameters *nalt* and χ on the numerical solution. Conversely, the parameters controlling the adaptation length (i.e. α_d, α_e and b_L) did not influence significantly our numerical output, only α_d slightly affecting the solution. Moreover, the variation of n, at least within the range suited for the study channel, did not affect substantially our computational solution. In contrast, Lai and Greimann (2011) ran long-time simulations of a basically erosional case (Tachia River, China, downstream of the Shih-Gang Dam) by SRH-1D, finding higher sensitivity of the computed amount of eroded sediment to Manning's coefficient (which was varied in the same range of our simulations) than to the parameters *nalt* and χ. A prevailing role played by Manning's coefficient was also underlined by Ruark et al. (2011), who simulated a lab depositional case study by SRH-1D. On one hand, this fact could be explained by the relatively wide range considered in the investigation (i.e. 0.015-0.065). Moreover, the very comprehensive sensitivity analysis performed by those authors to

evaluate the effects of varying the model parameters on the computed bed elevation, revealed a complex interaction and a comparable influence of nearly all the investigated parameters.

Finally, it should be underlined that the simulations well reproduced the negligible deposition of very fine sediment, i.e. with diameter roughly below 0.1 mm, irrespectively from the parameters values. This peculiarity, documented in the field, is a relevant aspect of our investigated CSF: in fact, as it has been well established (e.g. Kemp et al., 2011; Owens et al., 2005), streambed clogging by very fine sediment can be critical for freshwater habitats, thus justifying the current research efforts concerning fine sediment dynamics (Smith et al., 2015).

5 Hydraulic dredging from Ambiesta Reservoir

This chapter reports on the hydraulic dredging of the Ambiesta Reservoir This operation was carried out for a total of 68 days during high flow season. The SSC in the downstream river was controlled regulating the amount of pumped sediment and the diluting water flow. The hydraulic dredging at the Ambiesta Reservoir was expensive; however, it allows restoring the safety operations of the bottom outlet without interfering with the normal reservoir operation.

5.1 Materials and methods

5.1.1 Study area

The Ambiesta Reservoir is located in North-Eastern Italy within the southern edge of the Alps (Figure 5.1). The Ambiesta Dam was closed in 1959 and impounds the Ambiesta River 6.0 km downstream of its springs and 4.8 km upstream its inlet into the Tagliamento River, the last morphologically intact river in the Alps (Tockner et al., 2003). The dam crest is at 486.5 m AMSL, the power intake at 444.8 m AMSL. The Ambiesta project comprises a surface spillway at 481 m AMSL (equipped with a 3 m high and 8 m long flap gate, Figure 5.2) and a 2.5 m diameter bottom outlet at 433.2 m AMSL. Both these structures bypass water from just upstream of the reservoir into the Ambiesta River by means of few hundreds meter long galleries. A further bottom outlet, a 1.2 m diameter pipe, is located into the body of the dam at 432.8 m AMSL. The original gross and effective storage capacity of the reservoir were 3.885×10^6 m^3 and 3.132×10^6 m^3, respectively. A 2011 reservoir bathymetry indicated a historical loss of gross storage capacity of 0.535×10^6 m^3. According to the estimates provided by the company managing the hydropower system in the area, the average annual rate of storage loss is less than 0.2%.

The catchment area at the Ambiesta dam is 9 Km^2. The diversion of water released from the Ampezzo HPP (55 MW installed capacity, 455 m effective head, Figure 5.1) and from numerous other intakes located in the surrounding streams (i.e. Lumiei, Tagliamento and Degano rivers) increases the catchment area up to 647 km^2. The basin develops in the Alpine and pre-Alpine area of Friuli that mainly consists of limestone, calcareous flysch and molasse (Tockner et al. 2003) and is characterized by minor anthropogenic activities.

The Ambiesta Reservoir performs the daily regulation of the incoming water volumes, thus feeding the Somplago HPP (166 MW installed capacity, 280 m effective head) that drains water into Lake Cavazzo (18.75×10^6 m^3). This lake has a small catchment (i.e. 9 km^2) and is mainly fed by the water released by the Somplago HPP. The size of sediment deposited into the Ambiesta Reservoir is

mostly fine-grained (80% silt and 20% clay) as a result of the peculiarities of the water supply (water is sand trapped at intakes or is provided by the Lumiei Reservoir).

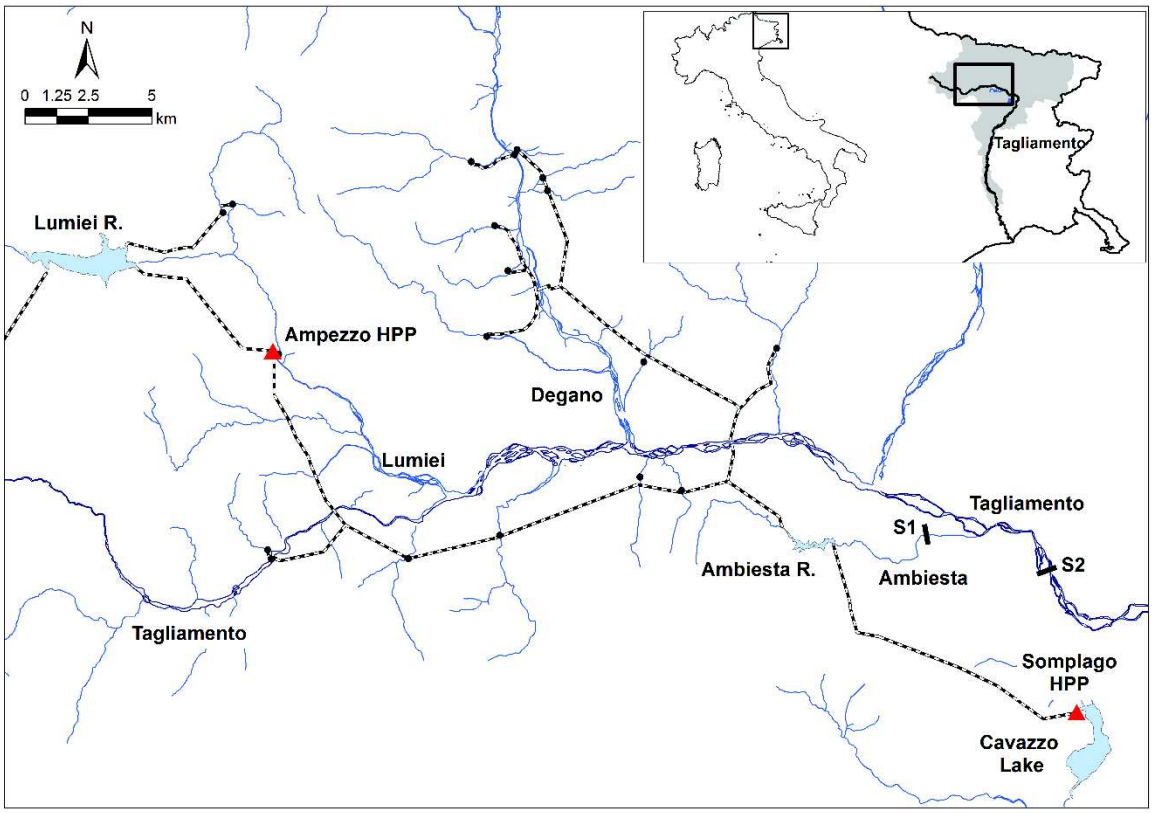

Figure 5.1. Study area. Location in Italy and in the Tagliamento basin. Main tributaries, water ducts (dashed lines), hydropower plants (HPPs- red triangles), reservoir (R.) and monitoring sites (S1 and S2).

Figure 5.2. (a) Ambiesta dam and (b) its surface spillway (outside the body of the dam).

Flow regime is influenced by both spring snowmelt and autumn precipitation, thus showing a bimodal flow pattern with peaks in May and October. The mean annual inflow at Ambiesta Reservoir is ca. 15 m^3/s, 20% of which consists of water discharged by the Ampezzo HPP. No flow is released downstream of the dam; the mean annual flow of the Ambiesta River at Tagliamento inlet is 0.4 m^3/s thanks to the water drained from the residual basin (i.e. 4.7 km^2).

The Ambiesta River downstream of the Ambiesta Reservoir flows for approximately 3.3 km mainly through a deeply incised canyon characterized by step-pool morphology (Montgomery and Buffington, 1997) and average slope of 0.039. Access is rather difficult, except for the final 1.7 km where the profile is smoother with average slope of 0.004. This part has a pool-riffle morphology.

5.1.2 Dredging operation

The 2014 hydraulic dredging of the Ambiesta Reservoir was planned to remove 25,000-35,000 m^3 of sediments burying the bottom outlets. The dredging area was defined in 5,000-6,000 m^2. This operation was carried out without interfering with the normal reservoir operation. The hydraulic dredges system consisted in a hull equipped with suction pipeline that picked up the sediment dislodged by the cutter-head thanks to a submerged ladder pump. The sediment pumped from the reservoir bottom were transported towards the surface spillway by means of a polyethylene pipe provided with floats (Figure 5.3). The sediment, together with the dilution water flow, were then discharged to the Ambiesta River through the bypass gallery. The pumping system was designed for discharging 0.04-0.08 m^3/s with a solid concentration of 200-300 g/l. The water discharge used for dilution purpose and for increasing the downstream transport capacity was fixed in at least 1.6 m^3/s.

Figure 5.3. Hydraulic dredging. The sediment mixed with water was discharged through the surface spillway to the Ambiesta River.

The months of October and November were selected accounting for the high water availability (see Section 5.1.1) and environmental requirements. In particular, the trout spawning period (December-February) and the spring (i.e. when trout are in their early life-stage) were avoided. Furthermore, the high flow period in April-May was also excluded for not reducing the water availability for the irrigation occurring in the following months.

As reported for the sediment flushing operations in the previous chapters, an SSC limit was set applying the N&J dose/response model. Similarly to the sediment flushing operations at Cancano Reservoir (see Section 3.1.2), a SEV of 11 was accepted corresponding to a fish mortality of 20-40%.

Accounting for 60 days duration, the SSC threshold was fixed to 1.5 g/l at S2, a Tagliamento River reach located 2.7 km downstream of the Ambiesta confluence (Figure 5.1).

5.1.3 Sediment monitoring

Optical turbidimeters (Lange Controller SC100®) were installed to continuously record SSC and OD at S1 (3.7 Km downstream of the dam) and S2 (Figure 5.1). The turbidimeter was factory calibrated with a suspension of Fuller's earth and provided an SSC output (a mean value each 15 minutes with 3 Hz sampling frequency). The probe was supported by a steel frame installed on the stream bank. Water and sediment samples were collected during the first two days of operation to calibrate the turbidimeters in-situ. These samples were randomly taken during daytime as close as possible to the probes by means of 1-liter handheld buckets (n=13 at S1 and n=11 at S2). The SSC of these samples was measured in the lab using the Standard Method 2540 D-F (APHA et al., 2005). The raw SSC data (SSC_{TUR}) were correlated to the corresponding lab data (SSC_{LAB}) and linear functions (SSC_{LAB}=A* SSC_{TUR}), one per station, were obtained through standard least-squares fitting. The agreement between the two measures was generally good and determination coefficient R^2 typically exceeded 0.96. The coefficients (A) of the linear functions were then used to modify the factory calibration curve of the turbidimeters in order to have reliable real-time SSC output. The total amount of removed sediment was assessed through ADCP bathymetric surveys in the reservoir carried out before and after the dredging operation.

5.1.4 Riverbed sampling

The accessible part of the Ambiesta River (see Section 5.1.1 and Figure 5.4) was surveyed by visual inspection in order to examine the riverbed alteration one month before and after the dredging operation. Riverbed sampling was performed at three transects, approximately 20 m equally spaced: S1A, S1B and S1C (from upstream to downstream). The most downstream transect S1C is located ca. 100 m upstream of S1. A pebble count (as per Wolman, 1954) was performed between S1A and S1C to determine the bed surface grain distribution (Figure 5.4). The representative percentiles D_{16}, D_{50} and D_{84} were 8 mm, 17 mm and 51 mm, respectively. Each transect was sampled in three points, two about one meter from the river edge and one in its centre. The silt/clay content in the uppermost layer of the riverbed was detected through the resuspension technique reported in the Section 3.1.3 by means of a McNeil corer. In the post-dredging survey, care was taken to sample the riverbed in the same points as in the pre-dredging survey. Furthermore, volumetric riverbed sampling was performed at each transect close to the central point already collected. Sampling was carried out using a 0.6 m high cylinder with a 0.5 m diameter. Water depth at the sampling points ranged from 0.1 to 0.25 m. Particles larger than 31.5 mm were measured and weighted in the field. All three axes were

measured and the corresponding sieve diameter was estimated from the particle intermediate and shortest axis dimensions (Bunte and Abt, 2001). The remaining subsamples of 4.5-7 kg were dried and sieved in laboratory. Overall, the analysed samples weighted 10-25 kg. As indicated by Rex and Carmichael (2002), one litre of turbid water was also collected after the removal of core samples to take the finer materials into account (see Section 4.1.3).

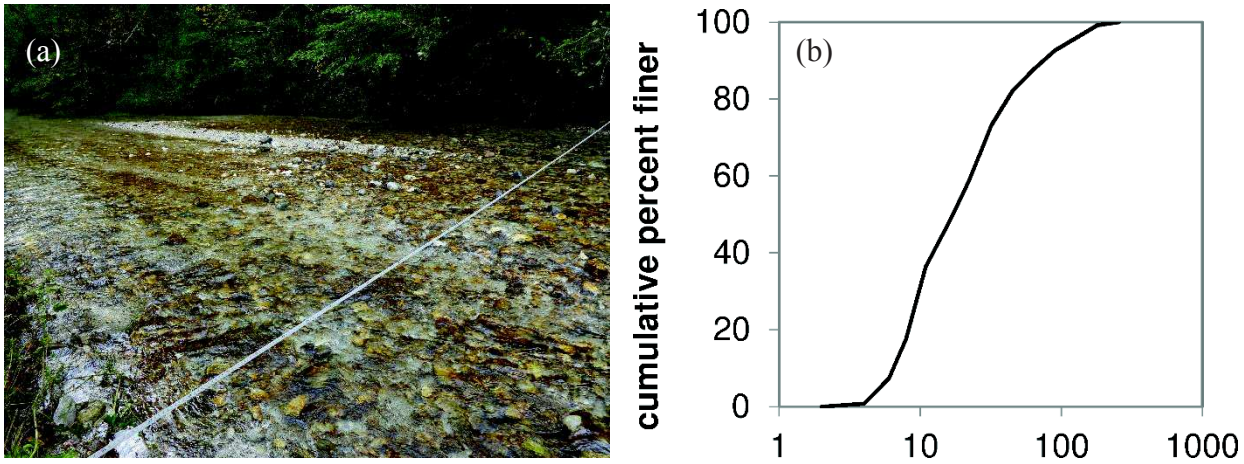

Figure 5.4. Monitored Ambiesta River just upstream of S1. (a) Photos taken before the dredging at S1 and (b) cumulative size distribution from Wolman pebble counts.

5.1.5 Biomonitoring

The impact of dredging from the Ambiesta Reservoir on the downstream aquatic ecosystem was evaluated through a pre-post monitoring of benthic macroinvertebrates and fish communities at S1. Benthic macroinvertebrates were collected one time before the dredging operation (in September 2014, i.e. pre-dredging sample) and three times after the works (in January, April and October 2015, i.e. post-dredging samples). Fish were sampled in September 2014 in a reach of approximately 1,700 m^2 to assess the community before the operations and then were removed to avoid a relevant fish mortality. However, to depict the recolonization of the monitored stream reach, fish sampling was also carried out after the works (i.e. in April and October 2014). The sampling procedures and data analysis were the same adopted for evaluating the sediment flushing effects (see Section 4.1.4).

5.2 Results

5.2.1 The hydraulic dredging operation and sediment monitoring

The dredging operation was carried out between the October 2nd and December 12th 2014, for a total of 68 days without affecting the ordinary hydropower production at Somplago HPP. The sediment removal was interrupted for two days (November, 5th and 6th) due to heavy rainfall. During this event, a daily maximum precipitation of 285 mm was measured at Ambiesta Dam (see Figure

5.5). The operation allowed to remove a total sediment volume of sediment of 30,600 m^3, estimated through bathymetric survey.

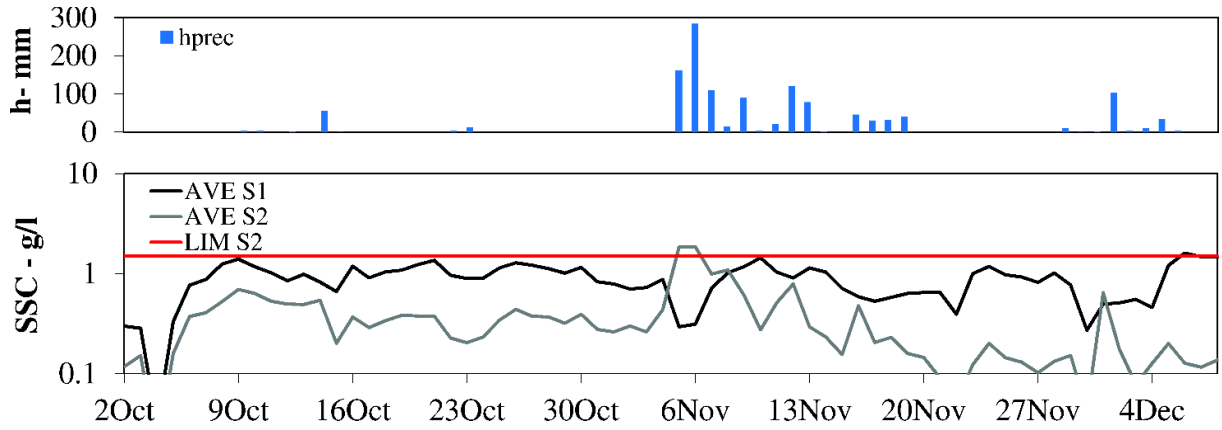

Figure 5.5. Time histories of daily average SSC at S1 (AVE S1) and S2 (AVE S2), SSC threshold at S2 (LIM S2) and daily precipitation height measured at Ambiesta Dam (hprec).

The Q released from the surface spillway of the dam did not change significantly neither during the day nor in the course of the dredging operation. In particular, Q generally ranged between 1.7 and 1.8 m^3/s; higher Q were discharged only during the two days that followed the above mentioned precipitation with mean and maximum daily value of 2.6 m^3/s and 4 m^3/s, respectively.

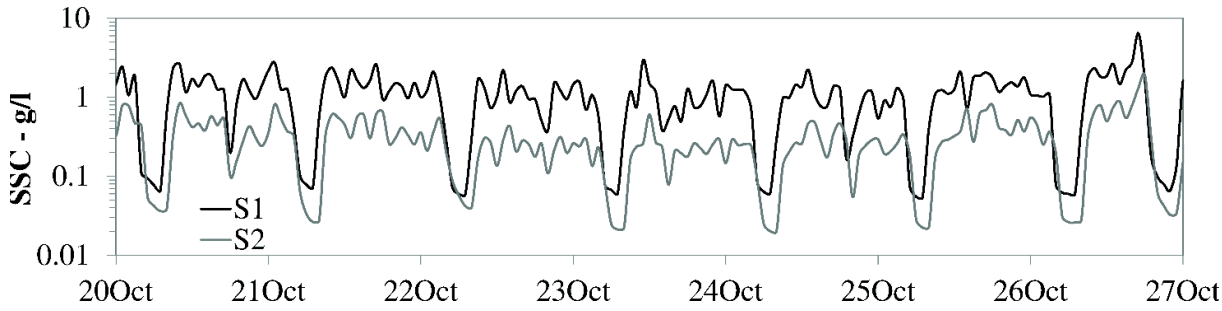

Figure 5.6. Example of time histories of hourly averaged SSC at S1 and S2.

The SSC pattern detected downstream of the dam showed regular daily pulses in response to the dredging activities (Figure 5.6). At S1, SSC peaked 2-8 g/l during daytime, dropping to less than 0.1 g/l during night-time (Figure 5.6). The daily averaged SSC at S1 was lower than 1.6 g/l; the maximum hourly SSC was generally 2-6 times higher than the daily averaged SSC (Figure 5.5). The SSC averaged on the whole operation was 0.9 g/l at S1. At S2, SSC was usually approximately 2/3 lower than at S1 with peaks less than 1-2 g/l during the days without precipitation. On the other hand, the rainfall clearly influenced the SSC at S2 (Figure 5.5). In particular, the daily average SSC at S2 during the rainy days was about twice higher than in the sunny days. This relevant SSC increase was not recorded at S1 due to the smaller natural catchment (see Section 5.1.1). Comparing the SSC

threshold of 1.5 g/l with the daily average SSC at S2, the limit was exceeded only during the two days of heavy rainfall when the dredging operation was interrupted (Figure 5.5, see Section 5.1.2). The SSC averaged on the dredging days was 0.3 g/l at S2 that is significantly lower than the mentioned threshold. In particular, SSC higher than 1.5 g/l was measured ca. 1.5% and 15% of the operation time at S2 and S1, respectively (Table 5.1). The SSC average on the whole operation at S1 was 0.9 g/l.

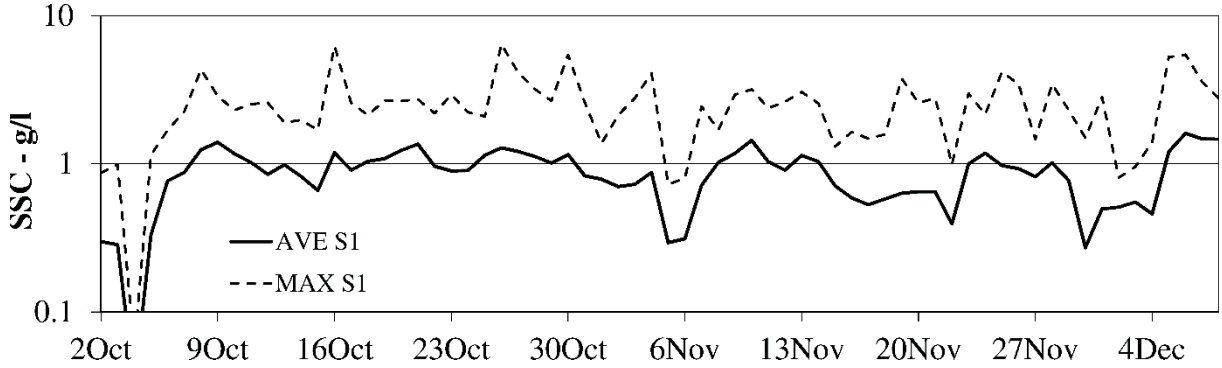

Figure 5.7. Time histories of daily averaged SSC (continuous line) and maximum hourly SSC (dashed lines) at S1 for the 2014 dredging operation.

SSC-g/l	5	4	3	2	1.5	1	0.5	0.1	0.05	0.01
Dur S1-%	0.5	0.9	2.0	6.4	15.4	37.5	61.8	85.3	95.2	100.0
Dur S2-%	0.0	0.0	0.2	0.6	1.5	5.7	18.8	72.5	83.2	97.8

Table 5.1. Duration of SSC at S1 and S2. Duration (Dur) is expressed as percentage of the overall operation time.

5.2.2 Riverbed sampling

Photographs of the three monitored transects (i.e. S1A, S1B and S1C) are provided in Figure 5.8, Figure 5.9 and Figure 5.10, respectively. Silt/clay deposits were not observed at these sections. Occasional silt/clay deposits were found in the rest of the surveyed reach, presumably in areas wetted during the flood or characterized by slow flow during the dredging operation.

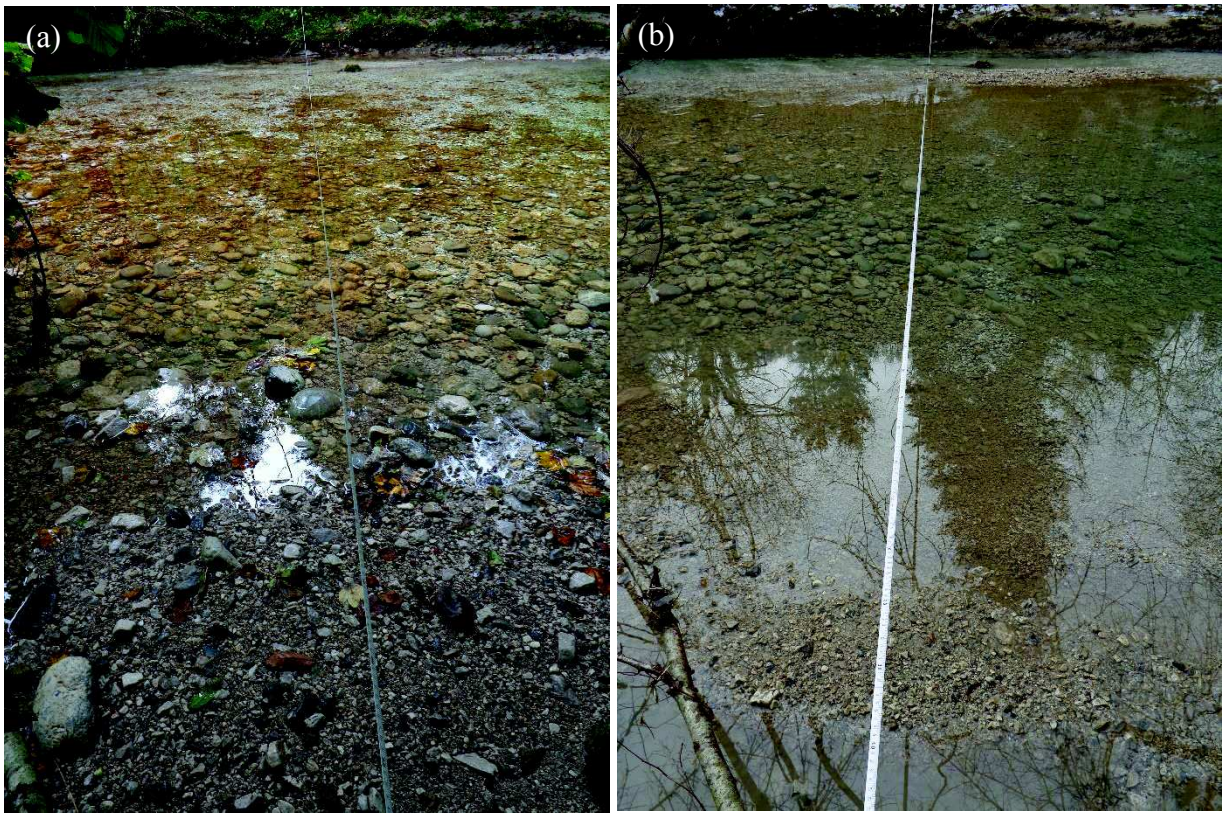

Figure 5.8. Photos taken one month (a) before and (b) after the dredging operation at S1A.

Figure 5.9. Photos taken one month (a) before and (b) after the dredging operation at S1B.

Figure 5.10. Photos taken one month (a) before and (b) after the dredging operation at S1C.

Grain-size distribution of the volumetric samples are provided in Figure 5.11. The percentage of silt/clay in the pre-dredging samples ranged between 0.1% and 0.4%. This percentage increased of approximately 1% in two (i.e. S1A and S1B) of the three sampling sampled transects; in the last one (i.e. S1C) it remained constant. The silt/clay content (mass per unit area) ranged from 0.11 to 0.35 kg/m^2 and from 0.27 to 1.06 kg/m^2, respectively in the pre and post-dredging samples collected with the resuspension technique (Table 5.2). The increase per unit area varied between 0.24 and 0.7 kg/m^2 as transect average.

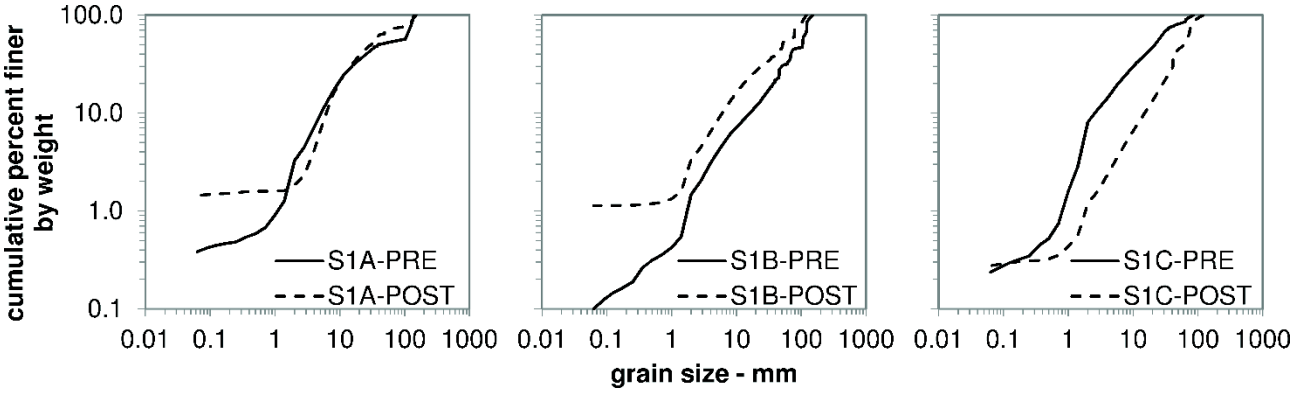

Figure 5.11. Grain size distribution of the McNeil samples at S1A, S1B and S1C.

section	sample position	Silt/clay content –		difference –	average difference –
		Pre	Post	Post-Pre	Post-Pre
S1A	right	0.14	0.66	0.52	0.27
	center	0.29	0.32	0.03	
	left	0.20	0.46	0.26	
S1B	right	0.28	0.50	0.22	0.24
	center	0.35	0.27	-0.08	
	left	0.13	0.73	0.60	
S1C	right	0.13	0.84	0.71	0.70
	center	0.11	1.06	0.95	
	left	0.27	0.73	0.46	

Table 5.2. Silt/clay content in the uppermost layer of the riverbed of the three monitored transects. Pre and Post indicate the sampling respectively carried out one month before and one month after the 2014 dredging operation.

5.2.3 Biomonitoring

The pre-dredging community of benthic macroinvertebrates collected at S1 was composed mainly of Coleoptera Elmidae, Plecoptera Leuctridae, Ephemeroptera Baetidae and Diptera Athericidae, Limoniidae and Chironomidae (Table 5.3). In the sample just after dredging, no relevant density reduction occurred while a non-negligible decrease in family richness (i.e. N families) and diversity (i.e. Shannon-Wiener) was detected (Table 5.4). Indeed, the first post-dredging sample was composed of 15 families with the dominance of only two taxa, Elmidae and Trichoptera Hydropsychidae (Table 5.3). However, an almost complete recovery of the benthic community occurred in spring, when some taxa (i.e. Baetidae and Ephemerellidae) boomed probably due to their life-cycle (Table 5.3). The Plecoptera Leuctridae and Diptera Athericidae appear the only taxa that did not recover the pre-dredging densities after one year from the monitored event (Table 5.3).

Although these changes in the benthic communities, the quality, defined through the STAR_ICMi, remained good for all the study period (Table 5.4).

As fish monitoring, before the dredging event the community was mainly composed of brown trout (Salmo trutta trutta) and bullhead (Cottus gobio) (Table 5.5). However, in the first post-dredging sample a community similar to the pre-flushing one was detected indicating that fish habitat conditions were not affected (i.e. that negligible substrate alteration due to sediment deposition occurred) (Table 5.5).

Taxon	Family	2014 (Pre)	2015 (Post)		
		September	January	April	October
Plecoptera	**Leuctridae**	90	7	3	27
	Nemouridae	14	1	8	1
Ephemeroptera	**Baetidae**	87	0	749	194
	Ephemerellidae	2	0	432	1
Trichoptera	**Hydropsychidae**	34	157	46	46
	Rhyacophilidae	2	0	14	3
Coleoptera	**Elmidae**	154	268	186	195
Diptera	**Chironomidae**	70	10	131	52
	Athericidae	90	15	40	31
	Simuliidae	13	0	130	22
	Limoniidae	10	15	33	17
Oligochaeta	**Lumbriculidae**	11	13	10	6
Other taxa	**-**	39	10	117	21

Table 5.3 Composition of the benthic macroinvertebrate communities collected at S1 before and after dredging. Density (individuals/m^2) is reported for each family sampled.

Metric	2014 (Pre)	2015 (Post)		
	September	January	April	October
Density (ind/m^2)	616	496	1899	616
N families	28	15	25	24
EPT	13	10	10	11
Shannon-Wiener	2.26	1.27	1.89	1.92
STAR_ICMi	0.89 (G)	0.76 (G)	0.80 (G)	0.79 (G)

Table 5.4 Metrics relative to the structure of the benthic macroinvertebrate communities collected at S1 before and after dredging.

Fish species	2014 (Pre)	2015 (Post)	
	September	April	October
Brown trout	140	146	82
Bullhead	170	105	170

Table 5.5 Main fish species collected at S1 before and after dredging. Density (individuals/ha) is reported for each species sampled.

5.3 Discussion

5.3.1 Dredging monitoring and management consideration

Dredging in lakes and reservoirs is mostly performed to construct and maintain commercial navigation. Dredging in reservoirs not used for navigation rarely involves more than 1×10^6 m^3 of sediment removal per site (Morris and Fan, 1997). This is focused on the cleaning of specific areas such hydropower intakes and bottom outlets due to the high costs (Morris and Fan, 1997). These costs induced to analyse other cheaper sediment strategies. For example, Ji et al. (2011) studied the possibility of replacing dredging at the Nakdon River Estuary Barrage (South Corea) with sediment flushing. However, an interesting application of reservoir dredging is the creation of a bottom channel in order to facilitate the transfer of turbidity currents during floods (Boillat et al., 2000).

The hydraulic dredging at the Ambiesta Reservoir was mainly carried out for restoring the safety operations of the bottom outlets. The operation was then oriented to the removal of a specific volume (i.e. ca. 30,000 m^3 of sediment) within a defined area. The Ambiesta Reservoir is an off-channel reservoir (Kondolf et al., 2014a) and is generally filled with diverted water with low sediment concentration of very fine sediment (i.e. silt/clay). Even if dredging is expensive compared to sediment flushing operation, it was selected because it allows to maintain the ordinary operation of the Somplago HPP that has been the most important source of water for Lake Cavazzo since the dam construction. Furthermore, it was not possible to perform a sediment flushing operation during high flow season due to the low capacity of the bottom outlets buried by the sediments. The cost of the dredging operation may be estimated in ca. 55 €/m^3 including the dredging works and the loss of hydropower. In particular, the cost of the dredging works accounted for ca. 70% of the sediment removal cost. Morris (2014) reported dredging costs of 5-15 \$/m^3 expected for 2013. This relevant difference is likely due to the small amount of sediment removed and the need to release water for dilution purpose (i.e. overall 9.9×10^6 m^3) for a long period (i.e. 68 days). The ratio between the volume of removed sediment and the volume of water used was 0.003. This value is in the range found for the CSFs performed in the Lake Como catchment in the last decade (see Section 6.3).

The SSC in the downstream river could be completely controlled during a hydraulic dredging operation regulating the amount of pumped sediment and of water used for dilution. On the contrary, SSC control during CSF operations could be difficult in some phases as reported for the Cancano CSFs (see Section 3.2.1). In this case study, the SSC limit of 1.5 g/l, fixed at S2 along the Tagliamento River, was largely respected (see Section 5.2.1). The SSC averaged on the whole period was 0.3 g/l at S2. Using this value, the SEV value computed by the N&J model was 10, reducing the predicted

fish mortality to 0-20%. Computed SEV at S1 was ca. 10.6 that corresponds to a fish mortality between 0-20% and 20-40%.

The SSC was calibrated in-situ in order to improve the reliability of the SSC records used for managing the dredging operation. For this purpose, the samples collected had a SSC lower than 1.5 g/l and 0.5 g/l at S1 and S2, respectively. SSCs higher than these values were recorded for the 15-20% of the overall operation time (Table 5.1). These SSC data were corrected extrapolating the calibration curve. Therefore, even if the in-situ calibration of the probe can be useful for the real-time management of the operation, further sampling are needed during all the dredging period allowing for a posteriori calibration of the probe that avoids extrapolations.

Riverbed sampling, even if performed only at few transects, seems to indicate a marginal sediment deposition. This result can be compared with those found for the 2011 Cancano (see Section 3.2.2) and the 2008 Valgrosina (Espa et al. 2013) CSFs. In fact, during these operations, silt/clay sediment was released and analogous field surveys were conducted in the downstream rivers. The range of fine sediment increase found in the Ambiesta case-study is relatively smaller (i.e. 0.3-0.7 kg/m^2) than those found in these study cases. In fact, a range of 0.5-1 kg/m^2 and 1-2.5 kg/m^2 as transect average was reported downstream from the Cancano and Valgrosina reservoirs, respectively. This difference may be related to the lower SSC detected at the Ambiesta monitoring site (i.e. 0.9 g/l as average) compared with 3.1-7.9 g/l and 3.5 g/l recorded at Cancano and Valgrosina stations. However, in all study cases the estimated deposition represent a very low fraction of the evacuated sediment.

The low impact of dredging on benthic macroinvertebrates and the fast recovery of both benthic and fish communities observed after the works seem to agree with the relatively low SSCs recorded during the event and the negligible fine sediment deposition. No relevant reduction of benthos density was observed in the first post-dredging sample as instead occurred after all of the monitored CSF operations (see Section 6.5), indicating a less severe effect due to an event (i.e. dredging) that lasted longer but showed significantly lower SSCs without high SSC peak. The decision of removing fish from S1 allowed to avoid a fish mortality that according to N&J model could be of more than 20% (i.e. SEV=10.6).

In conclusion, the results of this case study indicates that if sediment removal operations are performed controlling the SSC in the outflowing water and avoiding SSC peaks, the downstream environmental impacts can be effectively limited.

6 Overall discussion on CSFs

The evacuation of large amounts of sediments from reservoirs during sediment flushing operations can significantly impair the downstream environments. Only in recent years, the attention has been directed not only at maximizing the efficiency of sediment removal but also at developing strategies to minimize the environmental impacts that, up to now, limit sediment flushing feasibility. Morris (2014) recently identified the following mitigation measures:

- the use of biological as well as hydrologic criteria in selecting flushing dates (i.e. during high-flow periods but not during fish spawning),
- the availability of tributaries inflow, and thus of clear water releases for dilution and cleaning the riverbed after the sediment releases,
- the planning of more frequent flushing events resulting in smaller sediment releases during each event.

These general indications can be useful but specific approach may be developed taking into account site-specific considerations related to technical, economical and ecological constrains. Moreover, sediment flushing needs to be controlled limiting the sediment concentration of the sluiced water but existing thresholds for sediment concentration (Bilotta and Brazier, 2008) are generally unsuitable for flushing management (Crosa et al., 2010).

The CSFs at Cancano Reservoir (CR, Chapter 3) and at Madesimo Reservoir (MR, Chapter 4), along with previous CSFs carried out annually at Valgrosina Reservoir from 2006 to 2009 (VR, Espa et al., 2013) and at Sernio Reservoir in 2009 and 2010 (SR, Espa et al., 2015) can be considered as pilot case studies for improving the sustainable management of Alpine reservoirs through sediment flushing. The location of the investigated reservoirs, the hydropower systems and the monitoring sites are showed in Figure 6.1; the main characteristics of the reservoirs and hydropower plants are presented in Table 6.1.

In the following, the main findings from these case studies will be discussed highlighting not only the increased eco-sustainability of sediment flushing by controlling the sediment concentration in the downstream river but also the limits of the approach and the need of other ecosystem-based management criteria.

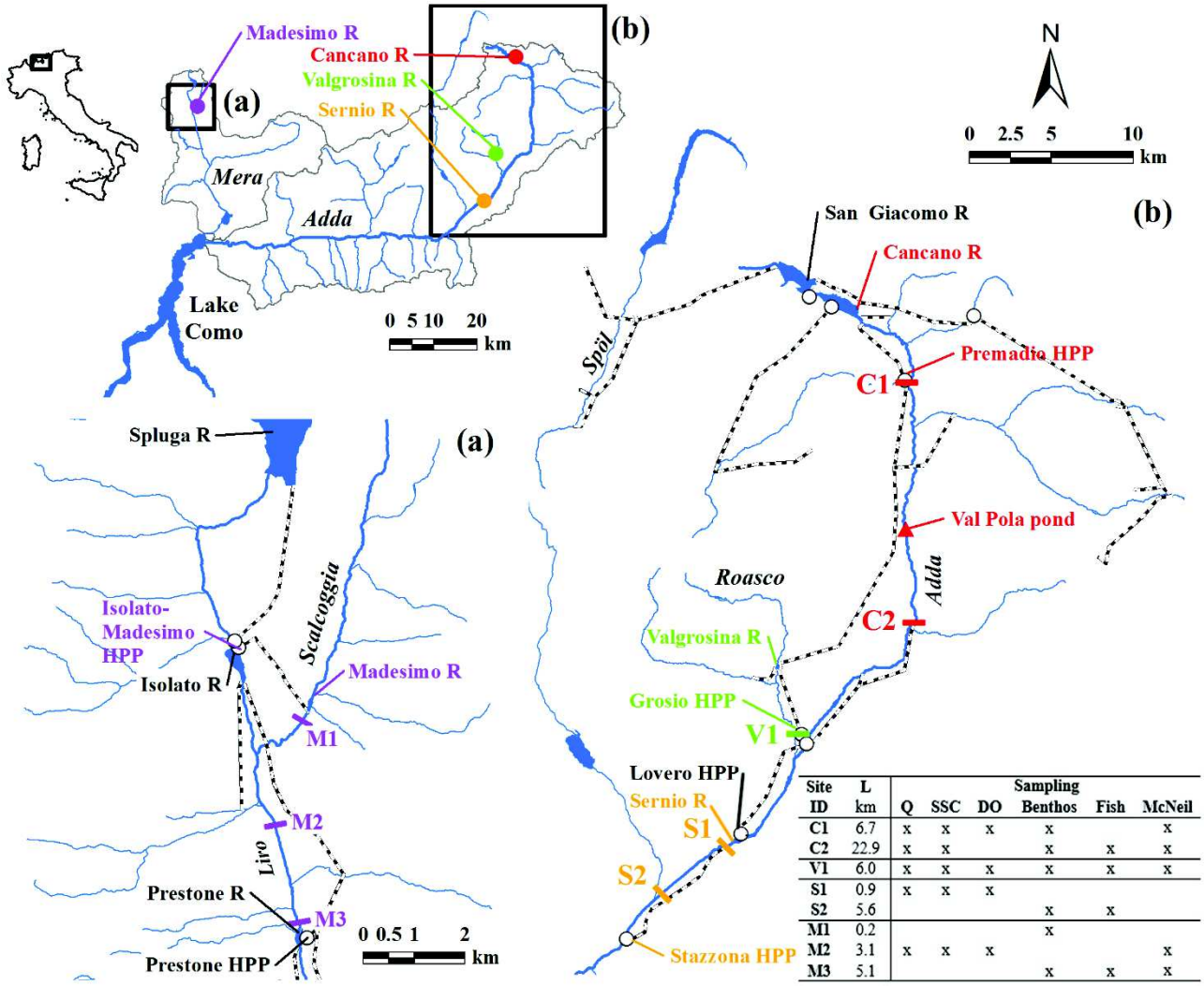

Site ID	L km	Sampling Q	SSC	DO	Benthos	Fish	McNeil
C1	6.7	x	x	x	x		x
C2	22.9	x	x		x	x	x
V1	6.0	x	x	x	x	x	x
S1	0.9	x	x	x			
S2	5.6				x	x	
M1	0.2				x		
M2	3.1	x	x	x			x
M3	5.1				x	x	x

Figure 6.1 Coloured circles indicate the four flushed reservoirs (R) located in the catchments of the Adda and Mera rivers, i.e. the main tributaries of Lake Como, northern Italy. Hydropower systems (dashed lines and white circles indicate the main ducts and hydropower plants - HPPs, respectively) and monitoring sites in the Liro Stream basin (a) and in the Upper Adda River basin (b). The table reports the distance from the dam of the monitoring sites (L) and the field surveys performed at each site.

Reservoir	Cancano	Valgrosina	Sernio	Madesimo
CAP ($\times 10^6$ m^3)	124	1.3	0.7	0.13
Z_{TOP} (m_{AMSL})	1901	1210	497	1524
A_{TOT}* (km^2)	370	712	885	25
MAR ($\times 10^6$ m^3)	271	533	757	41
HPP	**Premadio**	**Grosio**	**Stazzona**	**Isolato-Madesimo**
IC (MW)	226	430	30	17.3
EH (m)	647	600	88.7	273.5
Q_{MAX} (m^3/s)	40	80	40	8

*A_{TOT} corresponds to natural catchment area (A_{NAT}) for SR and MR, while for CR and VR A_{NAT} is 20 and 60 km^2, respectively.

Table 6.1 Main characteristics of the flushed reservoirs (CAP= capacity, Z_{TOP}= elevation of the top of active pool, A_{TOT}= total catchment area, MAR= mean annual runoff) and of the hydropower plants (HPPs) they supplied (IC= installed capacity, EH= effective head, Q_{MAX}= maximum power station discharge).

6.1 Planning phase

The CSFs performed in the Lake Como catchment in the last decade were planned considering the restrictions set by the local Authorities:

-the respect of SSC thresholds at specific sites downstream of the reservoir,

-the pre-/post-event monitoring of the ecological status (*sensu* WFD) of the downstream watercourses, that could be only temporarily deteriorated.

The SSC thresholds as average value over the whole flushing period and the ED were established using the N&J model and taking into account site-specific aspects (e.g. the needs of other river stakeholders and technical constrains). These limits are reported in the Table 6.2.

Reservoir	Period	Site	SSC_{LIM}	ED	SEV
CR	Feb-Apr	C2	3	40-50	11
VR	Aug-Sep	V1	4	12-13	10
SR	May-Jul	S1	1.5	15*	10
MR	Oct	M2	10	3	10

Table 6.2 Planning of the investigated CSFs: period of flushing, SSC_{LIM}= SSC threshold fixed at a site downstream of the flushed reservoir (Figure 6.1), ED= duration of exposure, and SEV= severity of ill effect.

The other features common to all of the CSFs included:

- emptying the reservoir and employing mechanical equipment only during daytime, thus releasing clear water during night-time,
- implementing mitigation measures and defining monitoring sites,
- real-time monitoring of SSC and DO and eventually re-design the on-going activities,
- surveying the physical effects along the wadeable river downstream of the reservoir (i.e. sediment deposition and riverbed substrate alteration),
- investigating the effects on benthic macroinvertebrates and their recovery, also evaluating the ecological status through a specific normative index (i.e. STAR_ICMi, see Section 6.5.3),
- surveying brown trout populations and comparing the observed effects with those predicted by the N&J model.

The planned mitigation measures mainly consisted in increasing Q in the rivers downstream of reservoirs through the regulation of tributaries intakes or the water releases from other reservoirs, thus enhancing the dilution and the transport capacity of evacuated sediments. Only for the CSFs at CR, these measures also included an instream settling basin for trapping sediment and the possibility of diverting the sluiced waters off-stream, conveying them to VR, in case of intolerable SSC (i.e. above 50 g/l) (see Section 3.1.2).

Different seasons were selected to carry out the works, mainly due to the size of outlet facilities and the needs of other river stakeholders. In general, the period for performing the CSFs was selected avoiding:

- the most sensitive period for trout (from December-February, i.e. the spawning period, to spring, i.e. when the trout are in their early life-stages),
- the large seasonal inflow for the safety employment of the earth-moving equipment and, in some cases, for the small hydraulic capacity of the bottom outlets (e.g. at VR and CR), with the only exception of the CSFs at SR.

At SR, the CSFs were planned during maximum seasonal runoff, but on non-consecutive days to improve the environmental sustainability (Espa et al., 2015). At CR, several technical difficulties, such as the degree of silting of the bottom outlet and its low capacity, led to the execution of the works between late winter and early spring, with low temperatures and low water flow (Section 3.1.2).

During the planning phase of CSFs, the N&J model allowed for the estimation of SSC and ED through the following five steps.

1) Selection of target fish species for defining the regression coefficients

The N&J model has the following formula:

$$SEV = A + B \times \ln(ED) + C \times \ln(SSC)$$

where A, B, C are regression coefficients, ED is the duration of exposure in hours and SSC is the suspended sediment concentration averaged on the whole duration in mg/l. Different regression coefficients are reported by Newcombe and Jensen (1996) as a function of fish species, thus the most adequate for the study context may be selected. The coefficients indicated for Salmonids-all ages (i.e. A=1.0642, B=0.6068, C=0.7384) were applied for the reported CSFs as brown trout is the dominant species in the study area.

2) Selection of tolerable SEV

The tolerable effects on target species may be selected as a function of the ecological status of the impacted river and/or the need to protect specific fish species or specific life stages, etc. SEV varies between 0 and 14; in particular, SEVs equal to 10,11,12,13,14 correspond to fish mortalities in the ranges 0-20, 20-40, 40-60, 60-80, 80-100%, respectively.

3) Definition of target volume (V_{sed}) or mass (M_{sed}) of sediment

It is necessary to quantify the volume to be silted, for example through bathymetric surveys. Then, adopting the appropriate bulk density, the volume can be converted in mass.

4) Selection of season and estimation of available Q

The season when the CSFs will be perform has to be defined taking into account multiple aspects, such as technical constrains, the need to control the amount of flushed sediment, needs of other river stakeholders and environmental aspects (e.g. most sensitive period for fish). The selected season has to be evaluated by a multidisciplinary team including river ecologist, water resources managers, hydropower engineers, and fluvial geomorphologists. The season influences not only the water

availability for sediment desilting, downstream dilution and riverbed cleaning but also the costs and efficiency of CSFs. Then, the available Q may be reasonably estimated as a function of the selected season. On one hand, it is advisable to perform the CSFs during the maximum seasonal runoff (White, 2001) to preserve the natural distribution of sediment load. On the other hand, the flushing "velocity" may have to be limited not only to avoid SSC peaks but also due to other further constraints (e.g. the operational feasibility of increasing Q, the need to avoid large Q to limit the carrying capacity of the flow, the digging rate of mechanical equipment, safety conditions for working in reservoirs, etc.).

5) Computation of SSC and ED

Once M_{sed} and Q are fixed, SSC is only a function of ED; therefore, if SEV is also established, ED and SSC are unequivocally determined using the N&J model. An alternative approach is to start from an estimate of the available clear water volume to conduct the CSFs; this case is immediately re-conducted to the previous one, as Q is the water volume divided by ED.

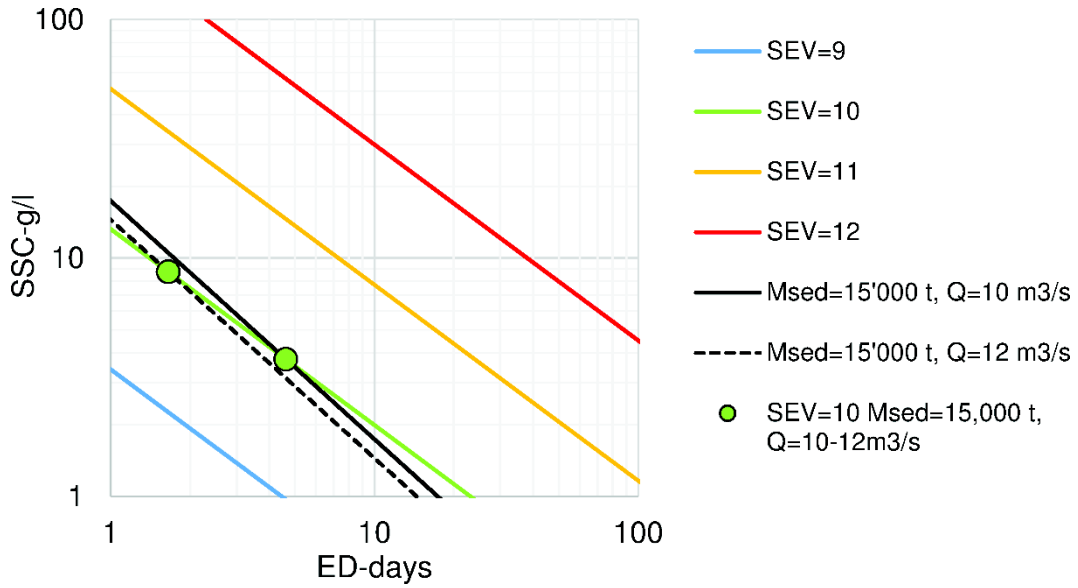

Figure 6.2 Examples of application of the Newcombe and Jensen (1996) model

The water availability strongly influences the computed flushing scenario. For example, taking into account an available Q ranging from 10 m^3/s (Case 1) to 12 m^3/s (Case 2), a target mass of 15,000 t and a tolerable SEV of 10, the model identifies the following two extreme scenarios characterized by significantly different SSC-ED pairs (Figure 6.2):

- Case 1: SSC=4 g/l and ED=4.5 days,
- Case 2: SSC=40 g/l and ED=1.5 days.

6.2 SSC peaks and DO reduction: the need of multiple SSC threshold approach

In all of the discussed CSFs, the SSC trends had a similar pattern. In fact, the SSCs were usually characterized by regular daily pulses due to the employment of mechanical equipment to dislodge the sediments during daytime activities, frequently coupled to an increase of water into the emptied reservoir or/and in the downstream river. Observed SSC averaged on the whole operation at sites where the thresholds were set, ranged from 0.3 to 4.7 g/l (Table 6.3). With the only exception of M2 (see Chapter 0 for further details), we assumed that the turbidimeter readings were representative of the average SSC at a given cross-section, due to the high turbulence that characterized the flow at the monitoring sites. For most of the time, the CSFs could be managed keeping the daily average SSC below the threshold. Critical phases (i.e. periods when it was not operationally possible to regulate the amount of flushed sediment) occurred during the works at VR and CR.

At VR, a critical phase occurred at the beginning of the first CSF in 2006. The high peak was due to the removal of sediment occluding the outlets (e.g. two pipes of 1.2 m of diameter) that remained closed for a long period (at least 10 years up to 2006). This CSF was the only one at VR for which the SSC threshold was not respected (Espa et al. 2013) and was useful to acquire experience for preventing erroneous operation in the following CSFs.

Reservoir	Year	ED	Site	Q_{AVE}	SSC_{AVE}	SSC_{MAX}	M_{TOT}
CR	2010	46	C1	1.0	3.5	30.2	14.6
			C2	3.4	0.3	3.3	4.6
	2011	53	C1	1.3	7.9	68.9	70.9
			C2	4.8	0.3	6.1	13.9
	2012	40	C1	0.9	5.9	99.2	26.1
			C2	3.4	0.8	38.2	12.1
VR	2006	13	V1	3.2	4.7	50.0	17.0
	2007	12		4.4	3.0	11.9	14.0
	2008	13		4.6	3.5	13.6	18.7
	2009	13		3.5	4.0	48.2	18.0
SR	2009	16*	S1	70	0.8	6.2	74.9
	2010	6*		60	0.73	3.6	24.0
MR	2010	3	M2	10	2.6	16.6	21.9

*non-consecutive days

Table 6.3 Main results of the physical monitoring of the CSFs (ED= duration of exposure, Q_{AVE}= average water discharge, SSC_{AVE}= average SSC, SSC_{MAX}= maximum SSC, M_{TOT} = total flowed mass).

At CR, the low capacity of the bottom outlet buried by more than 15 m thick deposits led the works to be operationally difficult with two main critical phases. A first critical phase occurred at the end of the 2011 CSF due to the combined effect of the opening of the bottom outlet and the increasing of the runoff into the CR (determined by a noticeable temperature increase that caused the rapid snowmelt runoff). During the first day of this critical phase, the sluiced water was diverted out of the

Adda River, towards the VR, thus allowing for the reduction of the SSC peak (see Section 3.2.1). A second critical phase took place at the beginning of the 2012 CSF, during the final emptying of the reservoir through its bottom outlet. This critical phase was shorter if compared to the previous one (less than one day), and off-stream diversion was deemed unnecessary. Nevertheless, during this phase, the absolute maximum SSC was detected at C2 (Table 6.3; Section 3.2.1).

These experiences highlighted the need of predicting critical phases in regulating the sediment release, and of planning specific measures to tackle them. Despite short in time, critical phases may spoil the efforts made to increase the sustainability of the operations since a sharp increase of the SSC may have strong impacts on the downstream ecosystems. At CR, some efforts were made to manage this problem by diverting the evacuated water off-stream. VR case studies indicated that the control of flushing operations could be improved by planning periodical removals (Espa et al. 2013).

The rapid SSC increase can combine with a rapid DO decrease creating critical condition for fish. For example, during the 1999 coordinated flushing event from Dashidaira and Unazuki reservoirs (Japan), Sumi and Kanazawa (2006) recorded the lowest DO levels (i.e. ca 6 mg/l) in correspondence of the SSC peaks (i.e. 161 and 52.1 g/l detected just downstream of the Dashidaira and Unazuki dams, respectively). The Authors reported that DO was monitored so as not to fall below 4 mg/l, i.e. two times the value that poses a risk to fish living in the downstream river (i.e. Kurobe River). Other studies reported that during flushing operation the oxygen depletion progresses to hypoxia (e.g. Baoligao et al., 2016; Buermann et al., 1995). In particular, recently, Baoligao et al. (2016) found a significant relationship between DO and SSC measured in the Yellow River downstream of the Xiaolangdi Reservoir (China) during the 2009 and 2010 flushing operations. DO decreased (from 8 mg/l at 25°C) to 3 and 1.1 mg/l and SSC increased to 80 and 65 g/l during the 2009 and 2010 event, respectively. In our case studies, the DO seems not to be a limiting factor. The DO levels remained above 10 mg/l (i.e. 90% oxygen saturation) during the CSFs at VR and SR. For the VR, this finding can be explained by the low water residence time (1 day), which avoids any hypolimnetic water stagnation, with the absence of significant polluting sources in the watershed drained by the reservoir water collecting system, and by considering the low water temperatures (daily water temperature excursion 7–11°C) (Espa et al., 2013). On the other hand, DO randomly measured during daytime at C1, reached lower levels than at V1 with values kept above 6 mg/l during the 2010 critical phase.

If a DO reduction is expected, the Garric et al. (1990) model can represent an alternative approach to the N&J model. This model predicts the ED that would not be exceeded by limiting at 10% the mortality rate of brown trout fry as a function of SSC and DO. However, the investigated range of DO is 0-6 mg/l, well below the DO recorded in our case studies.

For limiting the impact of SSC peaks, the SSC threshold as average value on the whole operation may be coupled with a SSC peak threshold. In general, this may be evaluated taking into account not only the effect of SSC peaks but also the possible DO reduction. The relationship between SSC and DO is site-specific and it is influenced by physical and chemical processes such as the absorption and release of organic matter and metal ions oxidation (e.g. Bilotta et al., 2008). For instance, a two threshold approach for SSC was applied only for the CSFs at SR. In particular, the SSC threshold averaged on the whole working day (i.e. 1.5 g/l) was coupled with an alert threshold to adjust the ongoing activity (i.e. 3.0 g/l) (Espa et al., 2015). This approach was used to further reduce the environmental impacts in the downstream Adda River reach characterized by a high environmental quality in an area of high tourist amenity. In particular, during the first CSF at SR, several days were employed in the gradual opening of the gates regulating the pondage outflow, for being confident to not exceed the SSC thresholds. A similar approach, with different SSC thresholds, was applied for the *environmentally friendly flushing* at Genissiat Reservoir (France). The sediment flushing from this reservoir is scheduled every 3 years for a duration of approximately 10 days fixing three different thresholds related to specific durations (Peteuil et al., 2013):

- the entire operation (SSC threshold equal to 5 g/l),
- a continuous period of 6 hours (SSC threshold equal to 10 g/l),
- a continuous period of 30 minutes (SSC threshold equal to 15 g/l).

Lombardy Region (2006) suggested to avoid SSC peaks higher than 30-40 g/l and proposed a multiple threshold approach fixing the SSC threshold as average value on the overall operation, the daily averaged SSC and the SSC peak (as average value on two hours). In particular, the daily and the peak SSC thresholds would be set at a value equal to two and six times the overall SSC threshold, respectively. Recently, Baoligao et al. (2016) proposed an overall SSC threshold equal to 32 g/l for a flushing duration of 66 h at Xiaolangdi Reservoir. The proposed threshold resulted from site-specific field investigations and laboratory experiments on a target fish (*Cyprinus carpio*) that can tolerate high SSC due to the naturally high SSC characterizing the Yellow River. This value is quite high if compared with the other ones previously reported. In conclusion, site-specific studies are crucial to evaluate the eco-sustainability of sediment flushing operations.

6.3 Cost and efficiency of sediment flushing

The cost estimated for the analysed CSFs for removing the unit volume of sediment ranged from 5 to 45 €/m^3. These costs include the loss of hydropower and the expenses connected to mechanical excavation. The lowest value is related to the 2009 CSF at SR that was performed taking advantage of the large water availability. It is similar to the cost of the 2012 sediment flushing at the Genissiat Reservoir (ca. 4 €/t; Peteuil et al., 2013). The 2010 CSF at CR was instead the most expensive one, due to the mentioned technical constraints that allowed performing flushing only during the low-flow season. This high cost is comparable to the maximum value (50 US$/m^3) for dry excavation by conventional earth-moving equipment in Los Angeles County reported by Morris and Fan (1997).

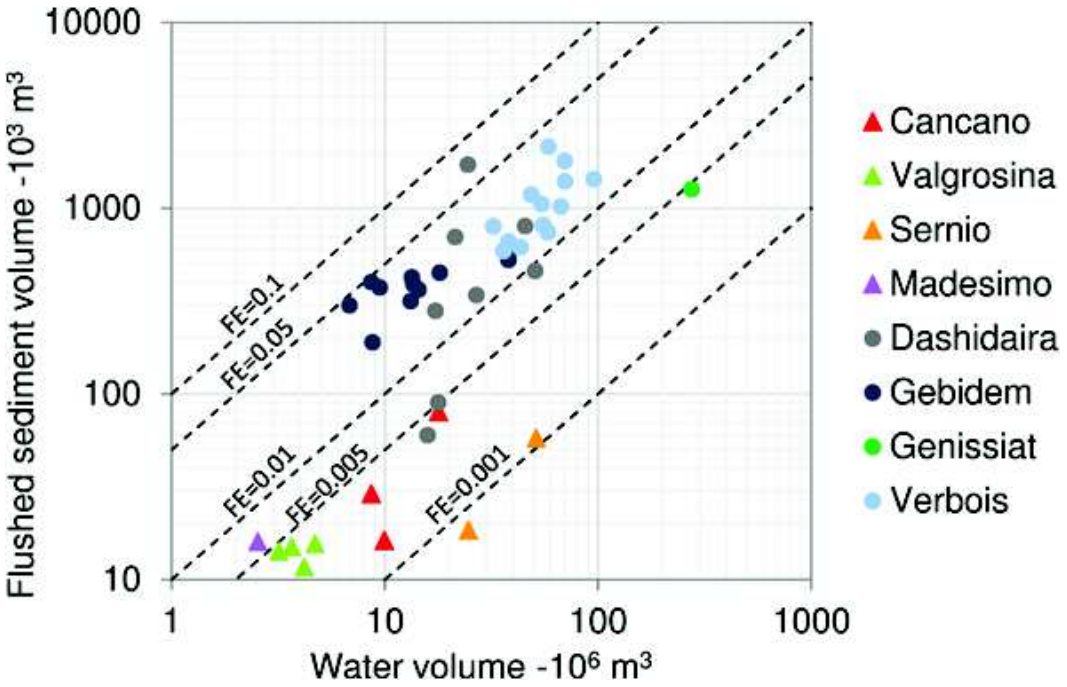

Figure 6.3 Flushing efficiency (FE). Comparison of the reported CSFOs with other worldwide sediment flushing operations. References: Sumi & Kanazawa (2006) for 9 events at Dashidaira Dam from 1995 to 2004, Meile et al. (2014) for 10 events at Gebidem Dam from 2004 to 2013, Peteuil et al. (2013) for 2012 event at Gebidem Dam, Cohen & Briod (1989) for 13 events from 1945 to 1981 at Verbois Dam.

The average daily flushed sediment ranged between 300 t/day for the 2010 CSF from CR to approximately 7000 t/day for the 2010 CSF from MR. Sediment flushing efficiency (FE) varied between approximately 0.001 and 0.006 (Figure 6.3). This parameter was calculated as the ratio between the volume of evacuated sediment and the corresponding volume of water employed in the CSF (including water for dilution purpose released in the downstream river). Only for the CSF at MR, the volume of sediment removed from the reservoir was quantified through bathymetry so, for the other case studies, the flowed mass through the most upstream monitoring sites (Table 6.3) was adopted for estimating the sediment volume. The density used to convert the sediment mass to a

volume was estimated by applying the procedure reported in Yang (2006), i.e. taking into account the composition of the reservoir sediment, the reservoir level regulation during normal operating conditions and the number of years of operation.

Compared with sediment flushing from Dashidaira Dam (Japan), Gebidem and Verbois dams (Switzerland) and Genissiat Dam (France) (Figure 6.3), our case studies had a lower flushed sediment volume (less than 100,000 m^3). On the other hand, the water volume used for the CSFs at CR and SR was of the same order of magnitude of those used for all of these events with the only exception of the Genissiat flushing that was characterized by the highest water volume. However, the FE of the Genissiat flushing sits in the range found for our CSFs. The low FE of our CSFs as well as of the Genissiat flushing is strictly linked to the SSC thresholds applied for limiting the environmental impacts. If the N&J model is considered, the FE of CSFs could be estimated by the ratio between the SSC threshold and the density of sediment deposited in reservoir. Thus, accounting for a density varying between 1,000 and 1,500 kg/m^3, a range of FE values could be found for each SSC threshold as showed in the Figure 6.4. In particular, if SEV limit is fixed at 11 and ED ranges between 3 and 53 days (as in our case studies), FE would be lower than 0.005-0.01 (Figure 6.4).

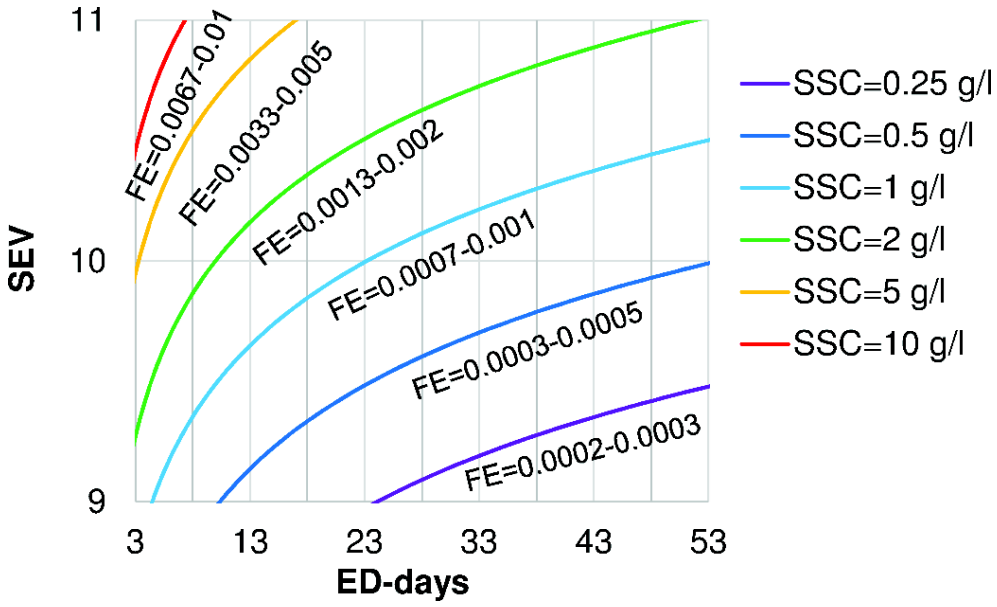

Figure 6.4 How SEV influences FE for the range of ED (i.e. 3-53 days) of the CSFs.

Morris and Fan (1997) reported that FEs vary widely and are heavily influenced by ED, but the range of values reported by the Authors is generally higher (i.e. up to 0.13) than that of our case studies. Furthermore, Sumi (2005) found that FE of different sediment flushing around the world ranged between 0.01 and 0.15 and suggested that it is necessary to limit it to approximately 0.05 or less for limiting environmental impacts. Although, the values of FE found in our CSFs and in the 2012 Genissiat sediment flushing are approximately one order of magnitude lower than those reported by Sumi (2005), non-negligible environmental impacts were detected (Section 6.5). Therefore, even

if the SSC thresholds and, as a consequence the FE, would be fixed taking into account site-specific conditions, the FE threshold value proposed by Sumi (2005) probably is still not enough conservative to ensure the control and the mitigation of the environmental impacts of sediment flushing.

6.4 Riverbed alteration

6.4.1 Flushing of silt/clay material

After the 2011 CSF at CR, only a slight increase of the silt/clay content was found in the riverbed wetted by MF, ranging from 0.5 to 1 kg/m^2 (average values computed for each transect). Similarly, after the 2008 CSF at VR, the samples of each transect showed an average increase of 1 and 2.5 kg/m^2. During these two CSFs, most of the sediment was transported in suspension and the deposition was limited (Espa et al., 2013; Section 3.2.2). Moreover, the deposition, as estimated with McNeil samples only in the riverbed wetted by MF, appeared to represent a very low fraction of the evacuated sediment and the increases of fines after flushing seemed not to represent a permanent alteration of the streambed substrate (Espa et al., 2013; Section 3.2.2). However, it should be noted that just few transects (i.e. two and four transects downstream of VR and CR, respectively) were surveyed and caution should be exercised in interpreting the results.

The maximum silt/clay content detected after the 2011 CSF at CR and the 2008 CSF at VR was 3.0 kg/m^2 and 4.3 kg/m^2, respectively. These values are comparable with the maximum ones (i.e. 3.9 kg/m^2) found by Piquè et al. (2014) for the Isàbena River (Spain) that naturally drains highly erodible badlands, and with the values found by Collins and Walling (2007) that examined 29 sites in the Frome and Piddle catchments (UK) (2.6 and 4.3 kg/m^2, respectively). Recently, Duerdoth et al. (2015) investigated depositional patches at 12 sites characterized by different substrate composition across different area of England and Wales, using an effective methodology for producing reach-scale estimates of deposited fine-grained sediment. They found surface sediment mass up to approximately 7 and 2 kg/m^2 at sites with coarse and moderate substrate, respectively, while the total surface mass varied up to more than 10 kg/m^2.

6.4.2 Flushing of silt/clay and sand material

After the CSF at MR, the content of particles smaller than 2 mm in the riverbed increased from 1 to 30 kg/m^2 (average values computed for three transects). The silt/clay content did not show a remarkable change, with mean values of approximately 1 kg/m^2. The grain size of sand deposits was mostly coarser than 250 μm. This fraction was not detected in suspension and thus it was mostly transported as bed load. The thickness of the deposits above the coarse surface layer was measured with a graduated iron rod at eight sites (Section 4.1.3). Mean values from 0 to 20 cm (i.e. up to 300-

450 kg/m^2) were found. Evans & Wilcox (2014), investigating the riverbed infiltration of contaminated fine sediment (< 2 mm) released after a dam removal, did not found these sediments within the bed material. The Authors suggested that, in natural systems, high sediment supply and mobile bed may limit seal formation and persistence. Even if further field surveys are needed, these results may indicate that the investigated deposition along the Liro River may be shortly reworked and transported downstream. However, the post-CSF habitat alteration affected the macroinvertebrate community (see Section 6.5.2).

6.5 Biological impacts

6.5.1 Short-term effects on benthos

The short-term effects of CSFs can be associated with the significant increase in streamflow and sediment concentration. Flood peaks can exert a particularly strong influence on the benthic fauna (McMullen and Lytle, 2012). Moreover, high SSC peaks can cause acute effects on benthos (Jones et al., 2012). Both the physical disturbances of the flowing waters (i.e. increased shear stress and river-bed overturn) and of the sediment load (i.e. abrasion by transported particles) probably contributed to impair the benthic communities during the CSFs by increasing the drift, and thus depleting the assemblages. Indeed, in the first post-CSF samples, collected within one month from the end of the works, a contraction of the benthic community, in terms of both density and richness, was detected at the monitoring sites (Figure 6.5).

In most cases, the decrease in density observed after CSFs exceeded 70% and family richness fell by 10-60%. In the case of density, a similar response to different doses might suggest an asymptotic behaviour, i.e. an analogous response of the benthic assemblage once certain SSC thresholds are exceeded. In fact, detectable impacts of SSC on invertebrate communities usually occur at values of few hundreds mg/l (Doeg and Milledge, 1991; García Molinos and Donohue, 2011), i.e. values considerably lower than those recorded during the CSFs. The lowest density reductions showed in Figure 6.5 were usually detected when the density of the pre-CSF sample was already low (e.g. the 2010 pre-CSF sample at SR; Espa et al., 2015). The correlation (R^2= 0.26, p= 0.02) between sediment dose and richness reduction led us to interpret this as taxon-specific response to this kind of perturbation, as discussed in the following Section 6.5.2.

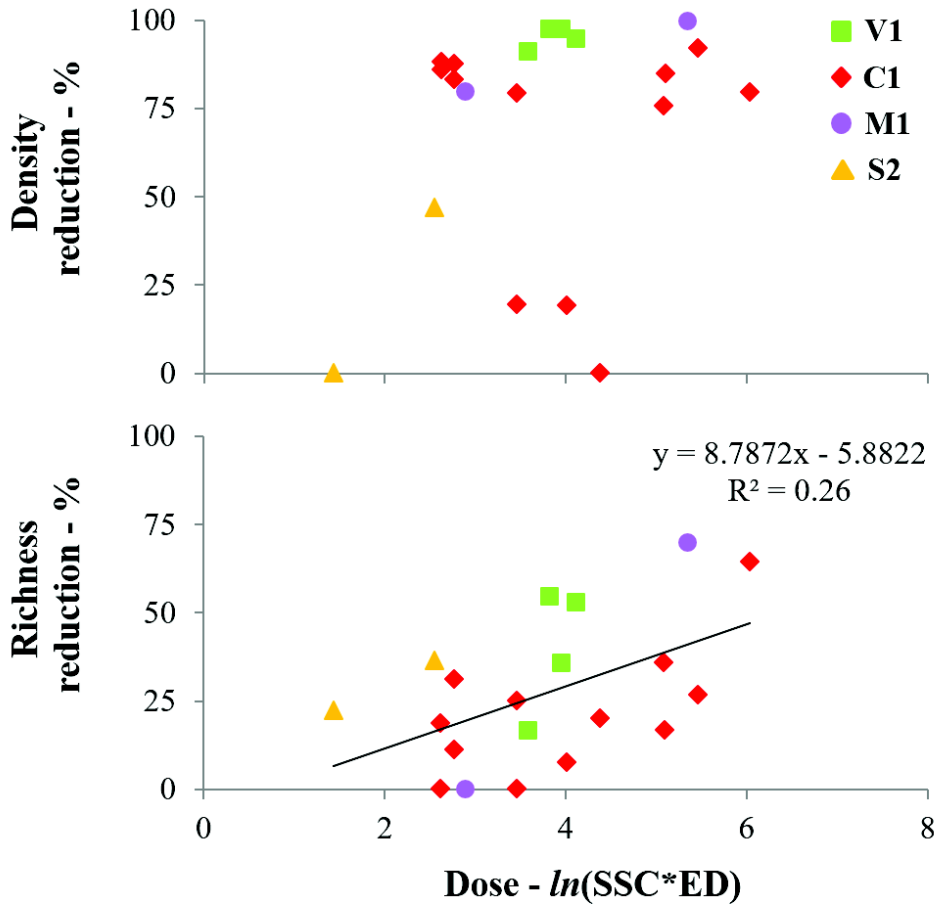

Figure 6.5 Percentage reduction of macroinvertebrate density and richness after CSFs as a function of the sediment dose. Percentage reduction was computed by comparing the first post-CSF sample to the corresponding pre-CSF one. The dose was computed according to Newcombe and Jensen (1996) as the natural logarithm of the average SSC (g/l) times the ED of the flushing event (days). Different symbols indicate the four analysed sites: square= V1, diamond= C1, circle= M1, triangle= S2.

6.5.2 Log-term effects on benthos

The long-term effects of CSFs can be mainly associated with the sediment deposition, which can determine persisting habitat alteration (Jones et al., 2012), thus tangling the recolonization of the benthic taxa. The time employed by the macroinvertebrate communities to re-gain previous density and richness after CSFs was different in the various case studies (Figure 6.6). For example, at V1 the benthic assemblages recovered in both density and richness within three months after the end of the works, while at C1 they recovered after approximately 250-300 days. At M1 nor density neither richness recovered to the pre-CSF values within a year after the CSF. These differences might be justified by different factors:

- the persisting riverbed alteration,
- the recolonization potential of a site, that is strictly dependent on its position in the fluvial landscape,
- the proximity of the flushing period to the high-flow season, that is known to cause a benthos contraction in Alpine rivers (Espa et al., 2015).

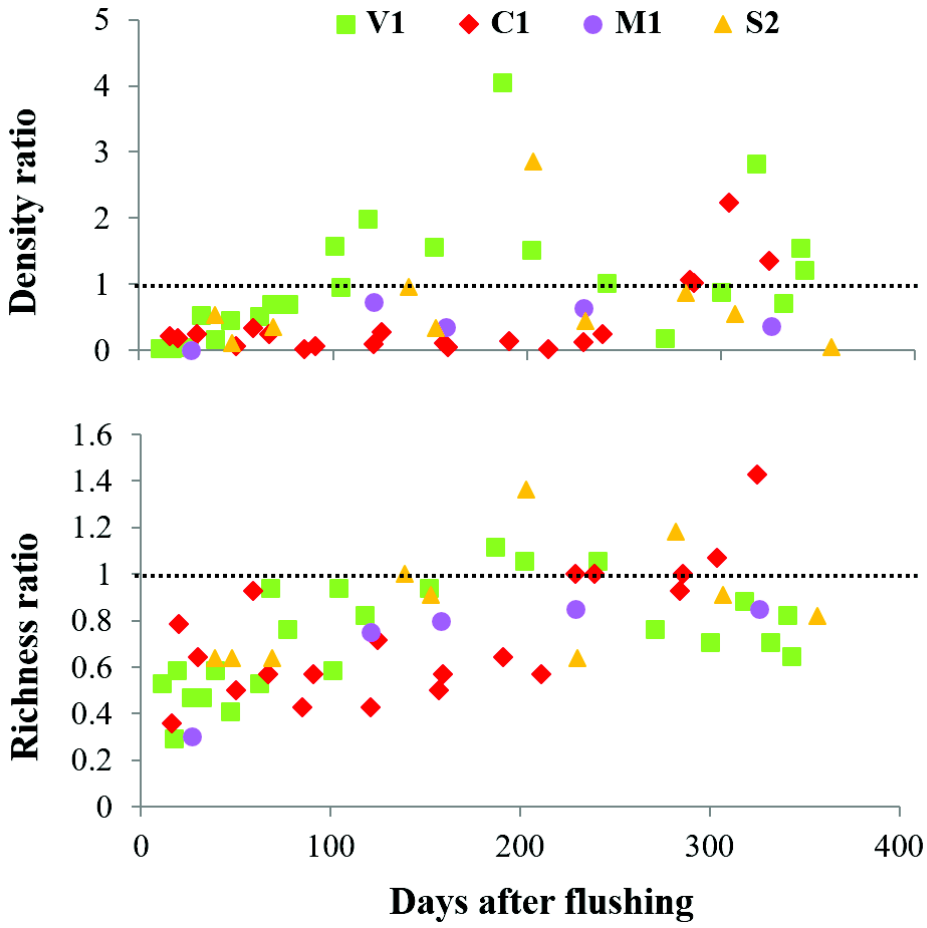

Figure 6.6 Temporal evolution of the density and richness of the benthic communities after the CSFs. Density and richness are expressed as ratios of the current value to the value detected in the corresponding pre-CSF sampling. Data related to the most upstream sites were used: V1, C1, M1, S2 (Figure 6.1).

At M1, in fact, a relevant sediment deposition was detected three weeks after the CSF (Section 4.2.1.2), while at the other investigated sites the deposition was considerably lower (i.e. approximately two orders of magnitude). At C1, the high-flow season, short after the CSF, could have delayed the benthos recovery.

The sampled data showed also a spatial gradient of the impact, proportionally to SSC that was larger at the upstream reaches. At the downstream sites (i.e. M3 and C2, Figure 6.1) a faster recovery was generally observed. For example, at M3 the recovery occurred within nine months. However, in all of the cases showed in Figure 6.7 a considerable change in community composition was observed immediately after the CSFs (i.e. between pre- and I post-CSF samples), while assemblages collected after one year from the end of the works (i.e. II post-CSF samples) nearly approached the pre-CSF ones.

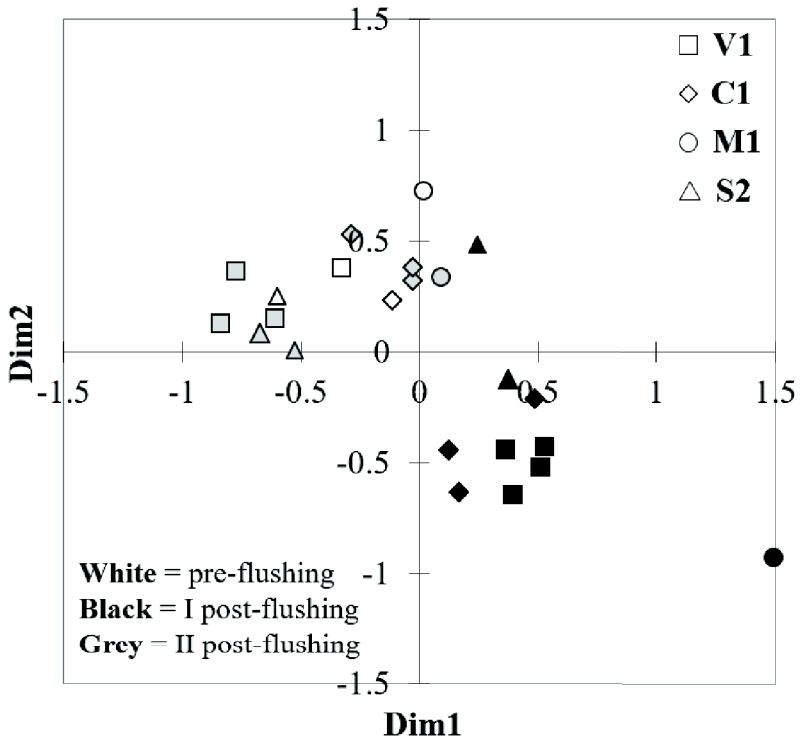

Figure 6.7 NMDS (stress value= 0.089) using Bray-Curtis distances of the macroinvertebrate assemblages collected at V1 (squares), C1 (diamonds), M1 (circles) and S2 (triangles). Pre-CSF, I post-CSF (i.e. samples collected within a month after flushing) and II post-CSF (i.e. samples collected after one year from the end of the works) samples are indicated in white, black and grey, respectively.

In Figure 6.8 the average composition of the macroinvertebrate communities of the pre-, I post- and II post-CSF samples is reported. Like most of the benthic communities found in regulated Alpine rivers (e.g. Monaghan et al., 2005; Yoshimura et al., 2006), the ones collected at the biomonitoring sites before the CSFs were composed of few resilient taxa. Just a few weeks after the CSFs, Leuctridae, Naemouridae, Baetidae, Rhyacophilidae and Chironomidae were detected in the benthos samples, while no or few specimens of Heptageniidae and Limnephilidae were collected. On these occasions, overall densities were very low, with Baetidae, Chironomidae and Naemouridae making up more than 50% of the community, demonstrating high resilience to the flushing disturbances probably due to their rapid reproduction and high tendency to drift (Matthaei et al., 1996).

Thus, the occurrence of CSF appears to temporary modify the macroinvertebrate community, allowing species with a fast life cycle and good colonizing ability to re-establish, and disadvantaging taxa that need stable environments to complete their life cycles. However, no cumulative effects, i.e. a progressive decline of the benthic community in the course of the years, were detected (Espa et al., 2013). The ability of lotic macroinvertebrate communities to recover from ecosystem disturbances is extensively documented in literature and it is confirmed by our field evidences. In particular, as observed in case of pulsing events, such as floods (e.g. Robinson et al., 2004) or pesticide applications (e.g. Crosa et al., 2001), the recovery can be relatively rapid, i.e. few months. Buendia et al. (2013a, 2013b, 2014) reported that in a mountainous river (i.e. Isábena River, Spain) naturally affected by

high suspended sediment loads, both invertebrate assemblage composition and patterns of turnover in assemblages were influenced by seasonal and habitat-specific rates of sedimentation. Assemblages appeared to exhibit resilience after high-flow events that removed the fine material (Buendia et al., 2014).

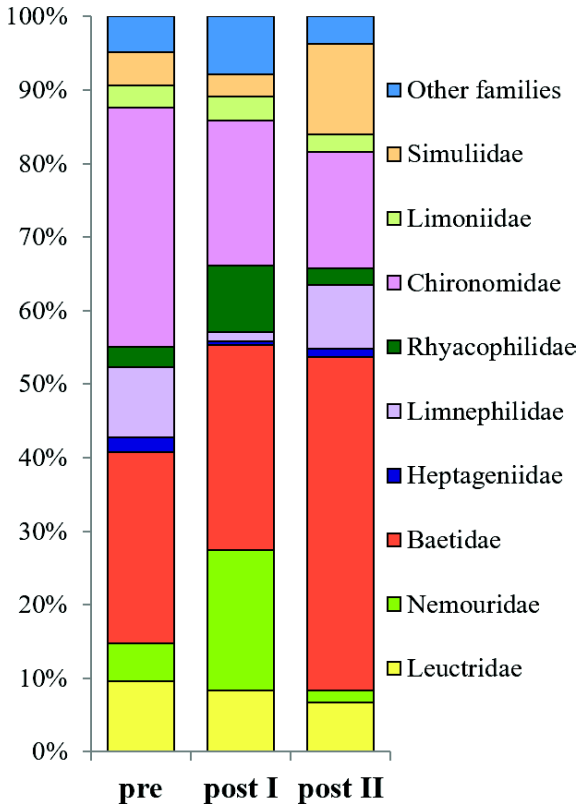

Figure 6.8 Average composition of the pre-CSF (i.e. pre), I post-CSF (i.e. post I) and II post-CSF (i.e. post II) samples collected at V1, C1, S2 and M1.

6.5.3 STAR_ICMi index for ecological quality

Currently, in the investigated area, sediment flushing would be carried out respecting WFD constraints on the ecological quality of the downstream freshwater ecosystems (see Section 6.1). In our case studies the ecological quality was evaluated through the application of the benthos based normative index, STAR_ICMi (Espa et al. 2015; Section 3.1.4).

As showed in the Figure 6.9, the response of this index to CSFs differed between sites. As expected, at M1 the quality decreased from good to moderate just after the CSF and slowly recovered, probably following the riverbed recovery. On the contrary, at C1 the index did not show the expected quality drop just after flushing but its reduction was mainly influenced by other factors (i.e. perturbation due to high flow in summer) as discussed in Section 3.2.3. Moreover, also within the same site the response to similar flushing events markedly differed, as detected for V1. However, only a temporary deterioration of the ecological status of downstream watercourses resulted from the CSFs as required by the Authorities (see Section 6.1).

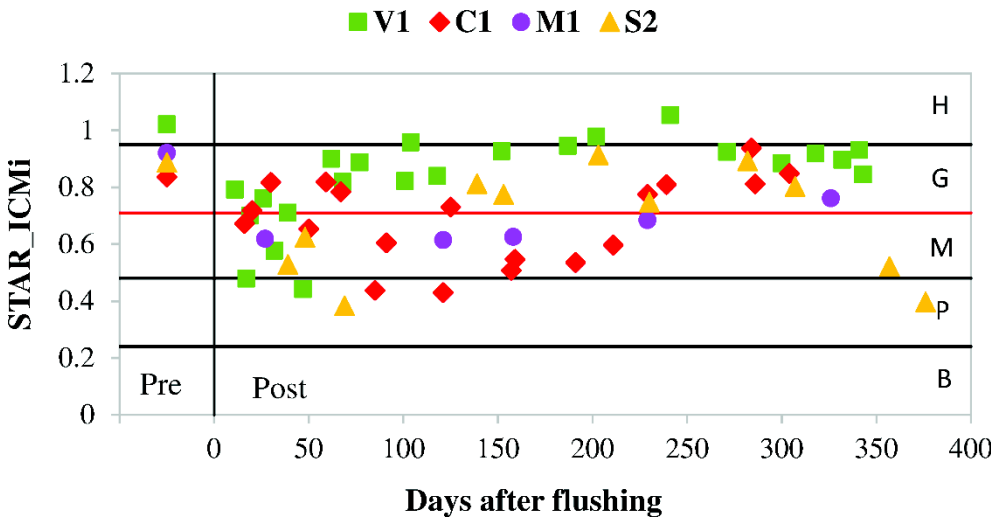

Figure 6.9 Temporal evolution of the STAR_ICM index. Data related to the most upstream sites were used: V1, C1, M1, S2 (Figure 6.1).The quality classes associated to the STAR_ICM index are reported: H= high, G= good, M= moderate, P= poor, B= bad.

As reported by Espa et al. (2015), care should be taken when evaluating the ecological stream quality through the STAR_ICMi since it would seem to overestimate the status of the benthic community in certain circumstances. Although assemblage composition, density, and diversity values could suggest a rather poor state of the benthic community, the STAR_ICMi frequently ranked among good quality class. This discrepancy is likely to be explained by the relatively high weighting assigned to the metric associated to organic pollution (e.g. Average Score Per Taxon; Sandin and Hering, 2004), which is not of concern at the monitoring sites. Moreover, the STAR_ICMi does not take into account the sample density that is markedly influenced by CSFs (Figure 6.5). Indexes developed to evaluate sediment pressure, like the Proportion of Sediment-sensitive Invertebrates (Extence et al., 2013) used in UK, consider both the sensitivity of the benthos taxa to the specific perturbation and the abundance of each taxon within a sample. Thus, a similar index would be developed for the Alpine benthic fauna and could represent an useful and adequate tool for flushing management.

6.5.4 Effects on trout and suitability of the N&J model

The total density of the brown trout populations decreased after almost all of the CSFs, with the largest reductions of approximately 50% (Table 6.4). Moreover, a selective pressure of the CSFs on juveniles (i.e. 0+) was demonstrated by the different responses to the CSFs of different age classes (Table 6.4). The CSFs at CR were carried out in the period of more marked sensitivity of trout to enhanced fine sediment loads (Kemp et al., 2011), i.e. the incubation stage (over winter in the study area). Furthermore, at M3, the average sediment deposition of approximately 30 kg/m^2 could have interfered with trout spawning since the proportion of sand in the substrate that is critical for Salmonids embryos and eggs was exceeded (Section 4.3.1).

In some cases, the density drops predicted using the N&J model underestimated the observed ones (Table 6.4). However, at C2, the density reductions of adults (i.e. ≥2+) could have been overestimated due to the fishing activity occurring at this site. In general, the results of the trout monitoring demonstrated that the N&J model can support the planning of sediment evacuation through CSF, providing a first estimate of the impact of flushing on fish fauna. Taking into account the complexity of the biological effects under study, this model can be indeed considered adequate for predicting the order of magnitude of the impacts of CSFs on the trout populations in the investigated sites. However, the application of the SEV model for the investigated CSFs can be questioned as discussed in the following.

Site	Year	Observed DR (%)				Expected
		0^+	1^+	$\geq 2^+$	Total	Total
V1	2006	69	30	(-60)	31	20-40
	2007	78	35	10	54	0-20
	2008	14	(-14)	(-8)	(-3)	20-40
	2009	35	8	5	19	20-40
C2	2010	96	25	0	45	0-20
	2011	75	29	52	47	0-20
	2012	100	(-9)	23	13	0-20
M3	2010	75	40	45	52	0-20

Table 6.4 Percentage density reduction (DR) of trout after the CSFs. The observed values (total population and subdivided into three age classes) are compared to the ones computed according to the Newcombe and Jensen [1996] model (calculated adopting the formula for Salmonids - all ages). The monitored sites are: V1, C2 and M3 (Figure 6.1). Brown trout surveys were performed few weeks before and after the CSFs.

First, the N&J model predicts the same SEV for short ED and high SSC and for long ED and low SSC. For example, a SEV equal to 11 is predicted for SSC=4 g/l and ED=5.5 day (Case 1) and for SSC=40 g/l and ED=1.5 days (Case 2) (see Section 6.1 and Figure 6.2). In the Case 1, the effect of the high SSC could have a relevant short-term effect due for example to gill abrasion. In the Case 2, the long-term effects could instead to be more significant than in Case 1. If there are no technical constrains, a shortest operations may be preferred. Nevertheless, the model does not take into account the possible reduction of DO level (see Section 6.2). Recently, Baoligao et al. (2016) highlighted that the computed SEV values underestimates the fish mortality rates detected in laboratory experiments on a target fish (*Cyprinus carpio*). In fact, in experiments with SSCs higher than 89 g/l and ED less than 1 hours, the model predicted SEV smaller than 9 but fish mortality rates were of 100% due to the combined effect of the DO reduction with the SSC increase. Furthermore, the SSC used for SEV estimation is averaged on the whole operation but CSFs with similar average SSC and different SSC peaks may cause very different impacts. Therefore, a particular attention would be given to select the flushing scenario and to manage SSC peaks (see Section 6.2).

Second, several alternatives (i.e. different pairs SSC-ED) could be found with similar predicted impacts on fish but non-negligible differences in the amount of flushed sediment. For example, if the

CSF is planned for 50 days duration and a SEV ranging between 10 (0-20% mortality) and 11 (20-40% mortality) is accepted, the SSC threshold may vary from ca. 0.5 g/l (Case A) to 2 g/l (Case B) (Figure 6.10). On the other hand, in the Case B the flushed sediment may be four times larger than in the Case A. Therefore, the model may be applied for a pre-assessment of different scenarios that may be then evaluated taking into account site-specific considerations. The environmental impacts found after the first CSF may allow changing the thresholds, balancing the need to improve flushing efficiency and limit the environmental impacts (see Section 6.2). Environmental factors, such as the availability of suitable habitat or food, may indeed determine different response to the same dose.

Finally, the site where the SSC threshold is fixed may be carefully evaluated including ecological aspects and technical constrains. The SSC generally decreases moving downstream due to water dilution and sedimentation. The SSC reduction was especially relevant downstream of the CR (Section 3.2.1). As a consequence, the predicted impact at C1 (i.e. the upstream site, Figure 6.1) is much heavier than at C2 (Figure 6.10).

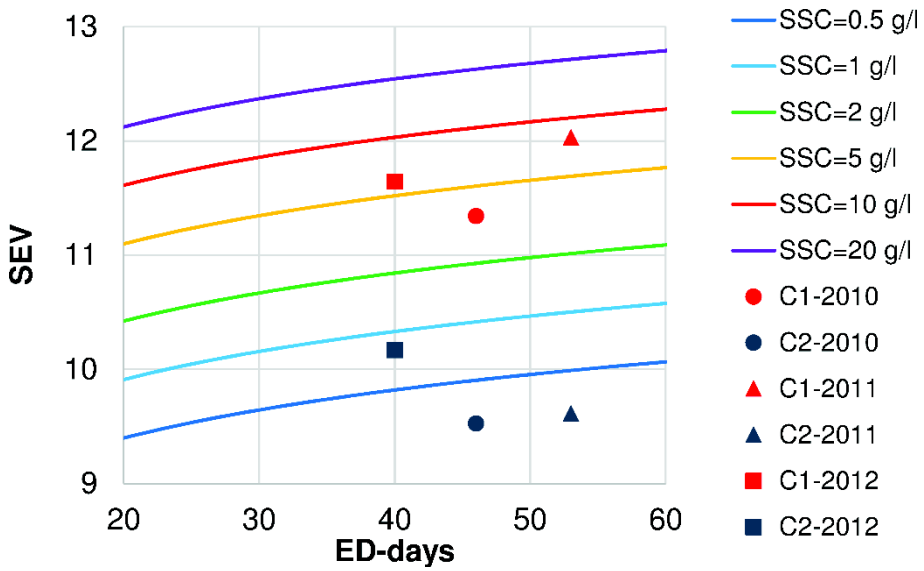

Figure 6.10. N&J model for Salmonids (all ages) and computed SEV values for CSFs from CR at C1 and C2

Ecosystem-based management criteria that include not only the effect of SSC and ED of the perturbation but also the riverbed substrate alteration are especially needed if the sand fraction of the flushed sediment is relevant. The riverbed alteration may indeed reduce the recovery capacity of macroinvertebrate community (Section 4.2.2.1 and Section 6.5.2) and the availability of trout spawning habitat.

7 Conclusion

7.1 Planning CSFs and sediment monitoring

The N&J model seems to be useful to guide the planning of sediment flushing operations towards a framework of environmental sustainability as it provides a first estimate of the impact on fish, thus allowing to fix SSC thresholds. On the other hand, low SEV variations result from significantly varying the input parameters of this formula. Consequently, it is possible to identify several alternatives with similar SEV values but with different flushing efficiency and operational cost. Furthermore, its application requires special caution if the operation is characterized by high-predicted SSC. If the target sediment volume to be removed is set, a short operation requires a higher water discharge and higher SSC, and other potential perturbations, such as hydropeaking effects and DO reduction, would be carefully evaluated. Furthermore, the duration of the operation and the water discharge might be defined taking also into account the needs to deal with critical phases in controlling the amount of flushed sediment. Therefore, the planning phase could be very complex, balancing conflicting interests (e.g. FE maximization and environmental impact mitigation), and remaining some aspects basically undetermined. Finally, the accurate monitoring of the environmental impacts of flushing operations would be the key element for getting improved site-specific and flushing-specific SSC thresholds. Studying sediment transport and environmental impacts of floods in the same area could be also useful for a comparison with the effects of CSFs.

Controlling the sediment concentration while flushing a reservoir is operationally difficult. The raw SSC data, continuously measured by means of turbidimeters, were used to control the operations and eventually re-design the on-going activities. Suspended sediment samples were generally exploited for the a posteriori calibration of the raw SSC data. The correction of the raw SSC was strictly linked with the grain size of the suspended sediment, it was site-specific and, for the same site, it may change for different CSF events.

7.2 Downstream riverbed alteration and sediment transport modeling

A relevant difference in the downstream riverbed alteration was found as a function of the size of the flushed sediment. When flushed material was primarily silt and clay (i.e. CR and VR case studies), deposition rates of few kg/m^2 were measured in the riverbed wetted by minimum flow. Otherwise, deposits up to 450 kg/m^2 were detected when an important fraction of the flushed sediments was sand (i.e. MR case study). These results suggest that, if the sediment in the reservoir are expected to be mainly sand, it might be important to evaluate not only the short-term effect of the SSC but also the long-term effect of the riverbed alteration.

If the amount of sand in the flushed sediment is relevant, the sediment monitoring would be improved for allowing the quantification of the total load by means of depth-integrated samplers and bed load samplers performed during CSFs. Moreover, these samples could provide an important dataset for the validation of the sediment transport model, such as the SRH-1D model already calibrated through the MR case study. The performed simulations suggest that, after proper calibration, sediment transport modelling can offer the necessary support to plan CSFs aimed at minimizing environmental effects. In fact, the computed pattern of deposits was in good agreement with the measurements carried out in the downstream Liro River after the CSF, both in terms of average deposit thickness and grain-size of deposited sediment. Nevertheless, the analysed scenarios as well as the model outputs need to be carefully evaluated from a multidisciplinary perspective (river geomorphology and ecology, catchment hydrology and water resources, hydropower engineering and operational costs) to ensure adequate efficiency of the desilting operation while minimizing downstream effects. Moreover, the calibrated model could be usefully applied for studying the sediment transport dynamics occurred in the downstream river after the CSFs for evaluating the channel recovery.

7.3 Ecological impacts and eco-hydraulic models

As the ecological impacts, we found that CSFs had severe effects on both the benthic macroinvertebrate communities and trout populations. However, the benthic communities were able to recover to the pre-CSF conditions within few months up to one year after the end of the works, if a considerable riverbed alteration (i.e. sediment deposition) did not occur. Effects on trout were considerable, especially for juveniles. However, brown trout repopulation programs, based on the use of hatchery-reared fish for maintaining good recruitment levels are currently carried out in the study area and could be further improved after the CSFs.

The planning of eco-sustainable sediment flushing operations is currently hampered by the lack of an adequate set of reference study cases and reliable eco-hydraulic models to predict the flushing effects on the downstream aquatic ecosystem and the time required for their recovery. An attempt to cover this knowledge gas was done through the discussed CSFs. This dataset needs to be enlarged and the biomonitoring improved to develop eco-hydraulic criteria specific for such a complex perturbation. For example, the field surveys could be upgraded adopting a before/after and control/impact (BACI) approach (Underwood, 1992) and identifying the benthic macroinvertebrates to species level for evaluating the most sensitive taxa. Moreover, the biomonitoring of benthic macroinvertebrates and the sampling of the riverbed sediments may be coupled for a better assessment of the geomorphic changes on the benthic fauna. Riverbed sediments may be then sampled as close as possible to the benthos sampling points.

References

APHA, AWWA, WEF (2005) Standard Methods for the Examination of Water and Wastewater, 21st edition. American Public Health Association, Washington

Arcement GJ, Schneider VR (1989) Guide for Selecting Manning's roughness coefficients for natural channels and flood plains. US Geological Survey Water-Supply, Denver, Paper 2339

Ahn J, Yang CT (2015) Determination of recovery factor for simulation of non-equilibrium sedimentation in reservoir. *International Journal of Sediment Research* 30:68-73. Doi: 10.1016/S1001-6279(15)60007-5

Ahn J, Yang CT, Boyd PM, Pridal DB, Remus JI (2013) Numerical modeling of sediment flushing from Lewis and Clark Lake. *International Journal of Sediment Research* 28(2):182-193. Doi: 10.1016/S1001-6279(13)60030-X

Baoligao B, Xu F, Chen X, Wang X, Chen W (2016) Acute impacts of reservoir sediment flushing on fishes in the Yellow River. Journal of Hydro-environment Research. DOI: 10.1016/j.jher.2015.11.003

Bilotta GS, Brazier RE (2008) Understanding the influence of suspended solids on water quality and aquatic biota. *Water Research* 42:2849-2861. DOI: 10.1016/j.watres.2008.03.018.

Booker DJ, Snelder TH, Greenwood MJ, Crow SK (2015) Relationships between invertebrate communities and both hydrological regime and other environmental factors across New Zealand's rivers. *Ecohydrology* 8(1):13-32. DOI: 10.1002/eco.1481.

Brandt SA, Swenning J (1999) Sedimentological and geomorphological effects of reservoir flushing: the Cachì Reservoir, Costa Rica, 1996. *Geografiska Annaler Series A* 81(3):391-407. Retrieved from http://www.jstor.org/stable/521477

Brune GM (1953) Trap efficiency of reservoir. *Eos, Transactions American Geophysical Union* 34(3):407-418.

Bryce SA, Lomnicky GA, Kaufmann PR (2010) Protecting sediment-sensitive aquatic species in mountain streams through the application of biologically based streambed sediment criteria. *Journal of the North American Benthological Society* 29 (2):657-672. DOI: 10.1899/09-061.1

Buendia C, Gibbins CN, Vericat D, Batalla RJ, Douglas A (2013a) Detecting the structural and functional impacts of fine sediment on stream invertebrates. *Ecological Indicators* 25:184-196. DOI: 10.1016/j.ecolind.2012.09.027.

Buendia C, Gibbins CN, Vericat D., Batalla RJ (2013b) Reach and catchment-scale influences on invertebrate assemblages in a river with naturally high fine sediment loads. *Limnologica* 43:362-370. DOI: 10.1016/j.limno.2013.04.005

Buendia C, Gibbins CN, Vericat D, Batalla RJ (2014) Effects of flow and fine sediment dynamics on the turnover of stream invertebrate assemblages. *Ecohydrology* 7(4):1105-1123. DOI: 10.1002/eco.1443.

Buermann Y, Du Preez, HH, Steyn GJ, Harmse JT, Deacon A (1995) Suspended silt concentrations in the lower Olifants River (Mpumalanga) and the impact of silt releases from the Phalaborwa Barrage on water quality and fish survival. *KOEDOE* 38(2):11-34. DOI: 10.4102/koedoe.v38i2.312

Buffagni A, Erba S (2007) Macroinvertebrati acquatici e Direttiva 2000/60/EC (WFD) - Parte A. Metodo di campionamento per i fiumi guadabili, IRSA CNR Notiziario dei metodi Analitici 2007(1).

Bundi U (2010) *Alpine Waters. The Handbook of Environmental Chemistry*. Volume 06, Springer-Verlag, Berlin, Germany. 278 pp. DOI: 10.1007/978-3-540-88275-6.

Bunte K, Abt SR (2001) *Sampling surface and subsurface particle-size distributions in wadable gravel- and cobble-bed streams for analyses in sediment transport, hydraulics, and streambed monitoring*. U.S. Department of Agriculture, Forest Service, Rocky Mountain Research Station, Fort Collins. http://www.stream.fs.fed.us/publications/PDFs/rmrs_gtr74.pdf

Burgherr P, Ward JV (2001) Longitudinal and seasonal distribution patterns of the benthic fauna of an Alpine glacial stream (Val Roseg, Swiss Alps). *Freshwater Biology* 46:1705-1721. DOI: 10.1046/j.1365-2427.2001.00853.x.

Cerdan O, Govers G, Le Bissonnais Y, Van Oost K, Poesen J, Saby N, Gobin A, Vacca A, Quinton J, Auerswald K, Klik A, Kwaad FJPM, Raclot D, Ionita I, Rejman J, Rousseva S, Muxart T, Roxo MJ, Dostal T (2010) Rates and spatial variations of soil erosion in Europe: A study based on erosion plot data. *Geomorphology* 122:167-177

Chapman JM, Proulx CL, Veilleux MA, Levert C, Bliss S, André MÈ, Lapointe NW, Cooke SJ (2014) Clear as mud: a meta-analysis on the effects of sedimentation on freshwater fish and the effectiveness of sediment-control measures. *Water research,* 56:190-202. DOI: 10.1016/j.watres.2014.02.047

Cohen M, Briod P (1989) Les apports solides de l'Arve dans le Rhône genevois. *La houille blanche*, (3-4), 301-305.

Coker EH, Hotchkiss RH, Johnson DA (2009) Conversion of a Missouri River dam and reservoir to a sustainable system: sediment management. *Journal of the American Water Resources Association* 45(4): 815-827. DOI: 10.1111/j.1752-1688.2009.00324.x

Collins AL, Walling DE (2007) The storage and provenance of fine sediment on the channel bed of two contrasting lowland permeable catchments, UK. *River Research and Applications*, 23(4):429-450. DOI: 10.1002/rra.992

Collins AL, Naden PS, Sear DA, Jones JI, Foster IDL, Morrow K (2011) Sediment targets for informing river catchment management: international experience and prospects. *Hydrological Processes* 25:2112-2129. DOI: 10.1002/hyp.7965

Crosa G, Castelli E, Gentili G, Espa P (2010) Effects of suspended sediments from reservoir flushing on fish and macroinvertebrates in an alpine stream. *Aquatic Sciences* 72:85-95. DOI: 10.1007/s00027-009-0117-z

Doeg TJ, Milledge GA (1991) Effects of experimentally increasing suspended sediment concentrations on macroinvertebrate drift. *Australian Journal of Marine and Freshwater Research* 42:519-526. DOI: 10.1071/MF9910519

Duerdoth CP, Arnold A, Murphy JF, Naden PS, Scarlett P, Collins AL, Sear DA, Jones JI (2015) Assessment of a rapid method for quantitative reach-scale estimates of deposited fine sediment in rivers. *Geomorphology*, 230:37-50. DOI: 10.1016/j.geomorph.2014.11.003

Esmaeili T, Sumi T, Kantoush SA (2014) Experimental and numerical study of flushing channel formation in shallow reservoirs. *Journal of Japan Society of Civil Engineers, Ser.B1* (Hydraulic Engineering), 70(4):19-24. DOI: 0.2208/jscejhe.70.I_19

Esmaeili T, Sumi T, Kantoush SA, Kubota Y, Haun S (2015) Numerical study on flushing channel evolution, Case study of Dashidaira Reservoir, Kurobe River. *Journal of Japan Society of Civil Engineers, Ser.B1* (Hydraulic Engineering), 71(4):115-120. DOI: 10.2208/jscejhe.71.I_115

Espa P, Castelli E, Crosa G, Gentili G (2013) Environmental effects of storage preservation practices: controlled flushing of fine sediment from a small hydropower reservoir. *Environmental Management*, 52(1):261-276. DOI: 10.1007/s00267-013-0090-0

Espa P, Crosa G, Gentili G, Quadroni S, Petts G (2015) Downstream ecological impacts of controlled sediment flushing in an Alpine valley river: a case study. River Res Appl 31(8):931-942. DOI: 10.1002/rra.2788

Evans E, Wilcox AC (2014) Fine sediment infiltration dynamics in a gravel-bed river following a sediment pulse. River Res Appl 30(3):372-384. DOI: 10.1002/rra.2647

Extence CA, Chadd RP, England J, Dunbar MJ, Wood PJ, Taylor ED (2013) The assessment of fine sediment accumulation in rivers using macroinvertebrate community response. *River Research and Applications* 29(1):17-55. DOI: 10.1002/rra.1569.

Frémion F, Courtin-Nomade A, Bordas F, Lenain JF, Jugé P, Kestens T, Mourier B (2016) Impact of sediments resuspension on metal solubilization and water quality during recurrent reservoir sluicing management. *Science of the Total Environment*, 562:201-215. DOI: 10.1016/j.scitotenv.2016.03.178

Fruchard F, Camenen B (2012) Reservoir sedimentation: different type of flushing - friendly flushing example of Génissiat dam flushing. *ICOLD International Symposium on Dams for a changing world*, June 2012, Kyoto, Japan, 6 pp.

Gabbud C, Lane SN (2016) Ecosystem impacts of Alpine water intakes for hydropower: the challenge of sediment management. *WIREs Water* 3:41-61. DOI: 10.1002/wat2.1124

Gallerano F, Cannata G (2011) Compatibility of Reservoir Sediment Flushing and River Protection. *Journal of Hydraulic Engineering* 137(10):1111-1125. DOI: 10.1061/(ASCE)HY.1943-7900.0000419

García Molinos J, Donohue I (2011) Temporal variability within disturbance events regulates their effects on natural communities. *Oecologia* 166:795-806. DOI: 10.1007/s00442-011-1923-2.

Garric J, Migeon B, Vindimian E (1990) Lethal effects of draining on brown trout: a predictive model based on field and laboratory studies. *Water Research* 24:59–65. DOI: 10.1016/0043-1354(90)90065-E

Gibbins C, Batalla RJ, Vericat D (2010) Invertebrate drift and benthic exhaustion during disturbance: Response of mayflies (Ephemeroptera) to increasing shear stress and river-bed instability. *River Research and Applications* 26(4):499-511. DOI: 10.1002/rra.1282.

Graf WL (2005) Geomorphology and American dams: The scientific, social, and economic context. *Geomorphology* 71(1-2):3-26. DOI: 10.1016/j.geomorph.2004.05.005

Graf WL, Wohl EE, Sinha T, Sabo JL (2010) Sedimentation and sustainability of western American reservoirs. *Water Resources Research* 46(12). DOI: 10.1029/2009WR008836

Greimann B, Lai L, Huang J (2008) Two-Dimensional Total Sediment Load Model Equations. *Journal of Hydraulic Engineering* 134(8):1142-1146. DOI: 10.1061/(ASCE)0733-9429(2008)134:8(1142)

Han Q, He M (1990) A mathematical model for reservoir sedimentation and fluvial processes. *International Journal of Sediment Research* 5(2):43-84.

Haun S, Olsen NRB (2012a) Three-dimensional numerical modelling of reservoir flushing in a prototype scale. *International Journal of River Basin Management* 10(4):341-349. DOI: 10.1080/15715124.2012.736388

Haun S, Olsen NRB (2012b) Three-dimensional numerical modelling of the flushing process of the Kali Gandaki Hydropower Reservoir. *Lakes & Reservoirs: Research and Management* 17(1):25-33. DOI: 10.1111/j.1440-1770.2012.00491.x

Hilton S, Lisle TE (1993) *Measuring the fraction of pool volume filled with fine sediment*. USDA Forest Service Research, Note PSW-RN-414, Berkeley

Huang JV, Greimann B (2012) *SRH-1D 3.0 User's Manual*, Sedimentation and River Hydraulics-One Dimension, Version 3.0. U.S. Bureau of Reclamation, Technical Service Center, Denver

Jones JI, Murphy JF, Collins AL, Sear DA, Naden PS, Armitage PD (2012) The impact of fine sediment on macro-invertebrates. *River Research and Applications* 28(8):1055-1071. DOI: 10.1002/rra.1516.

Kemp P, Sear D, Collins A, Naden P, Jones I (2011) The impacts of fine sediment on riverine fish. *Hydrological Processes* 25 (11):1800-1821. DOI: 10.1002/hyp.7940

Kennen JG, Riva-Murray K, Beaulieu KM (2010) Determining hydrologic factors that influence stream macroinvertebrate assemblages in the north-eastern US. *Ecohydrology* 3:88-106. DOI: 10.1002/eco.99.

Khosronejad A (2009) Optimization of the Sefid-Roud Dam desiltation process using a sophisticated one-dimensional numerical model. *International Journal of Sediment Research* 24(2):189-200. DOI: 10.1016/S1001-6279(09)60026-3

Kondolf GM (1997) Profile: hungry water: effects of dams and gravel mining on river channels. *Environmental Management* 21(4):533-551. DOI: 10.1007/s002679900048

Kondolf GM (2000) Assessing salmonid spawning gravel quality. *Transactions of the American fisheries Society* 129(1):262-281. DOI: 10.1577/1548-8659(2000)129<0262:ASSGQ>2.0.CO;2.

Kondolf GM, Gao Y, Annandale GW, Morris GL, Jiang E, Zhang J, Cao Y, Carling P, Fu K, Guo Q, Hotchkiss R, Peteuil C, Sumi T, Wang HW, Wang Z, Wei Z, Wu C, Yang CT (2014a) Sustainable sediment management in reservoirs and regulated rivers: experiences from five continents. Earth's Future 2(5):256-280. DOI: 10.1002/2013EF000184

Kondolf GM, Rubin ZK, Minear JT (2014b). Dams on the Mekong: cumulative sediment starvation. *Water Resources Research* 50:5158–5169. DOI:10.1002/2013WR014651

Krone RB (1962) Flumes studies of the transport of sediment in estuarial shoaling processes. University of California, Hydraulic Engineering Laboratory and Sanitary Engineering Research Laboratory, Final Report, Berkeley

Interagency Committee (1957) *Some fundamentals of particle size analysis, a study of methods used in measurement and analysis of sediment loads in stream*. Subcommittee on Sedimentation. Interagency Committee on Water Resources, St. Anthony Falls Hydraulic Laboratory Minneapolis, Report n°12, Minneapolis

Lai YG, Greimann BP (2011) *SRH Model Applications and Progress Report on Bank Erosion and Turbidity Current Models*. U.S. Bureau of Reclamation, Technical Service Center, Denver

Lambert CP, Walling DE (1988) *Measurements of channel storage of suspended sediment in a gravel-bed rivers*. Catena 15:65–80. DOI: 10.1016/0341-8162(88)90017-3

Lapointe MF, Bergeron NE, Bérubé F, Pouliot M-A, Johnston P (2004) Interactive effects of substrate sand and silt contents, redd-scale hydraulic gradients, and interstitial velocities on egg-to-emergence survival of Atlantic salmon (*Salmo salar*). *Canadian Journal of Fisheries and Aquatic Sciences* 61:2271-2277. DOI: 10.1139/f04-236.

Larsen S, Ormerod SJ (2010) Low-level effects of inert sediments on temperate stream invertebrates. *Freshwater Biology* 55:476-486. DOI: 10.1111/j.1365-2427.2009.02282.x.

Larsen S, Pace G, Ormerod SJ (2011) Experimental effects of sediment deposition on the structure and function of macroinvertebrate assemblages in temperate streams. *River Research and Applications* 27:257-267. DOI: 10.1002/rra.1361.

Lee BS, You GJY (2013) An assessment of long-term overtopping risk and optimal termination time of dam under climate change. *Journal of Environmental Management* 121:57-71. DOI: 10.1016/j.jenvman.2013.02.025

Legalle M, Santoul F, Figuerola J, Mastrorillo S, Céréghino R (2005) Factors influencing the spatial distribution patterns of the bullhead (*Cottus gobio* L., Teleostei Cottidae): a multi-scale study. *Biodiversity and Conservation* 14(6):1319-1334. DOI: 10.1007/s10531-004-9673-7.

Liu J, Minami S, Otsuki H, Liu B, Ashida K (2004a) Environmental impacts of coordinated sediment flushing. *Journal of Hydraulic Research* 42(5):461-472. DOI: 10.1080/00221686.2004.9641216

Liu J, Minami S, Otsuki H, Liu B, Ashida K (2004b) Prediction of Concerted Sediment Flushing. *Journal of Hydraulic Engineering* 130(11):1089-1096. DOI: 10.1061/(ASCE)0733-9429(2004)130:11(1089)

Lombardy Region (2008) Definizione dell'impatto degli svasi dei bacini artificiali sull'ittiofaunae valutazione di misure di protezione, Quaderni della ricerca n° 90, Luglio 2008, Copyright Lombardy Region.

López R, Vericat D, Batalla R (2014) Evaluation of bed load transport formulae in a large regulated gravel bed river: The lower Ebro (NE Iberian Peninsula). *Journal of Hydrology* 510:164-181. DOI: 10.1016/j.jhydrol.2013.12.014

Louhi P, Mäki-Petäys A, Erkinaro J (2008) Spawning habitat of Atlantic salmon and brown trout: general criteria and intra-gravel factors. *River Research and Applications* 24:330-339. DOI: 10.1002/rra.1072.

Luce JJ, Lapointe MF, Roy AG, Ketterling DB (2013) The effects of sand abrasion of a predominantly stable stream bed on periphyton biomass losses. *Ecohydrology* 6(4):689–699. DOI:10.1002/eco.1332.

Manap N, Voulvoulis N (2014) Risk-based decision-making framework for the selection of sediment dredging option. *Science of the Total Environment* 496:607-623. DOI: 10.1016/j.scitotenv.2014.07.009

Manap N, Voulvoulis N (2015) Environmental management for dredging sediments – The requirement of developing nations. *Journal of Environmental Management* 147:338-348. DOI: 10.1016/j.jenvman.2014.09.024

Matthaei C, Uehlinger U, Meyer E, Frutiger A (1996) Recolonization by benthic invertebrates after experimental disturbance in a Swiss Prealpine river. *Freshwater Biology* 35(2):233-248. DOI: 10.1046/j.1365-2427.1996.00496.x.

McMullen LE, Lytle DA (2012) Quantifying invertebrate resistance to floods: A global-scale meta-analysis. *Ecological Applications* 22:2164-2175. DOI: 10.1890/11-1650.1.

McNeil WJ, Ahnell WH (1964) *Success of Pink Spawning Relative to Size of Spawning Bed Material*. U.S. Fish and Wildlife Service, Special Scientific Report-Fisheries No. 469, Washington

Meile T, Bretz NV, Imboden B, Boillat, JL (2014) Reservoir sedimentation management at Gebidem Dam (Switzerland). *River Flow 2014*, Special Session on Reservoir Sedimentation (No. EPFL-CONF-202033, pp. 245-255), CRC Press/Balkema

Michel C, Schmidt-Posthaus H, Burkhardt-Holm P (2013) Suspended sediment pulse effects in rainbow trout (*Oncorhynchus mykiss*) - relating apical and systemic responses. *Canadian Journal of Fisheries and Aquatic Sciences* 70(4):630-641. DOI: 10.1139/cjfas-2012-0376.

Mochizuki S, Kayaba Y, Tanida K (2008) Responses of benthic invertebrates in an experimental channel to artificial flushes. *Hydrobiologia* 603:73-81. DOI: 10.1007/s10750-007-9248-1.

Monaghan MT, Robinson CT, Spaak P, Ward JV (2005) Macroinvertebrate diversity in fragmented Alpine streams: implications for freshwater conservation. *Aquatic Sciences* 67(4):454-464. DOI: 10.1007/s00027-005-0787-0.

Monk WA, Wood PJ, Hannah DM, Extence CA, Chadd RP, Dunbar MJ (2012) How does macroinvertebrate taxonomic resolution influence ecohydrological relationships in riverine ecosystems. *Ecohydrology* 5(1):36-45. DOI: 10.1002/eco.192.

Montgomery DR, Buffington JM (1997) Channel-reach morphology in mountain drainage basins. *Geological Society of America Bulletin* 109(5):596-611. DOI: 10.1130/0016-7606(1997)109<0596:CRMIMD>2.3.CO;2

Morris GL, Fan J (1997) *Reservoir sedimentation handbook: design and management of dams, reservoirs, and watersheds for sustainable use*. McGraw-Hill, New York. ISBN: 007043302X

Morris GL (2014) Chapter 5: Sediment Management and Sustainable Use of Reservoirs. In: Wang, L.K., Yang, C.T. (Eds), Modern Water Resources Engineering. Humana Press, pp. 321-325. ISBN: 978-1-62703-595-8

Morris GL (2015) Management Alternatives to Combat Reservoir Sedimentation. *International Workshop on Sediment Bypass Tunnels*, April 2015, Zurich, Switzerland, 5 pp.

Mukundan R, Walling DE, Gellis AC, Slattery MC, Radcliffe DE (2012) Sediment source fingerprinting: transforming from a research tool to a management tool. *Journal of the American Water Resources Association* 48(6):1241-1257. DOI: 10.1111/j.1752-1688.2012.00685.x

Newcombe CP, Jensen JOT (1996) Channel suspended sediment and fisheries: a synthesis for quantitative assessment of risk and impact. *North American Journal of Fisheries Management* 16(4):693-727. DOI: 10.1577/1548-8675(1996)016<0693:CSSAFA>2.3.CO;2

OFEFP - Office fédéral de l'environnement des forêts et du paysage (2004) Méthodes d'analyse et d'appréciation des cours d'eau en Suisse. Poissons niveau R (région), Informations concernant la protection des eaux N°44, Berne. 63 pp.

Ortlepp J, Mürle U (2003) Effects of experimental flooding on brown trout (*Salmo trutta fario* L.): the River Spöl, Swiss National Park. *Aquatic Sciences* 65:232-238. DOI: 10.1007/s00027-003-0666-5.

Owens PN, Batalla RJ, Collins AJ, Gomez B, Hicks DM, Horowitz AJ, Kondolf GM, Marden M, Page MJ, Peacock DH, Petticrew EL, Salomons W, Trustrum NA (2005) Fine-grained sediment in river systems: environmental significance and management issues. River Research and Applications 21 (7):693-717. DOI: http://dx.doi.org/10.1002/rra.878

Palmieri A, Shah F, Dinar A (2001) Economics of reservoir sedimentation and sustainable management of dams. *Journal of Environmental Management* 61(2):149-163. DOI: 10.1006/jema.2000.0392

Palmieri A, Shah F, Annandale GW, Dinar A (2003) Reservoir conservation, vol. 1: the RESCON approach, The International Bank, Washington, D.C.

Partheniades E (1965) Erosion and deposition of cohesive soils. *Journal of the Hydraulics Division*, 91(1):105-139

Peter DH, Castella E, Slaveykova VI (2014) Effects of a reservoir flushing on trace metal partitioning, speciation and benthic invertebrates in the floodplain. *Environmental Science: Processes & Impacts* 16(12):2692-2702. DOI: 10.1039/C4EM00387J

Peteuil C, Fruchard F, Abadie F, Reynaud S, Camenen B, Guertault L (2013) Sustainable management of sediment fluxes in reservoir by environmental friendly flushing: the case study of Genissiat dam on upper Rhone River (France). *12th International Symposium on River Sedimentation*, Kyoto

Piqué G, López-Tarazón JA, Batalla RJ (2014) Variability of in-channel sediment storage in a river draining highly erodible areas the Isàbena, Ebro Basin. *Journal of Soils and Sediments*, 14(12): 2031-2044. DOI: 10.1007/s11368-014-0957-6

Poff NL, Allan JD (1995) Functional organization of stream fish assemblages in relation to hydrological variability. *Ecology* 76(2):606-627. DOI: 10.2307/1941217.

Quadroni S, Crosa G, Espa P, Gentili G., Zaccara S (2014) Eco-hydraulic survey of streams and rivers highly exploited for hydropower in the central Italian Alps. *Proceedings of the 10th International Symposium on Ecohydraulics*, Trondheim, Norway, June 23-27.

Rathburn SL, Wohl EE (2001) One-dimensional sediment transport modeling of pool recovery along a mountain channel after a reservoir sediment release. *Regulated Rivers: Research & Management* 17(3):251-273. DOI: 10.1002/rrr.617

Rathburn SL, Wohl EE (2003) Predicting fine sediment dynamics along a pool-riffle mountain channel. *Geomorphology* 55:111-124. DOI: 10.1016/S0169-555X(03)00135-1

Rathburn SL, Rubin ZK, Wohl EE (2013) Evaluating channel response to an extreme sedimentation event in the context of historical range of variability: Upper Colorado River, USA. *Earth Surface Processes and Landforms* 38(4):391-406. DOI: 10.1002/esp.3329

Rex JF, Carmichael NB (2002) Guidelines for monitoring fine sediment deposition in streams. Resources Information Standards Committee, Victoria

Robinson CT, Uehlinger U, Monaghan MT (2004) Stream ecosystem response to multiple experimental floods from a reservoir. *River Research and Applications* 20:359-377. DOI: 10.1002/rra.743.

Ruark MD, Niemann JD, Greimann BP, Arabi M (2011) Method for Assessing Impacts of Parameter Uncertainty in Sediment Transport Modeling Applications. *Journal of Hydraulic Engineering* 137(6):623-636. DOI: 10.1061/(ASCE)HY.1943-7900.0000343

Sandin L, Hering D. 2004. Comparing macroinvertebrate indices to detect organic pollution across Europe: a contribution to the EC Water Framework Directive intercalibration. Integrated Assessment of Running Waters in Europe. *Developments in Hydrobiology* 175:55–68. DOI: 10.1007/978-94-007-0993-5_4

Smith HG, Evrard O, Blake WH, Owens PN (2015) Preface - Addressing challenges to advance sediment fingerprinting research. *Journal of Soils and Sediments* 15:2033–2037. DOI: 10.1007/s11368-015-1231-2

Statzner B (2011) Mineral grains in caddisfly pupal cases and streambed sediments: Assessing resource use and its limitation across various river types. *Annales de Limnologie-International Journal of Limnology* 47(2):103-118. DOI: 10.1051/limn/2011004.

Sumi T (2005) Sediment flushing efficiency and selection of environmentally compatible reservoir sediment management measures. *International Symposium on Sediment Management and Dams*, 2nd EADC Symposium, 25-26 October 2005, Yokohama (Japan).

Sumi T, Kanazawa H (2006) Environmental study on sediment flushing in the Kurobe River. *22nd International Congress on Large Dams*, Barcelona, pp 219-242.

Thompson LC, Cocherell SA, Chun SN, Cech jr. JJ, Klimley AP (2011) Longitudinal movement of fish in response to a single-day flow pulse. *Environmental Biology of Fishes* 90:253-261. DOI: 10.1007/s10641-010-9738-2.

Tomlinson ML, Perrow MR (2003) *Ecology of the bullhead*. Conserving Natura 2000 Rivers Ecology Series No. 4. English Nature, Peterborough. 19 pp. ISBN: 185716 704 X.

Underwood AJ (1992) Beyond BACI: the detection of environmental impacts on populations in the real, but variable, world. *Journal of Experimental Marine Biology and Ecology*, 161(2):145-178. DOI: 10.1016/0022-0981(92)90094-Q

Unfer G, Hauer C, Lautsch E (2011) The influence of hydrology on the recruitment of brown trout in an Alpine river, the Ybbs River, Austria. *Ecology of Freshwater Fish* 20:438-448. DOI: 10.1111/j.1600-0633.2010.00456.x.

Utzinger J, Roth C, Peter A (1998) Effects of environmental parameters on the distribution of bullhead *Cottus gobio* with particular consideration of the effects of obstructions. Journal of *Applied Ecology* 35:882-892. DOI: 10.1111/j.1365-2664.1998.tb00006.x.

Valette E, Jodeau M. (2012) How to predict the sedimentological impacts of reservoir operations?. *6th Conference on Scour and Erosion*, Paris, pp 1329-1336.

Van Rijn LC (1993) *Principles of Sediment Transport in Rivers, Estuaries and Coastal Seas*. Aqua Publications, Amsterdam

Vanoni VA (1975) Sedimentation engineering, American Society of Civil Engineers, New York, USA. ISBN: 978-0-7844-0823-0

Vezza P, Parasiewicz P, Calles O, Spairani M, Comoglio C (2014) Modelling habitat requirements of bullhead (*Cottus gobio*) in Alpine streams. *Aquatic sciences* 76(1):1-15. DOI: 10.1007/s00027-013-0306-7.

Wang G, Wu B, Wang Z-Y (2005) Sedimentation problems and management strategies of Sanmenxia Reservoir, Yellow River, China. *Water Resources Research* 41(9) DOI: 10.1029/2004wr003919

White R. (2001) Evacuation of Sediments from Reservoirs. Thomas Telford Publishing, London, United Kingdom. 280 pp. ISBN: 9780727729538

White WR (2010) World water: resources, usage and the role of man- made reservoirs. Foundation for Water Research, Marlow

Wilcox AC, Peckarsky BL, Taylor BW, Encalada AC (2008) Hydraulic and geomorphic effects on mayfly drift in high-gradient streams at moderate discharges. *Ecohydrology* 1(2):176-186. DOI: 10.1002/eco.16.

Wild TB, Loucks DP (2014) Managing flow, sediment, and hydropower regimes in the Sre Pok, Se San, and Se Kong Rivers of the Mekong basin. *Water Resources Research* 50:5141– 5157. DOI:10.1002/2014WR015457

Wild TB, Loucks DP, Annandale GW, Kaini P (2015) Maintaining Sediment Flows through Hydropower Dams in the Mekong River Basin. *Journal of Water Resources Planning and Management* 142(1). DOI: 10.1061/(ASCE)WR.1943-5452.0000560

Wisser D, Frolking S, Hagen S, Bierkens MFP (2013) Beyond peak reservoir storage? A global estimate of decling water storage capacity in large reservoirs. *Water Resources Research* 49:1-8. DOI: 10.1002/wrcr.20452, 2013

Wohl EE, Cenderelli DA (2000) Sediment deposition and transport patterns following a reservoir sediment release. *Water Resources Research* 36(1):319-333. DOI: 10.1029/1999WR900272

Wohl EE, Rathburn S (2003) Mitigation of sedimentation hazards downstream from reservoirs. *International Journal of Sediment Research* 18(2):97-106.

Wohl EE, Bledsoe BP, Jacobson RB, Poff NL, Rathburn SL, Walters DM, Wilcox AC (2015) The natural sediment regime in rivers: broadening the foundation for ecosystem management. *BioScience* 65(4):358-371. DOI: 10.1093/biosci/biv002

Yang CT (1979) Unit stream power equations for total load. *Journal of Hydrology* 40:123-128. DOI: 10.1016/0022-1694(79)90092-1

Yang CT (1984) Unit stream power equations for gravel. *Journal of Hydraulic Engineering* 110(12):1783-1797. DOI: 10.1061/(ASCE)0733-9429(1984)110:12(1783)

Yang CT (2006) *Erosion and Sedimentation Manual*. Bureau of Reclamation, Technical Service Center, Denver

Yasarer LMW, Sturm BSM (2016) Potential impacts of climate change on reservoir services and management approaches. *Lake and Reservoir Management* 31(1):13-26. DOI: 10.1080/10402381.2015.1107665

Yoshimura C, Tockner K, Omura T, Moog O (2006) Species diversity and functional assessment of macroinvertebrate communities in Austrian rivers. *Limnology* 7:63-74. DOI: 10.1007/s10201-006-0170-4

Zarfl C, Lumsdon A E, Berlekamp J, Tydecks L, Tockner K (2015) A global boom in hydropower dam construction. *Aquatic Sciences* 77(1):161-170. DOI: 10.1007/s00027-014-0377-0

Papers published during the PhD

Espa P, Brignoli ML, Crosa G, Gentili G, Quadroni S. (2016) Controlled sediment flushing at the Cancano Reservoir (Italian Alps): management of the operation and downstream environmental impact. *Journal of Environmental management* 182:1-12. DOI: 10.1016/j.jenvman.2016.07.021

Quadroni S, Brignoli ML, Crosa G, Gentili G, Salmaso F, Zaccara S, Espa P (2016) Effects of sediment flushing from a small Alpine reservoir on downstream aquatic fauna. *Ecohydrology*. DOI: 10.1002/eco.1725

Brignoli ML, Espa P, Batalla RJ (2017) Sediment dynamics below a small alpine reservoir desilted by controlled flushing. *Journal of Soils and Sediments* DOI: 10.1007/s11368-017-1661-0

Brignoli ML, Espa P, Quadroni S, Crosa G, Gentili G, Batalla, RJ (2017) Experiences of controlled sediment flushing from four Alpine reservoirs. In: *River Sedimentation* – Wieprecht et al. (Eds), Taylor & Francis Group, London, ISBN 978-1-138-02945-3

Quadroni S, Crosa G, Zaccara S, Espa P, Brignoli ML, Gentili G, Batalla RJ (2017) Controlling sediment flushing to mitigate downstream environmental impacts. In: *River Sedimentation* – Wieprecht et al. (Eds), Taylor & Francis Group, London, ISBN 978-1-138-02945-3

Acknowledgements

I wish to express my sincere gratitude to my supervisor Paolo Espa and my colleague Silvia Quadroni for their continuous support to my Ph.D. research. My sincere thanks goes to Prof. Ramon J. Batalla and his research group for encouraging and supporting my research activity at the University of Lleida. I would also like to thank Dr. Damià Vericat and Prof. Maurizio Righetti for reviewing my Ph.D. dissertation. Last but not least, I wish to thank my husband Alberto that has supported me in field and lab work. He, together with my family, has always encouraged me to go ahead.

Symbols and abbreviations

AMSL	Above mean sea level
ANOSIM	Analyses of similarity
BCi	Bary-Curtis Index
b_L	Bedload adaptation length coefficient (SRH-1D model)
BS	Biomonitoring Sites
CR	Cancano Reservoir
CSF	Controlled sediment flushing
DO	Dissolved Oxygen
ED	Duration of exposure
EPT	Plecoptera and trichoptera families
FE	Flushinf efficiency
HPP	Hydropower plant
L_{tot}	Adaptation length (SRH-1D model)
MAF	Mean annual flow
MCDA	Multi-Criteria Decision Analysis
$M_{dep,tot}$	Total mass of deposited sediment
MF	Minimum flow
MR	Madesimo Reservoir
M_{sed}	Mass of sediment
n	Manning's roughness coefficient
nalt	Active layer thickness multiplier (SRH-1D model)
N&J	Newcombe and Jensen
NMDS	Non-metric Multidimensional Scaling
Q	Water discharge
R^2	Determination coefficient
SC	Sediment concentration
SD	Standard deviation
SEV	Severity of ill effect
SR	Sernio Reservoir
SRH-1D	Sedimentation and River Hydraulics-One Dimensional
SSC	Suspended sediment concentration
STAR_ICMi	Standardisation of River Classifications_Intercalibration Multimetric Index
TMDLs	Total maximum daily loads
VR	Valgrosina Reservoir
V_{sed}	Volume of sediment
WFD	Water Framework Directive
α_d	Suspended sediment recovery factor for deposition (SRH-1D model)
α_e	Suspended sediment recovery factor for erosion (SRH-1D model)
χ	Weight of bedload fraction (SRH-1D model)